Pavol Jozef Šafárik University in Košice
Faculty of Science

NEW TRENDS

IN CHEMISTRY, RESEARCH AND EDUCATION

at the Faculty of Science of Pavol Jozef Šafárik University in Košice 2021

Book of Abstracts

Košice 2021

Edited by: **Mária Kožurková**, Department of Biochemistry, Institute of Chemistry, Faculty of Science, Pavol Jozef Šafárik University in Košice, Moyzesova 11, 040 01 Košice, Slovak Republic
maria.kozurkova@upjs.sk

Reviewed by: **Katarína Reiffová**, Department of Analytical Chemistry, Institute of Chemistry, Faculty of Science, Pavol Jozef Šafárik University in Košice, Moyzesova 11, 040 01 Košice, Slovak Republic
katarina.reiffova@upjs.sk
Juraj Kuchár, Department of Inorganic Chemistry, Institute of Chemistry, Faculty of Science, Pavol Jozef Šafárik University in Košice, Moyzesova 11, 040 01 Košice, Slovak Republic
Juraj.kuchar@upjs.sk
Mariana Budovská, Department of Organic Chemistry, Institute of Chemistry, Faculty of Science, Pavol Jozef Šafárik University in Košice, Moyzesova 11, 040 01 Košice, Slovak Republic
mariana.budovska@upjs.sk
Ivana Šišoláková, Department of Physical Chemistry, Institute of Chemistry, Faculty of Science, Pavol Jozef Šafárik University in Košice, Moyzesova 11, 040 01 Košice, Slovak Republic
ivana.sisolakova@upjs.sk
Nataša Tomášková, Department of Biochemistry, Institute of Chemistry, Faculty of Science, Pavol Jozef Šafárik University in Košice, Moyzesova 11, 040 01 Košice, Slovak Republic
natasa.tomaskova@upjs.sk

Organized by: Institute of Chemistry
Faculty of Science, Pavol Jozef Šafárik University in Košice

Organisation Committee: Mária Kožurková
Mária Ganajová

Available at: www.unibook.upjs.sk
Publication date: 30.11.2021

ISBN 978-80-574-0048-6 (e-publication)

LIST OF CONTENTS

CONFERENCE PROGRAMME — 26th November 2021 — Aula M5

	08:25 - 08:30	**Z. Vargová: WELCOME AND OPENING**
INVITED LECTURES	**08:30 - 09:05**	**R. Halko:** *Slurry Sampling in Atomic Absorption Spectrometry.* Comenius University in Bratislava, Faculty of Natural Sciences, Department of Analytical Chemistry, Bratislava, Slovak Republic
	09:05 – 09:40	**M. Lísa:** *Monitoring of Metabolite Changes in Central Nervous System Disorders.* University of Hradec Králové, Faculty of Science, Department of Chemistry, Hradec Králové, Czech Republic
	09:40 – 10:15	**Š. Budzák:** *Computational Insights into Photoswitching Systems.* Department of Chemistry, Faculty of Natural Sciences, Matej Bel University, Banská Bystrica, Slovak Republic
	10:15 – 10:25	**COFFEE BREAK**
	10:25 – 11:00	**J. Mašlanková:** *Application of Zymography in Clinical-Biochemical Diagnostics*. Department of Medical and Clinical Biochemistry, Faculty of Medicine, Pavol Jozef Šafárik University in Košice, Slovak Republic
	11:00 – 12:00	**LUNCH**
PLENARY LECTURES	**12:00 – 12:20**	**V. Vojteková:** *Collision–Reaction Cells in the Analysis by Using ICP-MS Technology.* Department of Analytical Chemistry, Institute of Chemistry, Faculty of Science, Pavol Jozef Šafárik University in Košice, Slovak Republic
	12:20 – 12:40	**I. Šišoláková:** *Electrochemical Sensors as Novel Tool for Diseases Diagnostics.* Department of Physical Chemistry, Institute of Chemistry, Faculty of Science, Pavol Jozef Šafárik University in Košice, Slovak Republic
	12:40 – 13:00	**R. Varhač:** *Analysis of Glucose Oxidase Catalysed Reaction Measured by Fluorescence Spectroscopy.* Department of Biochemistry, Institute of Chemistry, Faculty of Science, Pavol Jozef Šafárik University in Košice, Slovak Republic
	13:00 – 13:10	**COFFEE BREAK**
	13:10 – 13:30	**J. Elečko:** *Iminosugars with Bicyclic Structure – Polyhydroxylated Indolizidines and Pyrrolizidines.* Department of Organic Chemistry, Institute of Chemistry, Faculty of Science, Pavol Jozef Šafárik University in Košice, Slovak Republic
	13:30 – 13:50	**Z. Vargová:** *Relationship between Structure and Biological Properties of Silver(I) Complexes.* Institute of Chemistry, Faculty of Science, Pavol Jozef Šafárik University in Košice, Slovak Republic
	13:50 – 14:10	**M. Ganajová:** *Formative Assessment in Teaching Science, Mathematics, and Informatics.* Department of Didactics of Chemistry, Institute of Chemistry, Faculty of Science, Pavol Jozef Šafárik University in Košice, Slovak Republic
INVITED LECTURE	**14:10 – 14:40**	**R. Šebesta:** *Green Asymmetric Organocatalysis*. Comenius University in Bratislava, Faculty of Natural Sciences, Department of Organic Chemistry, Bratislava, Slovak Republic
	14:40 – 15:30	**POSTER SESSION**
	15:30 – 15:35	**Z. Vargová: CONFERENCE CLOSING**

Slurry Sampling in Atomic Absorption Spectrometry

R. Halko[a]*, S. Procházková[a], K. Chovancová[a]
[a]Comenius University in Bratislava, Faculty of Natural Sciences, Department of Analytical Chemistry, Mlynská dolina, Ilkovičova 6, 842 15 Bratislava 4, Slovak Republic
*radoslav.halko@uniba.sk

This work presents a recent developments and applications of the slurry sampling in atomic absorption spectrometric techniques. Slurry sampling is an alternative approach for the minimization of sample preparation of solid samples before their analysis. The work is focused on the description of the basic critic factors of slurry sampling and some advantages or drawbacks of this technique are also discussed. Applications of combined sludge sampling with atomic absorption spectrometry for the determination of metals in various solid samples, such as environmental, biological, food and others, are also presented.

Acknowledgements

This work was supported by the Scientific Grant Agency of the Ministry of Education of the Slovak Republic, VEGA no. 1/0678/19 and the Slovak Research and Development Agency (APVV-17-0373).

Monitoring of Metabolite Changes in Central Nervous System Disorders

M. Lísa[a]*, E. Cífková[a], P. Lišková[a], O. Kozlov[a], H. Řehulková[a]
[a]University of Hradec Králové, Faculty of Science, Department of Chemistry, Rokitanského 62, Hradec Králové, Czech Republic
*miroslav.lisa@uhk.cz

Disorders of the central nervous system (CNS) represent a serious health problem in current medicine due to the continuously increasing incidence with significant human, medical, and economic effects on the population. Pathogenesis of CNS diseases is closely related to the changes of metabolites, naturally occurring low-molecular weight molecules (< 1 kDa) involved in metabolism pathways with many essential cellular functions. Metabolic profiling of the healthy and disease CNS in preclinical models or human samples may provide a better understanding of disease etiology and new biomarkers important for early diagnosis or monitoring of medical treatment. The goal of this work is the development of a powerful analytical platform for the monitoring of a wide range of polar metabolites and lipids in CNS disorders, providing a comprehensive insight into metabolic changes. The coupling of ultra-high performance liquid chromatography and ultra-high supercritical fluid chromatography with mass spectrometry (MS) is used in this work as a powerful analytical tool providing sensitive and selective detection of metabolites necessary for complex biological samples. New methods are developed for targeted and untargeted high-throughput quantitative metabolomic analysis. Optimized methods are validated for each biological matrix and internal standards and applied for monitoring of metabolite changes in clinical studies. Advanced data mining tools and multivariate statistical analysis are used in our workflow to identify potential biomarkers based on the mutual comparison of case and control groups. Results of the metabolomic study of the schizophrenia animal model will be presented.

Acknowledgements

This work was supported by project number 20-12289S sponsored by the Czech Science Foundation. Support of University of Hradec Králové (Faculty of Science no. VT2019- 2021 and SV2106-2021) is acknowledged.

Green Asymmetric Organocatalysis

R. Šebesta[a]*

[a]Comenius University in Bratislava, Faculty of Natural Sciences, Department of Organic Chemistry, Mlynská dolina, Ilkovičova 6, 842 15 Bratislava, Slovak Republic

*radovan.sebesta@uniba.sk

Current environmental challenges and the need for preparation of chiral compounds pose new demands on organic synthesis. Effective syntheses of chiral compounds that are needed as medicines, materials, or crop protection agents must be high stereoselectivity, but also need to fulfil stringent environmental criteria. Ideal synthesis should adhere to principles of green chemistry such as the elimination of dangerous compounds, or decrease of waste production. Asymmetric organocatalysis, that is the use of small chiral organic molecules as catalysts, offer great opportunities in the synthesis of important chiral compounds and at the same time enable implementation of green chemistry principles [1].

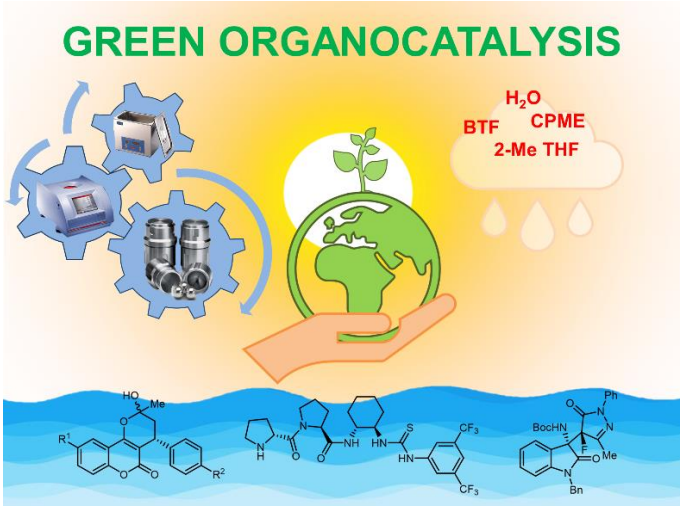

Enantioselective organocatalytic reactions, such as Michael additions, aminoxylation, and hydrazination of aldehydes can be performed in aqueous media or under solventless conditions using a ball mill [2]. The solventless methodology allows more effective catalysis using organocatalysts, which employ non-covalent interactions for activation [3]. Chiral thioureas and squaramides proved to be more enantioselective catalysts for Michael additions under solventless conditions than in solvents. The in-situ release of unstable alkyloxyacetaldehydes from acetals using acidic ionic liquids and microwave irradiation improved the organocatalytic synthesis of antiviral drug oseltamivir [4]. Greener solvent alternatives, such as 2-methyltetrahydrofurane enable highly enantioselective warfarin synthesis [5]. Ball-milling proved highly efficient for the asymmetric domino Mannich reaction/ fluorination with squaramide organocatalyst that afforded a range of functionalized oxindolyl fluoropyrazolones [6]. On the other hand, our newly designed peptide-thiourea organocatalyst was more effective in solution than under solvent-free conditions for Michael additions using heterocycle-containing reaction partners [7].

Acknowledgements

This work was supported by Slovak Research and Development Agency under the Contract no. APVV-18-0242 Grant Agency VEGA (VEGA-1-332-19).

References

[1] D. Krištofíková, V. Modrocká, M. Mečiarová, R. Šebesta, ChemSusChem **13** (2020) 2828-2858.
[2] E. Veverková, V. Poláčková, L. Liptáková, E. Kázmerová, M. Mečiarová, Š. Toma, R. Šebesta, ChemCatChem **4** (2012) 1013-1018; E. Veverková, V. Modrocká, R. Šebesta, Eur. J. Org. Chem. (2017) 1191-1195.
[3] M. Hestericová, R. Šebesta, Tetrahedron **70** (2014) 901-905.
[4] P. Tisovský, T. Peňaška, M. Mečiarová, R. Šebesta, ACS Sust. Chem. Eng. **3** (2015) 3429-3434.
[5] V. Modrocká, E. Veverková, M. Mečiarová, R. Šebesta, J. Org. Chem. **83** (2018) 13111-13120.
[6] D. Krištofíková, M. Mečiarová, E. Rakovský, R. Šebesta, ACS Sust. Chem. Eng. **8** (2020) 14417-14424.
[7] P. Čmelová, D. Vargová, R. Šebesta, J. Org. Chem. **86** (2021) 581-592.

Computational Insights into Photoswitching Systems

Š. Budzák[a]*, M. Medveď[a], M. Cigáň[b], D. Jacquemin[c]
[a]Department of Chemistry, Faculty of Natural Sciences, Matej Bel University, Tajovského 40, 974 01 Banská Bystrica, Slovak Republic
[b]Department of Organic Chemistry, Faculty of Natural Sciences, Comenius University, Ilkovičova 6, 842 15 Bratislava, Slovakia
[c] CEISAM Lab, UMR 6230, Université de Nantes, CNRS, 44000 Nantes, France
*simon.budzak@umb.sk

A photoswitch is a molecular entity that can change its structural and chemical properties upon absorption of electromagnetic radiation. The most noticeable families of organic photoswitches are azobenzenes [1], stilbenes [2], spiropyrans/merocyanines [3], diarylethenes [4] and hemithioindigos [5], which exploit either a Z/E double-bond photoisomerization, a photoactivated cyclization/ring opening reaction or a photo-initiated group transfer. Depending on the activation barrier(s) between the two states, a photoswitch can be either bistable (P-type) or thermally reversible (T-type). The bi-directional switching (P-type) employs two different wavelengths and thus relies on a change in the absorption spectrum upon photoswitching together with high thermal stabilities of the isomers. The T-type systems are driven by light from one form to the other, turning back to their original state through a thermal back reaction. The photochromic molecules are designed for a range of applications starting from adaptive sunscreen protection materials, through alternative materials for computer memories, ending with photo-pharmacological applications. Development in this field is rapid and recently several new classes of photoswitches were introduced while the older structural families are being optimized and refined. Van Dijken et al. [6] previously summarized the performance criteria for assessment of the quality of photoswitches. They include: a) addressability, defined as the separation of absorption maxima of the two forms ($\Delta\lambda_{max}$) and the ratio of the molar absorption coefficients (ε) of the two forms at the excitation wavelength; b) thermal stability, defined as the half-life ($\tau_{1/2}$) of back thermal reaction of the thermodynamically less stable form; c) efficiency, defined as the photoreaction quantum yield Φ and the photostationary state (PSS) composition, and d) reliability, defined as the fatigue resistance, i.e. resistance to competitive photoreaction pathways.
Thermal and light driven processes in photoswitches can be characterized by variety of tools. One of them is the computational chemistry, which offers insights into the photochemistry at molecular level, and is able to reveal small nuances of the structure-photoswitching relationship. Following general introduction, we will describe strong and weak points of theoretical predictions for the photochromic systems. In the ground state, we will demonstrate ability of the DFT methods to outline potential reaction pathways for thermal reactions – e.g. inversion vs. rotation mechanism in hydrazones and azobenzenes [7, 8]. The absorption spectrum can be modelled by TD-DFT methods with satisfactory precision even for large molecules, but the non-radiative deactivation and reactive phototransformations are methodological challenges for computational methods, especially when system size is considered [9]. Here we will show synergy between theoretical calculations and experimental measurements particularly for solvent dependent stimulated emission in hydrazone-based photoswitch. Interesting interpretations can be also obtained when modeling ultrafast transient spectra of studied molecules. Since transformations in the excited states are ultrafast by nature, we will show application of the nonadiabatic molecular dynamic to photoswitching systems.

Acknowledgements

This work has been supported by the Slovak Research and Development Agency and the Scientific Grant Agency, VEGA 1/0562/20 and APVV-20-0098, respectively.

References

[1] H. M. D. Bandara, S. C. Burdette, Chem. Soc. Rev. **41** (2012) 1809–1825.
[2] D. H. Waldeck, Chem. Rev. **91** (1991), 415-436.
[3] R. Klajn, Chem. Soc. Rev. **43** (2014), 148–184.
[4] M. Irie, T. Fukaminato, K. Matsuda, S. Kobatake, Chem. Rev. **114** (2014), 12174-12277.
[5] S. Wiedbrauk, H. Dube, Tetrahedron Lett. **56** (2015), 4266–4274.
[6] D. J. van Dijken, P. Kovaricek, S. P. Ihrig, S. Hecht, J. Am. Chem. Soc. **137** (2015), 14982-14991.
[7] B. Mravec, Š. Budzák, M. Medveď et al., J. Org. Chem. **86** (2021), 11633-11646.
[8] R. Travieso-Puente, Š Budzák, J. Chen et al., J. Am. Chem. Soc. **139** (2017), 3328-3331.
[9] P. Liesfeld, Y. Garmshausen, Š. Budzák et al., Angew. Chem. Int. Ed. **59** (2020), 19352-19358.

Application of Zymography in Clinical-Biochemical Diagnostics

J. Mašlanková[a*], I. Večurkovská[a], M. Mareková[a]
[a]Department of Medical and Clinical Biochemistry, Faculty of Medicine, Pavol Jozef Šafárik University in Košice, Trieda SNP 1, 040 11 Košice, Slovak Republic
*jana.maslankova@upjs.sk

One of the most reliable sensitive methods commonly used to monitor the expression and activity of hydrolytic enzymes in various biological samples, such as cells, tissues, and biological fluids, is the electrophoretic zymography method. It is a method of analysis of enzymes proteolytic activity by cleavage of the substrate, through which we can estimate, based on the size of the protein, which enzyme is present in a given biological sample. The proteins are first separated by electrophoresis in a polyacrylamide gel impregnated with a given protease substrate, which is cleaved by proteases during the subsequent incubation and, after staining**,** appears lytic zones, areas of destroyed substrate, shown as white stripes on a dark background. These visible zones on the gel are evidence of the proteases present. Thus, enzyme activity is detected by the absence of substrate in the gel, which can be visualized by transillumination. The activity of a particular protease is proportional to the intensity and thickness of the corresponding band on the zymogram, which can be evaluated electronically after scanning the gels using computer software. One of the main advantages of zymography is that this technique can also be used to assess the state of protease activation in a sample. Protease activation usually involves the release of the pro-domain (approximate size: 10 kDa) through a proteolytic and non-proteolytic cleavage mechanism. This process causes a decrease in the molecular weight of the active species of enzymes relative to the zymogen, which can be easily detected by zymography due to the difference in relative molecular weight [1].
The aim of our work is to apply zymography in the diagnosis of various types of diseases (carcinomas, neurodegenerative diseases, diabetes, periodontitis) in various biological materials (serum, plasma, tissue, tears, saliva, cell cultures) and use its potential in assessing disease progression as well as the suitability of the correct treatment procedure.

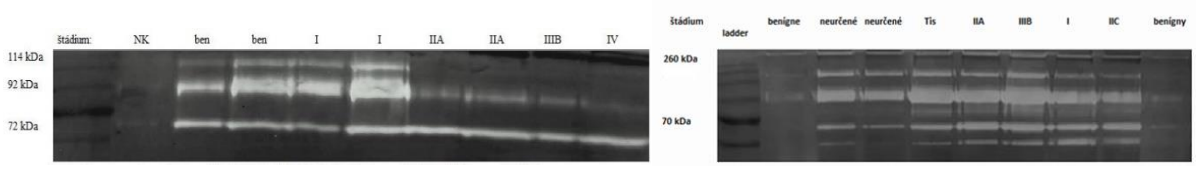

Figure 1 The zymogram of serum (left) and tissue (right) of patients with colorectal cancer.

Acknowledgements

This work was supported by the grants of the Slovak Grant Agency VEGA 1/0540/20 and VEGA1/0333/20.

References

[1] P. Bencsik, M. Bartekova, A. Görbe, K. Kiss, J. Pálóczi, J. Radosinska, G. Szűcs, P. Ferdinandy, Methods Mol. Biol. **1626** (2017) 53-70.

Collision–Reaction Cells in the Analysis by Using ICP-MS Technology

V. Vojteková[a]*
[a]Department of Analytical Chemistry, Institute of Chemistry, Faculty of Science, Pavol Jozef Šafárik University in Košice, Moyzesova 11, 040 01 Košice, Slovak Republic
*viera.vojtekova@upjs.sk

The contribution presents very interesting ion activation techniques employed in quadrupole and tandem mass spectrometry. After the in-source fragmentation and ion decompositions, the tandem mass spectrometry is followed.
There needs to be emphasized that the activation of ions is distinct from the ionization step, and that the interfering and analyzed ions are both characterized independently by their mass/charge ratios.
In collision-induced dissociation (CID), activation of the selected ions occurs by the molecules collision(s) with inert gas in a collision-reaction cell (CRC). The measurement can be realized at high (keV range) collision energies, using tandem sector and time-off-light instruments, or at low (eV range) energies, in tandem quadrupole and ion trapping instruments.
It can be performed using either single or multiple collisions with a selected gas and each of these factors influences the distribution of internal energy that the activated ion will possess [1, 2, 3].
The alternative process that can take place in the CRCs is called kinetic energy discrimination (KED). It is also realized in the collision mode of CRC, by using a non-reactive gas. The selective attenuation of polyatomic interferences is based on their size discrimination. KED exploits the fact that all polyatomic ions are larger than analyte ions of the same mass, so they collide with the cell gas more often as they pass through the cell, emerging with lower residual energy.
These low energy ions are excluded from the ion beam. KED requires the ions to undergo many collisions before the difference in residual energy between analyte and polyatomic ions is large enough to allow them to be separated. This fact requires a higher collision gas pressure in the CRC [4,5].
It can be stated that incorporation of collision–reaction cells into ICP-MS instruments is a very attractive and elegant way to overcome spectral interferences, which affects the accuracy of measurements [6,7]. Collision-reaction cells as the ionization and separation units of ICP-MS, are obviously placed in tandem behind a plasma torch and in front of the analyzing mass spectrometer.
The collision-reaction cells can promote reactive and non-reactive collisions, with resultant benefits in reduction of spectral interferences. This chemical and physico-chemical resolution technique can avert interferences that could require the use of the high resolution mass spectrometer.
This contribution wants to participate in the discussion on the applicability of CRC-ICP-QMS for routine analysis of the complicated mixtures. For accurate multi-element determinations of unknown and variable sample matrices, the advantages of collision mode using KED are indisputable.
Effective KED requires an instrument with the technology to minimize initial ion energy spread, simultaneously and efficiently transmit all masses through the cell, and maximize the number of collisions while reducing losses due to scattering.

Acknowledgements

This work was supported by folowing projects: EU ITMS 26220120064.

References

[1] J. T. Rowan, R. S. Houk, Appl. Spectrosc. **6** (1989) 976-980.
[2] I. Feldman, N. Jakubowski, D. Stuewer, Fresenius J. Anal. Chem. **365** (1999) 415-421.
[3] S. Wilbur, E. Soffey, E. Mc Curdy, Agilent ICP-MS Journal **19** (2004) 4-5.
[4] D. W. Koppenaal, G. C. Eiden, C. J. Barinaga, J. Anal. At. Spectrom. **19** (2004) 561-570.
[5] M. A. Amr, Adv. Appl. Sci. Res. **3** (2012) 2179-2191.
[6] S. D. Tanner, V. I. Baranov, D. R. Bandura, Spectrochim. Acta Part B **57** (2002) 1361-1452.
[7] E. McCurdy, G. Woods, J. Anal. At. Spectrom. **19** (2004) 607-615.

Electrochemical Sensors as Novel Tool for Diseases Diagnostics

I. Šišoláková[a]*, J. Shepa[a], R. Oriňaková[a]
[a]Department of Physical Chemistry, Institute of Chemistry, Faculty of Science, Pavol Jozef Šafárik University in Košice, Moyzesova 11, 040 01 Košice, Slovak Republic
*ivana.sisolakova@upjs.sk

Electrochemical sensors can be considered as the novel tool for fast, occurrence, and low-cost diseases diagnostics. Various worldwide serious diseases such as diabetes mellitus, cancer, Parkinson disease, Alzheimer, viruses' diseases can be diagnostic using electrochemical methods [1]. Our previous work has been focused on the development of a suitable electrochemical sensors for diabetes mellitus, epidermal growth factor receptor (EGFR), and various viruses diseases diagnostics. Since diabetes mellitus can be considered as the one of the most widespread disease worldwide, fast and cheap diagnosis is desirable. In our research various type of carbon electrodes modification for insulin (Figure 1) determination has been studied. As the most suitable material for modification nickel oxide (NiO) nanoparticles were chosen. The combination of polymer membrane, multi wide carbon nanotubes and NiONPs displayed the most suitable analytical characteristics like low limit of detection (), high sensitivity (), and suitable selectivity for insulin determination.

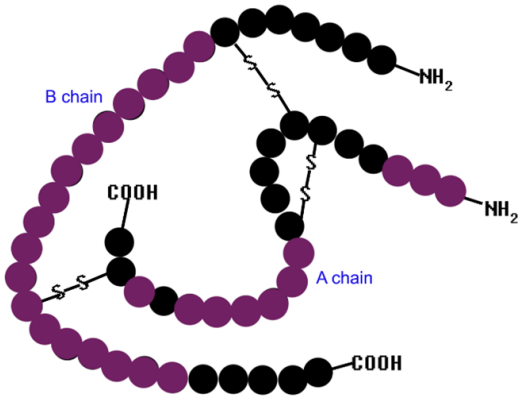

Figure 1 Insulin structure with the active parts of insulin in purple.

Electrochemical biosensors can be also used for EGFR diagnostic as a cancer precursor. This fast and cheap method can represent the revolution in fast cancer diagnostic. Various viruses diseases can be also diagnostics using electrochemical sensors (Figure 2). With small change of biological part of sensors we are able to prepare sensor for all viruses disease. Based on this research we can summarized that electrochemical sensor represents the novel suitable tool for various diseases diagnostics.

Figure 2 Modifiaction of electrochemical sensors for viruses detection.

Acknowledgements

This work has been supported by the project of the Slovak Research and Development Agency APVV-PP-COVID-20-0036 and Visegrad Fund project number 22020140.

References

[1] J. Hu, Y. Yu, M. Guo, M, Yuan, W. Liu, Biosens. Bioelectron. **77** (2016) 215-219.
[2] M. M. Qaid, M. M. Adbelrahman, Cogent Food Agric. **2** (2016) 1-18.

Analysis of Glucose Oxidase Catalysed Reaction Measured by Fluorescence Spectroscopy

R. Varhač[a]*
[a]Department of Biochemistry, Institute of Chemistry, Faculty of Science, Pavol Jozef Šafárik University in Košice, Moyzesova 11, 040 01 Košice, Slovak Republic
*rastislav.varhac@upjs.sk

Glucose oxidase (GOX, EC 1.1.3.4) is an oxidoreductase that catalyses oxidation of β-D-glucose to a D-glucono-δ-lactone in the presence of oxygen according to the following reaction:

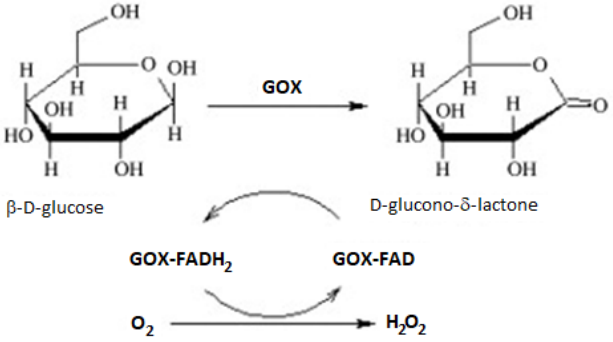

Based on the scheme, molecular oxygen present in a solution is necessary to regenerate (oxidise) GOX cofactor – flavin adenine dinucleotide (FAD) – for its employment in the next redox cycle. Fluorescence spectroscopy was used to monitor course of the reaction employing a fluorescent dye ruthenium-tris(4,7-diphenyl-1,10-phenanthroline) dichloride ($Ru(dpp)_3Cl_2$). The fluorescence emission of this dye is known to be quenched by a dissolved oxygen, which means the more oxygen is present in a solution the lesser signal we get and *vice versa*.
The obtained kinetic curves were analysed in two ways: (i) as original data and (ii) in their modified form. For original data analysis, Richards curve was used [1]:

$$F = \left(F_{min_0} + m \cdot t\right) + \frac{F_{max} - \left(F_{min_0} + m \cdot t\right)}{\left[1 + \left(\frac{t}{t_b}\right)^{-k}\right]^{s}}$$

where F_{mino} is a fluorescence signal at t = 0 s, F_{max} is a signal at the end of a reaction, m is a slope of the initial increase of the signal, t_b is a time of maximum signal increase, k characterizes the slope of the curve at its midpoint and s controls the asymmetry of the curve. The Richards curve was initially developed as a model to fit wide range of S-shaped growth curves. We observed the linear dependence of one (m) of the four altering parameters (m, t_b, k, s) on the initial concentration of glucose over the range 1 – 15 mM. Modification of the original time dependence was performed by its transformation based on the Stern-Volmer model [2]:

$$\frac{1}{F} = \frac{1}{F_0} + \frac{K_{SV}}{F_0}[Q]$$

where F_0 is a fluorescence intensity of $Ru(dpp)_3Cl_2$ in the absence of a quencher (O_2), F is a fluorescence intensity of $Ru(dpp)_3Cl_2$ in the presence of a quencher, [Q] is a concentration of dissolved O_2 and K_{SV} is the Stern-Volmer quenching constant. This approach allowed us to determine V_{max} and K_M values for the GOX-catalysed glucose oxidation as well as enzyme activity of GOX expressed in terms of molecular oxygen consumption per minute at optimal conditions.
Our results show a potential of fluorescence spectroscopy in its application to GOX-catalysed reaction. The major significance of the presented analysis is its application in the determination of the glucose concentration and calculation of enzyme activity from one set of measured data.

Acknowledgements

This work was supported by the research grant APVV-20-0340.

References

[1] F. J. Richards, J. Exp. Bot. **10** (1959) 290-300.
[2] O. Stern, M. Volmer, Z. Phys. **20** (1919) 183-188.

Iminosugars with Bicyclic Structure – Polyhydroxylated Indolizidines and Pyrrolizidines

J. Elečko[a]*
[a]Department of Organic Chemistry, Institute of Chemistry, Faculty of Science, Pavol Jozef Šafárik University in Košice, Moyzesova 11, 040 01 Košice, Slovak Republic
*jan.elecko@upjs.sk

Since the discovery of nojirimycin in 1966 there is significant interest in the large group of natural products called iminosugars. They are polyhydroxylated derivatives of mono and bicyclic heterocycles with endocyclic nitrogen atom with structure mimicking natural sugars. On the basis of structural resemblance, natural iminosugars can be divided into polyhydroxylated pyrrolidines, piperidines, indolozidines, pyrrolizidines and nortropanes [1].

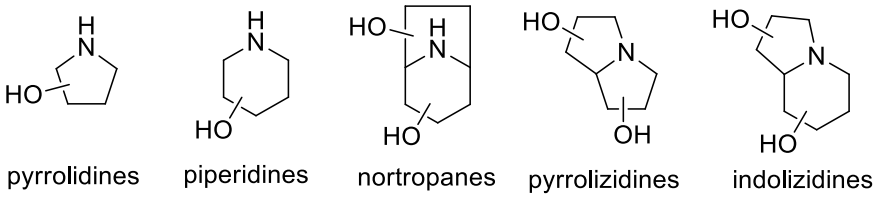

Thanks to their simple and small structure strictly related to carbohydrates, iminosugars are endowed with an excellent drug profile. The first recognized property of iminosugars was their ability to act as glycosidase and glycosyltransferase inhibitors, essentially acting in a competitive manner and exerting their activity mainly as antivirals and antidiabetics. Iminosugars have become the most popular class of carbohydrate-processing modulators, being able to alter the glycosylation profile of eukaryotic cells, to interfere in carbohydrate and glycoconjugate metabolism, to regulate the folding and transport of glycoproteins, and to stop the interaction mediated by host cell carbohydrates with infective agents. These compounds thus find their application as immune system modulators, anti-cancer agents and as therapeutic agents for the treatment of lysosomal storage disorders [2].
Due to promising therapeutic applications, variety of synthetic routes were developed and numbers of synthetic analogues were prepared [3]. We present our efferts on the field of synthesis of polyhydroxylated pyrrolizidine and indolizidine derivatives [4].

Acknowledgements

The present work was supported by the Slovak Grant Agency VEGA (1/0375/19) and by the Slovak Research and Development Agency (APVV-14-0883).

References

[1] N. Asano, R. J. Nash, R. J. Molyneux, G. W. J. Fleet, Tetrahedron: Asymmetry **11** (2000) 1645-1680.
[2] A. Guaragna *et al.*, Int. J. Mol. Sci. **21** (2020) 3353-3387.
[3] a) B. G. Davis, Tetrahedron: Asymmetry **20** (2009) 652-671; b) I. Conforti, A. Marra, Org. Biomol. Chem. **19** (2021) 5660-5697.
[4] a) J. Gonda, J. Elečko, M. Martinková, M. Fábian, Tetrahedron Letters **57** (2016) 2895-2897; b) J. Elečko, J. Gonda, M. Martinková, M. Vilková, Tetrahedron: Asymmetry **27** (2016) 346-351.

Relationship between Structure and Biological Properties of Silver(I) Complexes

Z. Vargová[a]*, M. Rendošová[a], G. Kuzderová[a], D. Sabolová[a], M. Vilková[a], R. Gyepes[b], P. Olejníková[c], M. Kello[d], D. Mudroňová[e]

[a]Institute of Chemistry, Faculty of Science, Pavol Jozef Šafárik University in Košice, Moyzesova 11, 040 01 Kosice, Slovak Republic

[b]Faculty of Science, Charles University, Hlavova 2030, 128 00 Prague, Czech Republic

[c]Department of Biochemistry and Microbiology, Slovak University of Technology, Radlinského 9, 812 37 Bratislava, Slovak Republic

[d]Department of Pharmacology, Faculty of Medicine, Pavol Jozef Šafárik University in Košice, Trieda SNP 1, 040 11 Kosice, Slovak Republic

[e]Department of Microbiology and Immunology, University of Veterinary Medicine and Pharmacy, Komenského 73, 041 81 Kosice, Slovak Republic

*zuzana.vargova@upjs.sk

For the second year in a row, humanity has been facing the pandemic caused by COVID-19 disease. The fact that this pandemic causes a huge loss of life is a direct impact of the activity of this strain of viruses. As healthcare has focused on addressing the current situation, many treatment processes have been delayed. Thus, it is natural that after two years, patients with various advanced infectious and cancerous diseases are beginning to appear in hospitals and outpatient clinics. This fact leads to the requirement for scientists to work intensively on the development of effective and selective antimicrobials and anticancer drugs. For this purpose, it is important to know what natural mechanisms the immune system in our organisms uses and to find approaches to help support this system.

All organisms, from bacteria to mammals, produce substances that they use to protect themselves against pathogens [1]. A vast majority of them are antimicrobial peptides (AMP) with short amino acid sequences, whose primarily function is protection against a wide spectrum of pathogens [2].

One of the ideas to help the immune system in acute infectious conditions is to combine antimicrobial metal ions (Ag^{+}, Zn^{2+}, Cu^{2+}) with effective organic ligands that are similar in structure and properties to antimicrobial peptides. Based on this, we have recently focused on ligands such as amino acids or on ligands that are part of biostructures, for example nicotinamide, pyridinecarboxylates. We found that silver(I) complexes of AgGly, AgAla and AgNam with ionic structure show higher AMB (antimicrobial) activity than neutral AgPhe complex, indicating that the cationic part of the structure may interact with negatively charged components of the cell membrane (Figure 1) [3, 4]. At the same time, we found that these ionic complexes are more effective against selected cancer cells than mentioned neutral complex. The contribution will focus on the antimicrobial and anticancer effects of selected silver(I) complexes prepared in our laboratory with emphasis on the relationship between their structure and biological activity.

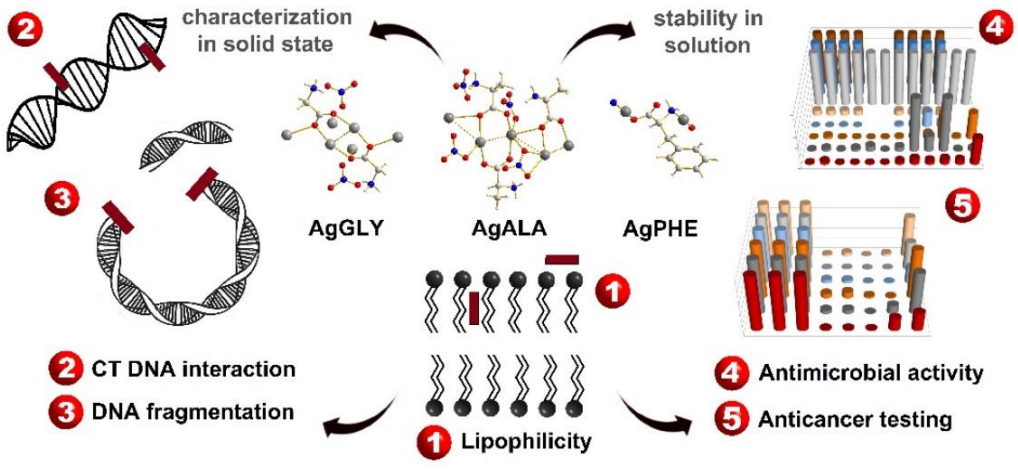

Figure 1 Biological properties of AgGly, AgAla and AgPhe complexes.

Acknowledgements

This work was supported by the grant of UPJŠ (VVGS 2020 1408), the Grant Agency of Ministry of the Education, Science, Research and Sport of the Slovak Republic (VEGA 1/0016/18, 1/0138/20, 1/0653/19, 1/0697/18).

References

[1] A. L. Tornesello, A. Borrelli, L. Buonaguro, F. M. Buonaguro, M. L. Tornesello, Molecules **25** (2020) 2850.
[2] N. Raheem, S. K. Straus, Front. Microbiol. **10** (2019) 2866.
[3] G. Kuzderová, M. Rendošová, R. Gyepes, M. Almáši, D. Sabolová, M. Vilková, P. Olejníková, D. Hudecová, M. Kello, Z. Vargová, J. Inorg. Biochem. **210** (2020) 111170.
[4] M. Rendošová, Z. Vargová, J. Kuchár, D. Sabolová, Š. Levoča, J. Kudláčová, H. Paulíková, D. Hudecová, V. Helebrandtová, M. Almáši, M. Vilková, M. Dušek, D. Bobáľová, J. Inorg. Biochem. **168** (2017) 1–12.

Formative Assessment in Teaching Science, Mathematics, and Informatics

M. Ganajová[a]*, I. Sotáková[a]
[a]Department of Didactics of Chemistry, Institute of Chemistry, Faculty of Science, Pavol Jozef Šafárik University in Košice, Moyzesova 11, 040 01 Košice, Slovak Republic
*maria.ganajova@upjs.sk

In the Slovak educational system, summative assessment prevails. The OECD evaluation team has brought attention to the need to improve students' understanding by using formative assessment [1].
Formative assessment is based on regular and interactive evaluation of students' work, it provides feedback on their learning in terms of the specified goals and indicates what the next steps in teaching should be [2].
The paper informs about the recently published monograph entitled *Formatívne hodnotenie vo výučbe prírodných vied, matematiky a informatiky (Formative Assessment in Teaching Science, Mathematics, and Informatics)* [3], which aims to disseminate the knowledge about theoretical, practical (application), and research aspects of formative assessment. It offers a complex insight into formative assessment in terms of historical development, characteristics, efficacy, pros and cons, implementation and monitoring, and feedback for students.
The monograph provides information about formative assessment strategies and tools useful in teaching science (biology, chemistry, physics), mathematics, and informatics at primary and secondary schools. It summarises research aimed at the verification of formative assessment efficacy. The results have shown that formative assessment develops conceptual understanding, scientific skills, and the skills necessary to successfully enter the labour market in the 21st century [4, 5].
However, Slovakia is still waiting for systematic and careful implementation of formative assessment in teaching. The presented monograph offers knowledge and experience, which can be used as a starting point for implementation of formative assessment in teaching at all levels of education and potentially also in the case of non-science subjects.
This is the first monograph of its kind in Slovakia to provide the readers with a framework to navigate the formative aspects of assessment. Hopefully, it will contribute to the development of subject didactics, general didactics, and pedagogy.

Acknowledgements

This work was supported by the VEGA No. 1/0265/17 "Formative Assessment in Natural Sciences, Mathematics and Informatics" and KEGA No. 004UPJŠ-4/2020 "Creation, Implementation, and Verification of the Effectiveness of Digital Library with the Formative Assessment Tools for the Natural Sciences, Mathematics and Informatics at the Elementary School" grants.

References

[1] C. Shewbridge, J. Van Bruggen, D. Nusche, P. Wright, *OECD Reviews of Evaluation and Assessment in Education: Slovak Republic 2014*. OECD Publishing.
[2] D. Wiliam, *What is Assessment for Learning.* Stud. Educ. Evaluation, **37** (2011) 3-14.
[3] M. Ganajová, B. Brestenská, J. Guniš, Z. Ješková, M. Kireš, A. Lešková, S. Lukáč, R. Orosová, I. Sotáková, K. Szarka, Ľ. Šnajder, *Formatívne hodnotenie vo výučbe prírodných vied, matematiky a informatiky*. 1. vyd. UPJŠ v Košiciach Vydavateľstvo ŠafárikPress, 2021.
[4] M. Babinčáková, M. Ganajová, I. Sotáková, P. Bernard, *Influence of Formative Assessment Classroom Techniques (FACTs) on Student's Outcomes in Chemistry at Secondary School*. J. Balt. Sci. Educ. **19** (2020) 36-49.
[5] M. Ganajová, I. Sotáková, S. Lukáč, Z. Ješková, V. Jurková, R. Orosová, *Formative Assessment as a Tool to Enhance the Development of Inquiry Skills in Science Education.* J. Balt. Sci. Educ. **20** (2021) 204-222.

HPLC Separation Using Cyclofructan Chiral Selectors

F. Dugas[a], T. Gondová[a]*
[a]Department of Analytical Chemistry, Institute of Chemistry, Faculty of Science, Pavol Jozef Šafárik University in Košice, Moyzesova 11, 040 01 Košice, Slovak Republic
*tatana.gondova@upjs.sk

High-performance liquid chromatography (HPLC) using chiral stationary phases is the most frequently used method for the separation of chiral compounds of biological and pharmacological importance. Direct HPLC separations of enantiomers are based on the application of various chiral selectors (and the chiral stationary phases made of them) such as amino acids, proteins, derivatized polysaccharides, cyclodextrins, cyclofructans, crown ethers, macrocyclic antibiotics and others.

Cyclofructans (CF) are unique group of chiral selectors. They are the macrocyclic oligosaccharides containing of six (CF6) or more β(2→1)-linked D-fructofuranose units. While native cyclofructans showed limited enantioselectivity, derivatized with aliphatic or aromatic functional groups possesed high degree of chiral resolution towards a variety of racemic compounds. The main advantages are their high loadability and versatility as they are able to enantioseparate neutral, acidic and basic analytes [1].

Aim of the work was to develop direct, simple and rapid enantioselective liquid chromatographic method for separation of racemic compound of pharmaceutical relevance using cyclofructans-based chiral stationary phases under various LC conditions and modes.

References

[1] J. Teixeira, M. E. Tiritan, M. M. M. Pinto, C. Fernandes, Molecules **24** (2019) 865.

Combination of Headspace Microextraction with Optical Probe for Sulfide Determination

A. Skok[a]*, A. Vishnikin[b], Y. Bazel[a]
[a]Department of Analytical Chemistry, Institute of Chemistry, Faculty of Science, Pavol Jozef Šafárik University in Košice, Moyzesova 11, 040 01 Košice, Slovak Republic
[b]Oles Honchar Dnipro National University, Gagarin Avenue 72, 49010, Dnipro, Ukraine
*arina.skok@student.upjs.sk

Comparing to classical analysis conducted in the cuvettes, measurements with the help of optical probe do not require the step of transferring analyte to the cuvette and allow to start recording of analytical signal immediately after start of processes in the studied system, that increases reproducibility and speed of analyses [1]. The optical probe can also be combined with microextraction, which simplifies the measurement procedure and minimizes the volume of solvents required. But now the usage of the optical probe in microextraction is quite limited [2,3]. At the same time, the main disadvantages of such a combination are the complexity of retention of the microdrop in the optical probe and its instability, which creates technical difficulties in the analysis and leads to low values of the accuracy of measurements.

A new approach for headspace micro-extraction combined with optical probe for the sulfide determination is proposed. It solves the problem of extraction phase retention and limitation of its volume and at the same time makes it possible to detect the analytical signal online.

The extraction solvent was kept in a plastic vial, fixed over the analyte solution. Analytical signal was measured with an optical probe immersed in acceptor phase. Determination of ions was based on the release of hydrogen sulfide from the donor phase after the addition of acid, followed by gas absorption of a 5,5`-dithiobis-(2-nitrobenzoic) acid solution. The use of an optical probe allows to reduce and simplify the determination by eliminating the stage of transfer of the extract to the cuvette. In a three-phase system, it is possible to perform rapid online determination of sulfide ions in samples that are cloudy, intensely colored, or contain large amounts of interfering substances. Reproducibility also increases significantly. Developed method has high reproducibility and selectivity and is comparable in sensitivity with other micro-extraction-spectrophotometric methods. The analytical capabilities of the new method were tested on the determination of sulfides in tap water and wine.

Procedure for sulfide determination. 5 mL of the aqueous solution is placed in a 10 mL vial. 200 µL of a 10^{-4} M DTNB solution having a pH 7 (phosphate buffer) are exposed in the headspace of the sample in a plastic vessel in which the optical probe is immersed. 5 mL of 10.00 % H_3PO_4 is added to 5 mL of the analyzed solution and stirred at 1000 rpm for 15 minutes at the room temperature. Recording of analytical signal starts immediately after acid addition. Analytical wavelength was chosen as 412 nm.

The calibration graph for the determination of sulfide is linear in the concentration range from 10^{-6} M to 8×10^{-6} M S^{2-}, the detection limit is 5.63×10^{-7} M (18 µg L^{-1}), the correlation coefficient R^2 - 0.9985. The equation of the calibration graph is $A = 0.05 + 90130 \times C$. The precision of the method in units of relative standard deviation (RSD) is 1.3 % (n=3; P=0.95) for 3.5×10^{-6} M S^{2-}.

The proposed method is highly selective, since there is no direct contact between the donor and acceptor phases. Only nitrite and sulfite ions cause interference effect even in small concentrations (10^{-7} M). In acidic medium nitrite anions can react with sulfide ions preventing its release in the form of hydrogen sulfide to the headspace. Sulfite ions in acidic medium produce SO_2, that also reacts with 5,5`-dithiobis- (2-nitrobenzoic) acid solution. Sulfite ions can be determined first with iodometry and then their impact can be recalculated from the hall absorbance.

References

[1] J. Tóth, Y. Bazeľ, Applied Spectroscopy, **73** (2019) 492-502.
[2] S. Zaruba, A. B. Vishnikin, J. Škrlíková, A. Diuzheva, I. Ozimaničová, V. Andruch, RSC Adv. **7** (2017) 29421-29427.
[3] S. Zaruba, A. B. Vishnikin, J. Škrlíková, V. Andruch, Anal. Chem. **88** (20) (2016) 10296–10300.

ensitive Spectrofluorimetric Determination of Nitrites with Hexacyanine 2 Dye

J. Tóth[a]*, Y. Bazeľ[a]

[a]Department of Analytical Chemistry, Institute of Chemistry, Faculty of Science, Pavol Jozef Šafárik University in Košice, Moyzesova 11, 040 01 Košice, Slovak Republic

*jantoth92@gmail.com

The sensitive kinetic determination of nitrites with spectrofluorimetric detection using Hexacyanine 2 dye is reported here. The nitrites can decompose the dye in an acidic environment that can be used for their determination. During the development of the analytical method, various variables were optimized like the concentration of hydrochloric acid, the concentration of dye, or the temperature of the reaction mixture. Under the optimal reaction conditions, the area under the synchronous spectra of dye was not in linear dependence against the concentration of nitrite. For that reason, a linearization procedure was done in accordance with [1] to ensure a linear calibration curve as shown in Fig. 1-B-2. The developed method was used for the determination of nitrite in water samples. The limit of detection was estimated at 1,54 µg L^{-1}, with a linear calibration curve in the range from 0 up to 20 µg L^{-1} and a relative standard deviation at 3,24 % (n = 5; 10,2 µg L^{-1}).

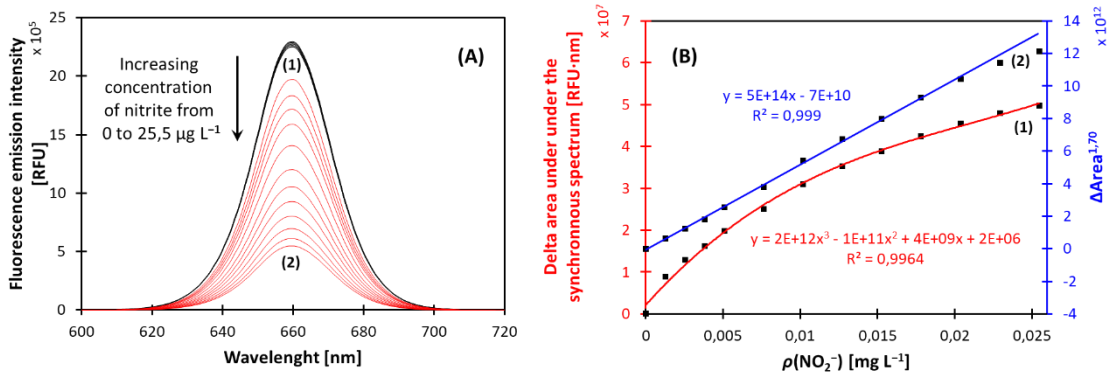

Figure 1 The effect of various nitrite concentration on synchronous spectra of dye (A) where (1) in the absence and (2) in the presence of analyte. The effect of various nitrite concentration on the area under the synchronous spectra (B) where (1) before and (2) after linearization. All results measured under the following conditions: c(HCl) = 0,152 mol L^{-1}; c(DYE) = 0,336 µmol L^{-1}; Temperature = 5 °C; Fixed time = 300 s; Integration limits = 600,5 - 720,5 nm.

References

[1] J. Tóth, Y. Bazeľ, Applied Spectroscopy **73** (2019) 492-502.

Extraction Methods and HPLC Determination of Selected Polyphenols in Slovak Berries

K. Trach[a]*, K. Reiffová[a]
[a]Department of Analytical Chemistry, Institute of Chemistry, Faculty of Science, Pavol Jozef Šafárik University in Košice, Moyzesova 11, 040 01, Košice, Slovak Republic
*kateryna.trach@student.upjs.sk

Polyphenols are secondary metabolites and pharmacoactive substances abundant in numerous plants. They exhibit antioxidant, antineoplastic activity, vaso-cardioprotective effects, and many others. Polyphenols are reported to be biomarkers thus can be used to assess environmental pollution [1]. Considering this, it is necessary to improve available and to investigate better preparation and quantification procedures for the analysis of these compounds. We intend to determine the quantitative composition of polyphenols in plants grown in different sites of Slovak Republic to analyze the correlation between quantities of polyphenolic compounds and the environmental pollution at the vegetation sites. As the object of analysis, we chose berries, which have diverse polyphenolic composition and can be evaluated throughout the territory of Slovakia. Below we present a preliminary literature review on composition, extraction, and analysis methods (see Table 1) in selected berries.

Table 1 Common extraction and determination methods of the polyphenols in berries of interest.

Source, botanical name, composition	
Extraction method details	Determination method
Black Currant, *Ríbes nígrum, Grossulariaceae*	
Phenolic Acids: caffeic; p-coumaric; ferulic; gallic; **Flavonoids:** myricetin; quercetin; kaempherol; **Anthocianins (glycosides):** cyanidin; delphinidin	
Ascorbic acid 50 % methanol and HCl [2]	HPLC UV-Vis, 260 nm - phenolic acids; catechins - 280 nm, hydroxycinnamic acids – 320; 360 nm [2]
1.5 mL of 10 % formic acid and 5 % acetonitrile [3].	HPLC-DAD; 360 nm -flavonols, 320 nm - phenolic acids, 520 nm - anthocyanins [3]
Blueberry, Bilberry, *Vaccinium myrtillus L., Ericaceae*	
Phenolic Acids: chlorogenic; caffeic; p-coumaric; ferulic; **Flavonoids:** myricetin (glycosides); quercetin; **Anthocianins (glycosides):** cyanidin; delphinidin; peonidin; petunidin; malvidin	
UAE, mixture MeOH:H_2O:acetic acid 70:29.5:0.5 [4]	HPLC-MS/MS [4]
Rowanberry, *Sórbus aucupária, Rosaceae*	
Phenolic Acids: neochlorogenic; chlorogenic;cryptochlorogenic; caffeyolshicimic; coumaryoylquinnic; dicaffeoylquinnic; **Flavonoids:** quercetin; rutin; hyperoside; isoquercetrine; **Anthocianins (glycosides):** cyanidin; delphinidin; peonidin; malvidin	
70% aqueous acetone with subsequent SPE (C18 solid phase). Sugars were eluted by HCl [5].	HPLC-DAD-FLD; excitation 280 nm; emission 324 nm [5]
Zymone et al. extracted polyphenols using 70 % ethanol and ultrasonic bath. [6]	HPLC-PDA; phenolic acids – 325 nm; flavonoids– 350 nm; anthocyanins – 535 nm [6]
Elderberry, *Sambucus nigra, Caprifoliaceae*	
Phenolic Acids: 3-4-5-caffeoylquinic; 3-feruloylquinic; p-coumaric; caffeic; 3,4-p-coumaroylquinic; chlorogenic; **Flavonoids:** quercetin; kaemferol; isothamnetin; naringenin; phloridzin; rutin; hyperoside; isoquercetrine; **Anthocianins (glycosides):** cyanidin; pelargonidin	
Extraction with methanol containing 3 % (v/v) formic acid and 1 % (w/v) 6-di-tert-butyl-4-methylphenol (BHT) in a cooled ultrasonic bath. [7]	HPLC-DAD-MS; 234-360 nm [7]

In addition, there is also a universal method. Jakobek et al. [8] analyzed polyphenols in different berries species, including black currant, elderberry, and blueberry. For extraction of flavonol and phenolic acids, a mixture of ascorbic acid, water, methanol, and HCl was used. The compounds were quantified by HPLC-PDA.

In general, described approaches of polyphenols extraction are low-cost simple to carry out, moreover, it is possible to establish a methodology for HPLC UV-Vis determination of the polyphenolic profiles in a greater number of berry plant species and originated products.

References

[1] A. Qayoom Mir, T. Yazdani, S. Ahmad et al., Caspian J. Env. Sci. **7** (2009) 9-16.
[2] S. Hakkinen, S. Karenlampi, I. Heinonen et al., J. Sci. Food Agric. **77** (1998) 543-551.
[3] M. Vagiri, A. Ekholm, S. Andersson et al., J. Agric. Food Chem. **60** (2012) 10501-10510.
[4] L. Kang, K. M. Thakali, G. Jensen et al., Plant Foods Hum. Nutr. **70** (2015) 56-62.
[5] P. Kylli, L. Nohynek, R. Puupponen-Pimia et al., J. Agric. Food Chem. **58** (2010) 11985-11992.
[6] K. Zymone, L. Raudone, R. Raudonis et al., Molecules **23** (2018) 1-117.
[7] M. Mikulic-Petkovsek, A. Ivancic, B. Todorovic et al., J. Food Sci. **80** (2015) C2180-C2190.
[8] L. Jakobek, M. Seruga, I. Novak et al., Dtsch. Lebensmitt. Rundsch. **103** (2007) 369-378.

Evaluation of Methods Suitable for Automated Separation and Determination of Polyphenols

O. Prystopiuk[a]*, K. Trach[a], Y. Bazel[a]
[a]Department of Analytical Chemistry, Institute of Chemistry, Faculty of Science, Pavol Jozef Šafárik University in Košice, Moyzesova 11, 040 01 Košice, Slovak Republic
*oleksandr.prystopiuk@student.upjs.sk

Natural phenolic compounds comprise 10 classes of herbal substances such as phenolic acids, anthocyanidins, flavonols, flavones, lignans, tannins, etc. [1]. These compounds have been extensively studied over decades as important multi-purpose secondary metabolites in plants [2]. Vegetables and fruits rich in phenolic compounds have been noticed to exhibit antioxidant, anti-carcinogenic, and other health-promoting properties [1]. During the last two decades, numerous berry plants, groceries, crops as well as algae [3], and mushrooms [4] have been evaluated as sources of polyphenols for the pharmaceutical and food industry. The spread of circular economy concepts and sustainability awareness in the industry has initiated investigations on the feasibility of commercial extraction of polyphenols from agricultural wastes and by-products [5].

One of the little-studied points on which we would like to focus is a quantification of polyphenols in fresh plant materials performed immediately after collection. To our knowledge, few papers are reporting the composition of phenolic compounds in fresh cultivated or wild-grown plant materials [6, 7]. Besides contributing to fundamental science, knowledge on the composition of polyphenols in a particular plant can be valuable in applied research and agriculture. For instance, qualitative and quantitative composition data can be directly utilized for the commercial evaluation of the plant as a source of specific compounds or the check of its feasibility in plants grown in specific cultivation places. Moreover, phenolic profiles can serve as a fingerprint for the authentification of various commercial products. Finally, such profiles can serve as indirect ecological markers [8], or signs of abiotic stress during the plant vegetation [9].

Among the other polyphenol-rich herbal matrices, berries of black currant (*Ríbes nígrum*), rowan (*Sórbus aucupária*), bilberry (*Vaccinium myrtillus*), and elderberry (*Sambucus nigrum*) have attracted our attention due to following reasons. (1) diverse composition, including phenolic acids, anthocyanins, flavonoids in both free and bound forms present unique challenges in the development of preparation extraction and analysis procedure. (2) well-studied composition investigated in deep-frozen and dried berries; (3) aforementioned berries are consumed as table fruits or in form of functional products in many countries including the Slovak Republic; (4) berries are cultivated industrially and have commercial value as sources of polyphenols; (5) area of vegetation is spread over the territory of the Slovak Republic and nearby countries.

Due to the extreme diversity of polyphenols, there are numerous methods of its separation and analysis. Modern methods that are used for the extraction of berry phenolics among the others comprise classical extraction (CE), microwave-assisted extraction (MAE), ultrasonic-assisted extraction (UAE), dispersive liquid-liquid microextraction (DLLME), solid-phase extraction (SPE). CE is a well-established method widely applied to berries [10]. Acid and alkaline hydrolysis have been introduced CE to release glycosylated and esterified forms respectively. The method described in [11] with modifications [12] can serve as a relevant example of CE applied to berries (see Fig. 1, a). The sequential procedure of alkaline/acidic hydrolysis was the further improvement of CE [13]. For instance, the sequence shown in Fig. 1, c includes alkaline hydrolysis for extraction of esterified polyphenols. However, it has been reported, that plant phenolics are generally undergoing undesirable degradation by extended extraction times [6]. Due to this UAE is used in most of the modern extraction procedures. DLLME is a newer extraction method, which has outperformed CE by reduction of used solvent amounts and short time of extraction. Vortex-assisted DLLME with diluted hydrochloric acid, ethanol, and acrylonitrile was successfully used for the determination of polyphenolic compounds in blueberries [6]. SPE allows to avoid exhaustive manual separation procedure and to separate classes of polyphenols by elution of the solid phase with the proper solvent. In addition, SPE allows eliminating such problems as incomplete phase separation, non-quantitative recovery [10]. Considering berry phenolics, a relevant example of SPE is the extraction of anthocyanins from the crude water extract of five berries (incl. black currant and blueberry) with Amberlite XAD7 (see Fig. 1, b) [14]. Another example is a dispersive SPE used as a separation step before UHPLC-MS-MS analysis of blackberry phenolic composition [15].

Analytical chemistry is capable to offer its vast toolbox of extraction, separation, and analysis methods to acquire the chemical composition in fresh plants. The latter, being combined with geospatial, climate, environmental information, etc. can serve as a good input dataset for obtaining the aforementioned indirect information. If to consider the practical application (e.g. on-site extraction with a portable device) the DLLME and SPE methods are foreseen for further development. They can be performed automatically with a robotic multi-purpose

autosampler (MPS) [16] or portable custom-made autosampler [17]. The latter is a gantry robot similar to those used in fused filament fabrication. It can be built with certain knowledge and based on low-cost components for hobby-grade 3D printers.

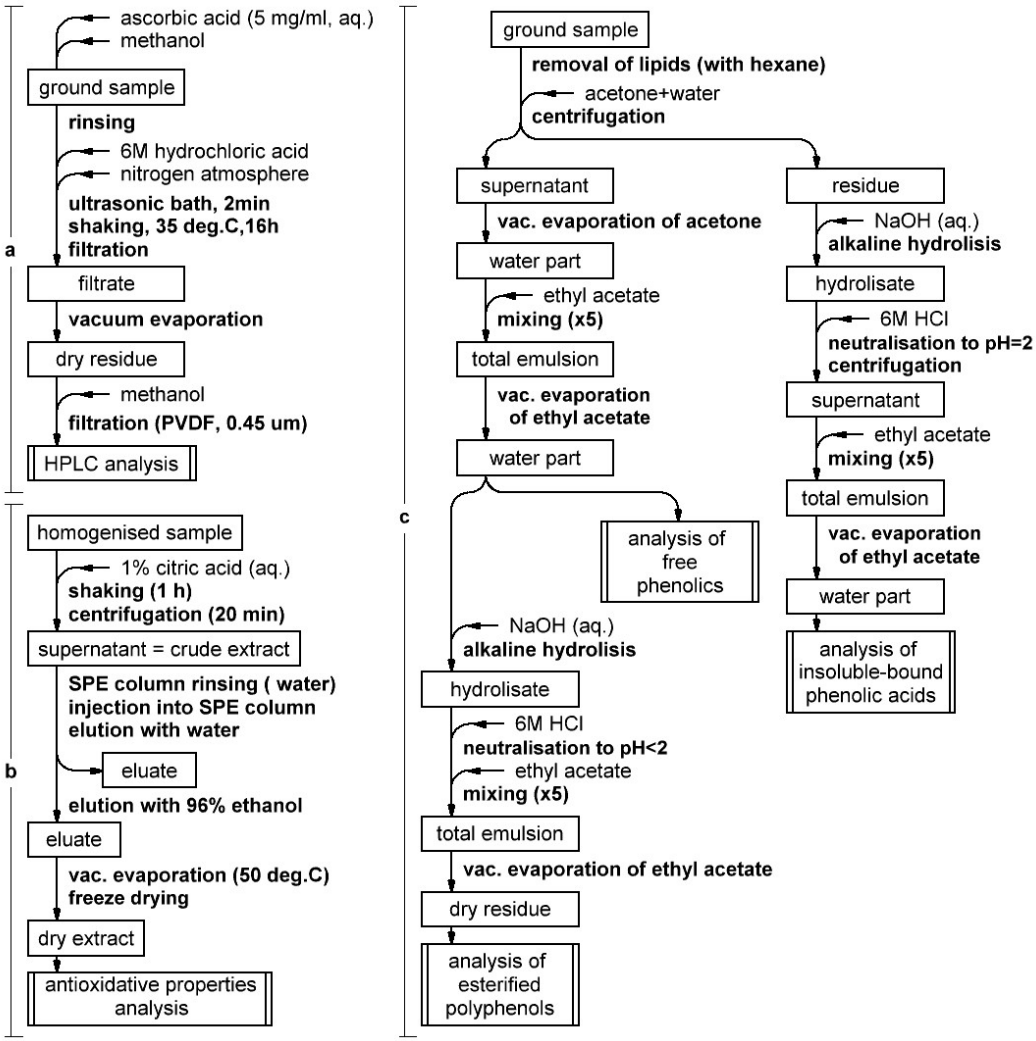

Figure 1 Procedures for the extraction and separation of the phenolic compounds from berries. a) – classical extraction with UAE [11, 12]; b) – solid-phase extraction [14]; c) – CE with sequential hydrolysis [13].

References

[1] J. Câmara, B. Albuquerque, J. Aguiar. Foods **10** (2021) 37.
[2] T. Swain, J. B. Harborne, C. F. Sumere, *Biochemistry of plant phenolics*. New York, Plenum Press. (1979).
[3] M. E. Wekre, K. Kåsin, J. Underhaug, Antioxidants (Basel) **8** (12) (2019) 612.
[4] N. Shomali, O. Onar, T. Alkan, Turk J Pharm Sci. **16** (2) (2019) 155-160.
[5] I. Mourtzinos, A. Goula, *Polyphenols in Agricultural Byproducts and Food Waste*; in *Polyphenols in Plants* (R. R. Watson, ed.), Academic Press, United Kingdom, 2019, pp. 23-44.
[6] Y. Xue, X.-S. Xu, L. Yong. Molecules **23** (2018) 2921.
[7] Zhu, Qin Yan; Zhang, Anqi; Tsang, David, J. Agric. Food Chem. **45** (12) (1997) 4624-4628.
[8] Z. Vaneková, M. Vanek, J. Škvarenina, Plants **9** (2020) 436.
[9] D. Treutter, Int. J. Mol. Sci. **11** (2010) 807-857.
[10] P. Garcia-Salas, A. Morales-Soto, A. Segura-Carretero, Molecules **15** (2010) 8813-8826.
[11] M. Hertog, P. Hollman, D. P. Venema, J. Agric. Food Chem. **40**(9) (1992) 1591-1598.
[12] S. Hakkinen, S. Karenlampi, M. Heinonen, J. Sci. Food. Agric. **77** (1998) 543-551
[13] Karabin, M., Halama, S., Jelinek, L., Kvasný Průmysl, **59** (12) (2013) 346-351.
[14] P. Denev, M. Ciz, G. Ambrozova, Food Chemistry **123** (4) (2010) 1055-1061.
[15] C. A. Rodrigues, A. E. Nicácio, J. S. Boeing, Food Chemistry **309** (2020) 0308-8146.
[16] S. Dugheri, G. Marrubini, N. Mucci, Acta Chromatographica **33** (2) (2021) 99-111.
[17] A. Hartmann, M. Luetscher, R. Wachter, Hydrol. Earth Syst. Sci. Discuss. **22** (8) (2018) 4281-4293.

Use of Infrared Spectrometry for Identification of Substances after their Separation by Liquid Chromatography

D. Pavelek[a]*, R. Halko[a]
[a]Comenius University in Bratislava, Faculty of Natural Sciences, Department of Analytical Chemistry, Mlynská dolina, Ilkovičova 6, 842 15 Bratislava 4, Slovak Republic
*pavelek7@uniba.sk

Introduction

Infrared spectrometry with Fourier transformation (FTIR) is one of the non-destructive optical methods that uses the infrared area of the electromagnetic spectrum to interact with molecules of substances. Infrared radiation has a longer wavelength and lower frequency than radiation than a visible spectrum region. The combination of liquid chromatography (LC) and FTIR may be very useful when specific detection or identification of separated compounds is required. [1] The benefit of FTIR to LC is in rapid and cheap identification of individual separate components of the mixture and the benefit of LC to FTIR is separation of the individual components of the mixture. The combination of LC with FTIR is not in such advanced stage development such as a combination of gas chromatography (GC) with FTIR due to several problems such as absorption of infrared (IR) radiation by mobile phase. [2,3] Because of this basic incompatibility, the combination of LC and FTIR is the subject of research more than twenty-five years. All mobile phases used in the LC absorb IR radiation with certain wavelengths, and whereas the mobile phase is present in a much higher concentration as sample components. The spectrum of samples can only be obtained in the range of spectrum without the absorption strips of the solvent (IR spectrum of mobile phase overlap the IR spectrum of samples). [3-5] The solution to this problem can be implemented in two ways:

1. The first is the use of a flow cell through which the eluent passes from the LC column, while continuously in FTIR records the IR spectrum. [2,6]
2. The second method works on the principle of eliminations of LC solvents prior to IR detection by interface that evaporates eluent and stores analytes to substrate. [7]

Experimental part

Chemicals: Deionized water prepared by Water for PS (Labconco, USA); Ethanol, Merck (Darmstadt, Germany); Caffeine, Sigma-Aldrich (China); Citric acid, Merck (Bratislava, Slovakia); L(+)-Ascorbic acid, Merck (Prague, Czech Republic); L(+)-tartaric acid, Merck (Bratislava, Slovakia); R-amygdalin BioXtra ≥97 % (HPLC) was obtained from Sigma Aldrich (St. Louis, USA); Vitamin B17 Amygdalin, Profivit (Slovakia); Vitamin D3, Cholecalciferol Profivit (Slovakia); Methanol 99 % for gradient elution, Merck (Darmstadt, Germany); Acetonitrile 99 % for gradient elution, Honeywell (Seezle, Germany); Lactic acid, Sigma-Aldrich (Japan); 85 % Formic acid, Merck (Darmstadt, Germany); Acetic acid 100 %, Merck (Darmstadt, Germany); Phosphoric acid 85 %, Merck (Czech Republic); Ammonium formate, Sigma-Aldrich (India); Ammonium acetate, Sigma-Aldrich (India); Ammonium dihydrogen phosphate, Merck (Darmstadt, Germany); Potassium bromide, Lachema (Brno, Czech); Nutrition Supplements Cytosan nutrition and Cytosan Inovum, ENERGY GROUP (Prague, Czech Republic).

Potassium bromide (KBr) tablet preparation: For measuring sample in KBr tablets, we used a KBR powder. Weight of KBr was 400 mg. After weighting, the KBr was dried to 100 °C. Weight of samples were 0.5 %, 1 % and 2 % to total weight of KBr. Then a sample and KBr were crushed and mixed together well. Thus, from mixture of samples and KBr, tablet was prepared by using a press and ready for analysis.

Preparation of solutions

Determination of the limit of detection of various analytes using IR spectrometry with transflective (R-A) technique: we prepared stock aqueous solutions from caffeine, citric acid, L(+)-ascorbic acid, L(+)-tartaric acid and amygdalin to 100 ml of a volumetric flask with a concentration of 1 mmol L^{-1}. Subsequently, we diluted them to a concentration of 0.1 and 0.5 mmol L^{-1}.

Study of influence of solutions on infrared spectrum of analytes using IR spectrometry with R-A technique: Mobile phases were prepared as mixtures: water : methanol, water : ethanol, water : lactic acid and water : acetonitrile in ratio 40 % : 60 %. At the same time, a stock solution of L(+)-ascorbic acid was prepared with concentration of 10 mmol L^{-1}. The fractions of the L(+)-ascorbic acid were diluted to mobile phases with concentration of 1 mmol L^{-1} and 0.1 mmol L^{-1}.

Study of influence of buffers on infrared spectrum of analytes using IR spectrometry with R-A technique: Three different buffers were prepared, which composed of weak acid and its salt: formic acid and ammonium formate, acetic acid and ammonium acetate and phosphoric acid and ammonium dihydrogen phosphate with concentration

of 10 mmol L^{-1}. The pH of buffer solutions were adjusted by using their appropriate acid. Mobile phases were consisted of methanol and prepared buffers in ratio 60:40. A stock solution of L(+)-ascorbic acid was prepared with concentration of 10 mmol L^{-1}. The fractions of the L(+)-ascorbic acid were diluted to mobile phases with concentration of 1 mmol L^{-1}.

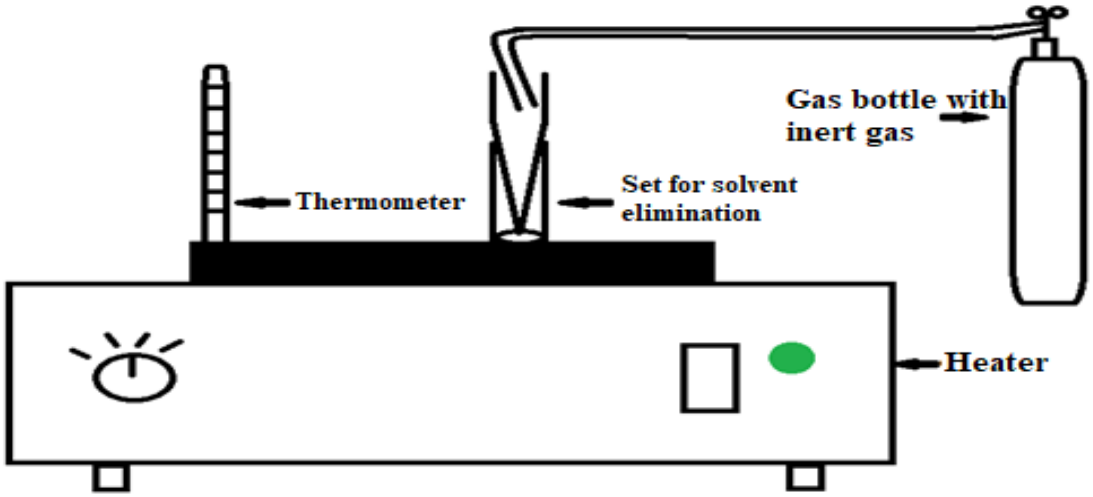

Figure 1 Scheme of apparatus for solvent elimination method.

Results and discussion

Study of influence of the surface of the R-A substrate material on the infrared spectrum: The first step of our experimental work was to study of influence of R-A substrate on IR spectrum obtained by IR spectrometry with R-A technique. Used materials selected as R-A substrates were stainless steel sheet, crystal of germanium, zinc selenide (ZnSe) crystal, silver plate, aluminum plane, polished gold layer, aluminum foil, metal layer on glass, and a piece of glossy polymer. From measured values of intensities of radiation falling on detector was chosen glossy and polished materials, that the most reflect the IR radiation as aluminum foil, silver plate, stainless steel sheet and polished gold layer. In the second part of this study, we were monitoring changes on the IR spectrums of caffeine measured on selected R-A substrates: silver plate, germanium crystal, aluminum foil, polished gold layer and stainless steel sheet. The most suitable R-A substrate in our case of caffeine analysis was aluminum foil and then germanium crystal. The choice of R-A substrate depends mainly on their physical properties such as its structure, smooth surface, etc. Surface irregularity and its deformation can bring the poor quality of measured IR spectrum. By cleaning the surface of R-A substrate from impurities or its careless treatment we can cause these shortcomings. In the selection of R-A substrate, we must also take care of the factors in the sample adjustment, for example the type of used solvent, the pH of the solvents and buffers, the temperature, the parameters used in the separation of the individual components of the mixture by separation methods and used solvent elimination method. In the third part of this study, we compared the quality of the IR spectrum of selected two samples of Cytosan Ivonum and Cytosan prepared by the solvent elimination method and KBr tablet method. In the solvent elimination method, we skipped the step of separating the individual components of the sample mixture and immediately passed (after dissolving the sample) to the solvent elimination step. Differences between the IR spectrum of samples prepared by both mentioned methods had minimal differences between themselves.

Determination of the limit of detection of various analytes using IR spectrometry with R-A technique: In this section, we have determined the limit of detection of various analytes with IR spectrometry with R-A technique - We determined the smallest detectable amount of sample. The aqueous solutions were gradually dosed into a pre-produced set for solvent elimination with a nitrogen stream and a temperature on the aluminum foil as R-A substrate with volume of 0.5; 1; 5; 10; 20; 30 µl. The heater, when the solvents was evaporating, was set to 100 ° C but the real heating temperature read from the thermometer was 82 ° C. After drying the sample, the IR analyte spectrum was recorded in reflection mode R-A technique. After all measurements, we have determined the smallest quantities of each sample that could be detected, according to the quality of the IR spectrum.

Studying the influence of different solvents on the infrared spectrum of analytes using IR spectrometry with R-A technique: In this section we have studied the impact of various composition of mobile phases commonly used in the LC on IR spectrum of analytes. At combination of reverse-phase high performance liquid chromatography (RP-HPLC) with IR spectrometry, suitable polar solvents with low boiling point should be selected. The solvent must be perfectly eliminated - analyte must be dry, as polar solvents exhibit their characteristic absorption strips in IR spectrum. Selected mobile phases that were applicable for separation of the analytes were water : methanol

and water : acetonitrile, thanks to their low boiling points and purity. Pollution of mobile phase water : ethanol was high, which was also reflected on the quality of the IR spectrum of measured analyte. A similar problem was at mobile phase water : lactic acid, where elimination of solvent water : lactic acid was deteriorated by the high boiling point of the lactic acid, which was not properly evaporated and was degrading the IR spectrum of analyte.

Study of influence of buffers on infrared spectrum of analytes using IR spectrometry with R-A technique: In this section, we studied the impact of different buffers on IR spectrum of analytes. Problems with buffer in combination of LC and IR spectrometry is that in the solvent elimination are mostly formed salt crystals derived from buffering solutions, where a weak acid, optionally a weak base is evaporated due to their low boiling points. These created salt crystals can leave their characteristic absorption strips in the IR spectrum of analyte and cover characteristic absorption strips of measured analyte because they also absorb IR radiation. Ammonium acetate and ammonium formate left a few characteristic absorption strips in IR spectrum of analyte, but IR spectrum of ammonium dihydrogen phosphate has covered a whole IR spectrum of analyte.

Qualitative Analysis: In a qualitative analysis, we have used all previously performed studies and applied them on analysis selected commercial nutritional samples by using an off-line combination of LC and IR spectrometry. From the nutritional samples of amygdalin, cholecalciferol and Cytosan, we have managed to separate selected fractions, eliminate their solvent and measure IR spectrums. From mixture of four analytes caffeine, L(+)-ascorbic acid, L(+)-tartaric acid and amygdalin, we have also managed to obtain individual fractions, where solvent was eliminated and IR spectrums were measured.

Conclusion

Method RP-HPLC-FTIR managed to be optimized for multi-component samples analysis by using performed studies and experiments.

Acknowledgement

This work was supported by the Scientific Grant Agency of the Ministry of Education of the Slovak Republic, VEGA no. 1/0678/19 and the Slovak Research and Development Agency (APVV-17-0373).

References

[1] G.W. Somsen, C. Gooijer, U. A. Brinkman, J. Chromatography A **856**(1-2) (1999).
[2] C. Fujimoto, G. Uematsu, K. Jinno, Chromatographia **20** (1985) 112-116.
[3] C. Fujimoto, T. Oosuka, K. Jinno, Anal. Chim. Acta **178** (1985) 159-167.
[4] J. C. Jones, D. Littlejohn, P. R. Griffiths, Appl. Spectroscopy **53**, 7 (1999) 792-799.
[5] S. D. Taylor, *In-line combination of LC with MS, NMR, UV and IR in drug analysis*, Doctoral Thesis, Sheffield Hallam University (United Kingdom), 2007.
[6] K. Jinno, C. Fujimoto, J. Chromatography A, **506** (1990) 443-460.
[7] C. D. Tran, G. Huang, V. I. Grishko, Anal. Chim. Acta **299** (1995) 361-369.

Isolation of Anabolic Androgenic Steroids from Oil-Based Samples

B. Benická[a*], E. Kupcová[a]
[a]Matej Bel University in Banská Bystrica, Faculty of Natural Sciences, Department of Chemistry,
Tajovského 40, 974 01 Banská Bystrica, Slovak Republic
*barbora.benicka@umb.sk

Anabolic androgenic steroids (AAS), synthetic derivatives of testosterone, are widely used by athletes owing to their muscle-building and performance-enhancing effects. Since AAS are prohibited substances, they are commonly available mostly on the black market. AAS are popular not only within the recreational athlete community, but their abuse is common in professional sport as well, making AAS one of the most frequently analyzed doping substances in the world, according to the World Anti-Doping Agency (WADA). Therefore, analytical methods providing rapid, sensitive and reliable determination of these substances in different types of matrices are developed.

This work describes an analytical method for simultaneous determination of four testosterone derivatives (testosterone propionate, testosterone phenylpropionate, testosterone isocaproate and testosterone decanoate) in an oil-based injectable dosage form. However, this kind of sample presents a challenge in the analysis of AAS and, therefore, a different approach to their isolation from such matrices was tested. Chromatographis analysis (HPLC-DAD) [1,2] was used to evaluate the efficiency of the extraction process.

References

[1] P. Kozlík, B. Tirčová, Steroids **115** (2016) 34-39.
[2] B. Tirčová, Z. Bosáková, P. Kozlík, Drug Test. Anal. **11** (2019) 355-360.

Determination of Benzodiazepines in Alcoholic Beverages Using Microextraction Technique Coupled with HPLC/DAD

A. Várfalvyová[a, b]*, E. Kupcová[a]
[a]Department of Chemistry, Faculty of Natural Sciences, Matej Bel University in Banská Bystrica, Tajovského 40, 974 01 Banská Bystrica, Slovak Republic
[a]Department of Analytical Chemistry, Institute of Chemistry, Faculty of Science, Pavol Jozef Šafárik University in Košice, Moyzesova 11, 040 01 Košice, Slovak Republic
*alica.varfalvyova@student.upjs.sk

Abstract
Benzodiazepines are a class of psychoactive drugs often used in drug facilitated crimes, especially robberies or rapes, making it important to develop sensitive and accurate methods for their determination. A new microextraction protocol was tested for the isolation of four benzodiazepines (alprazolam, bromazepam, diazepam, oxazepam) from alcoholic beverages which are the most common way of reaching the unaware victim. A simple and rapid extraction process was studied and tested, using 1 ml of sample, 100 µL of chloroform as an extraction solvent and 100 µL of acetone as a dispersive solvent. The extraction efficiency, ranging from 4 to 92 %, was evaluated by high performance liquid chromatography with diode array detection (HPLC/DAD) which was linear within the concentration range 1 – 250 mg/L and providing LODs from 0.02 to 6.60 µg/L for analyzed compounds.

Key words
Alcoholic beverages, benzodiazepines, diode array detection, high-performace liquid chromatograpgy, microextraction.

Hydrogen Peroxide Modification of Cytochrome c Trigger Protein Fast Degradation

N. Tomášková[a]*, P. Novák[c], T. Kožár[b], G. Yassaghi[c], P. Man[c], E. Sedlák[a, b]
[a]Department of Biochemistry, Institute of Chemistry, Faculty of Science, Pavol Jozef Šafárik University in Košice, Moyzesova 11, 040 01 Košice, Slovak Republic
[b]Center for Interdisciplinary Biosciences, Pavol Jozef Šafárik University in Košice, Jesenná 5, 041 54 Košice, Slovak Republic
[c]Institute of Microbiology - BioCeV, Vídeňská 1083, 142 20 Prague 4, Czech Republic
*natasa.tomaskova@upjs.sk

Cytochrome c (cyt c) is a small globular water-soluble mitochondrial protein with numerous functions in cells [1]. Out of its multiple interactions and functions, the two most intensively studied physiological functions are: (i) electron transfer in connection with its canonical function as an electron shuffle between Complex III and Complex IV in mitochondrial respiration and (ii) peroxidase activity in relation to preapoptotic events [2]. Mammalian cyt c consists of 104 amino acid residues (MW approximately 12 kDa) and contains one c-type heme prosthetic group, with six-coordinated iron, covalently attached to its polypeptide chain via two thioether bonds to cysteine residues [3]. Covalent attachment of heme group to polypeptide chain is typical only for mammalian peroxidases and type c cytochromes.

Classical peroxidases contain a five-coordinated heme, with the sixth site vacant, which is an inevitable feature for accessibility of the active site to substrate. Therefore, it has been puzzling for a long time how can cyt c have peroxidase-like activity with the six-coordinated heme iron. Findings obtained from cyt c mutational studies and from cyt c cardiolipin interaction studies, mimicking a situation in the intermembrane space in mitochondria, indicate that peroxidase-like activity is triggered by a conformational transition or increased dynamics leading to an increased fraction of five-coordinated species of cyt c [4]. Recently, an appealing proposal has been brought forward suggesting that cyt c self-activates its peroxidase-like activity by H_2O_2-triggered covalent modification at early steps of reaction with H_2O_2 [5]. This activation of the pre-catalytic native state can be considered, paradoxically, as the first stage of inactivation of cyt c, comparable to suicide inactivation processes typical for classical peroxidases [5].

In the current study, mass spectrometry analysis enabled us to detect the first-hit modifications of cyt c in the interaction with hydrogen peroxide. This detection points out likely a major pathway of radical transfer through the polypeptide chain from heme region to the protein surface. We suggest that the pathway Met80-Tyr67-Tyr74 for the radical transfer from heme region to the protein surface has a protective function for the active site of cyt c. We also explored an existence of protein channels connecting the heme iron with the protein surface. Locations of the channels suggest which amino acids in cyt c are mostly exposed to reactive oxidants (mostly superoxide anion radicals) originated at the heme region and thus prone to covalent modifications. Our findings concerning peroxidase-like activity, thermal stability, and mass spectrometry analyses of cyt c incubated with H_2O_2 support a model of cyt c reaction with H_2O_2 proposed by Yin et al. [6]. An existence of two major populations of cyt c clearly indicates that the oxidation/carbonylation of critical residues of cyt c leads to an efficient self-destruction of this protein by its increased peroxidase-like activity.

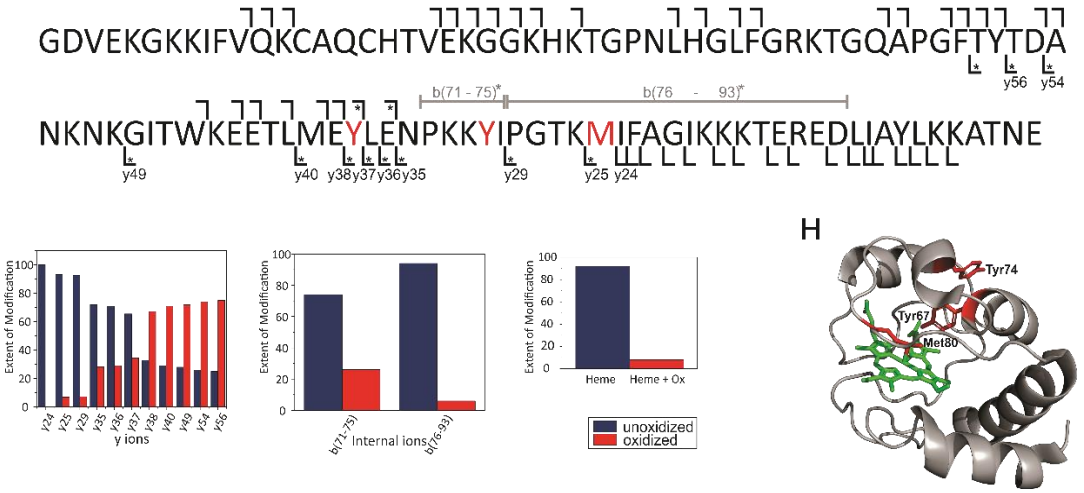

Figure 1 Top-down MS analysis of singly oxidized cyt *c* after treatment with 3 mM peroxide for 10 min.

Acknowledgements

This work was supported by the research grants provided by Slovak Research and Development Agency grant APVV 15-0069, the the Slovak Grant Agency VEGA no. 2/0009/17, and support under the Operational Program Integrated Infrastructure for the project Open Scientific Community for Modern Interdisciplinary Research in Medicine (OPENMED), grant 731077.

References

[1] D. Alvarez-Paggi, L. Hannibal, M. A. Castro, S. Oviedo-Rouco, V. Demicheli, V. Tortora, F. Tomasina, R. Radi, D. H. Murgida, Chem. Rev. **117** (2017)13382-13460.
[2] V. E. Kagan, V. A. Tyurin, J. Jiang, Y. Y. Tyurina, V. B. Ritov, A. A. Amoscato, A. N. Osipov, N. A. Belikova, A. A. Kapralov, V. Kini, I. I. Vlasova, Q. Zhao, M. Zou, P. Di, D. A. Svistunenko, I. V. Kurnikov, G. G. Borisenko, Nat. Chem. Biol. **1** (2005) 223–232.
[3] S. Zaidi, M. I. Hassan, A. Islam, F. Ahmad, Cell. Mol. Life Sci. **71** (2014) 229–255.
[4] N. Tomášková, R. Varhač, V. Lysáková, A. Musatov, E. Sedlák, Biochim. Biophys. Acta, Proteins Proteomics **1866** (2018) 1073-1083.
[5] B. Valderrama, M. Ayala, R. Vazquez-Duhalt, Chem. Biol. **9** (2002) 555–565.
[6] V. Yin, G. S. Shaw, L. Konermann, J. Am. Chem. Soc. **139** (2017) 15701–15709.

Synthesis of Novel 7-Hydroxy-2-Oxo-2*H*-4-Chromenyl Metal Chelators

A. Gucký[a]*, S. Hamuľaková[b], M. Kožurková[a]
[a]Department of Biochemistry, Institute of Chemistry, Faculty of Science, Pavol Jozef Šafárik University in Košice, Moyzesova 11, 040 01 Košice, Slovak Republic
[b]Department of Organic Chemistry, Institute of Chemistry, Faculty of Science, Pavol Jozef Šafárik University in Košice, Moyzesova 11, 040 01 Košice, Slovak Republic
*adrian.gucky@student.upjs.sk

Metal ions are essential for countless physiological processes occurring in the human body, as well as for the development and normal functioning of the brain. Dyshomeostasis of biometal ions, especially iron, copper and zinc, may, however, lead to the development of neurodegenerative disorders, such as Alzheimer's disease (AD) [1]. Metal ion chelation is therefore one of many potential therapeutic strategies against AD. In this context, numerous natural and synthetic compounds have been tested for their chelation properties so far [2]. Considering the complex and multifactorial nature of the disease, it is advantageous for potential drug candidates to target as many aspects of the neurodegenerative process as possible. Differently substituted coumarin derivatives exhibit a broad range of beneficial effects, such as antimicrobial, antioxidative, anti-inflammatory properties, as well as the ability to inhibit cholinesterases and monoamine oxidases [3]. Coumarin is therefore a desirable scaffold when considering the design of novel anti-Alzheimer therapeutics.

In our research, we have designed and synthesized three series of potential metal chelators **3a-c**, **4a-c** and **5a-d**, all of which contain the 7-hydroxy-2-oxo-2*H*-4-chromenyl moiety in their structure (Fig. 1). The key synthon **1** was submitted to an addition-elimination reaction with the corresponding dihydroxybenzaldehyde or trihydroxybenzaldehyde to afford target compounds **3a-c** and **4a-c** respectively, before being further modified into the thiosemicarbazide **2** *via* an addition reaction with phenyl isothiocyanate. Coumarin derivatives **5a-d** were obtained in a one-pot reaction of the intermediate **2** with the corresponding dihydroxybenzaldehyde and chloroacetyl chloride.

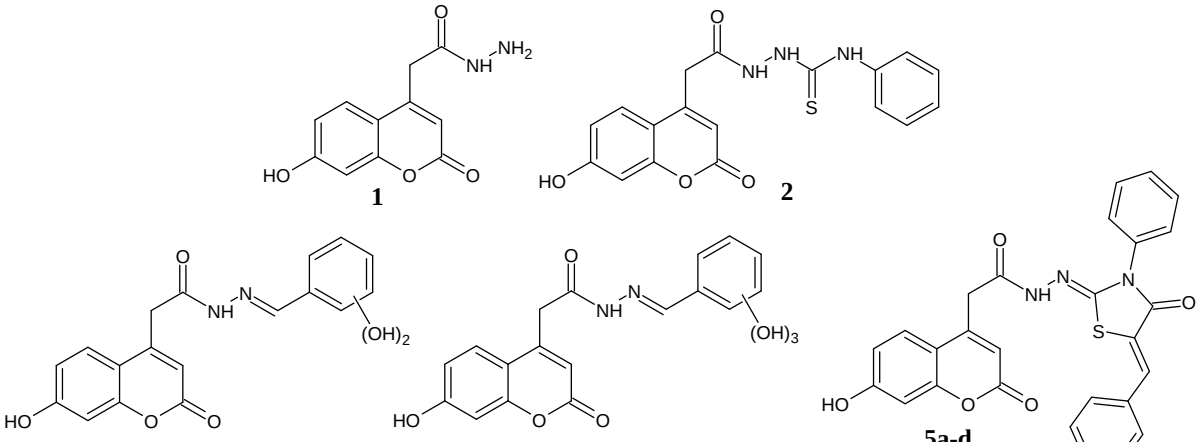

Figure 1 Chemical structure of key intermediates **1-2** and the newly synthesized derivatives **3a-c**, **4a-c** and **5a-d**.

Acknowledgements

The present work was supported by VEGA Grant no. 1/0760/20 and 1/00016/18.

References

[1] J. A. Duce, A. I. Bush, Prog. Neurobiol. **92** (2010) 1-18.
[2] G. J. Yang, H. Liu, D. L. Ma, C. H. Leung, J. Biol. Inorg. Chem. **24** (2019) 1159-1170.
[3] A. Stefanachi, F. Leonetti, L. Pisani, M. Catto, A. Carotti, Molecules **23** (2018) 250.

Topoisomerase Inhibitory Potential of 3,9-Disubstituted Acridine Derivatives

K. Krochtová[a]*, L. Janovec[b], M. Kožurková[a]
[a]Department of Biochemistry, Institute of Chemistry, Faculty of Science, Pavol Jozef Šafárik University in Košice, Moyzesova 11, 040 01 Košice, Slovak Republic
[b]Department of Organic Chemistry, Institute of Chemistry, Faculty of Science, Pavol Jozef Šafárik University in Košice, Moyzesova 11, 040 01 Košice, Slovak Republic
*kristina.krochtova@student.upjs.sk

DNA topoisomerases are enzymes involved in solving topological problems of DNA which arise during replication, transcription, recombination and reparation of DNA. In human we distinguish two main types of topoisomerases, topoisomerase I (hTop I) and topoisomerase II (hTop II), which differs by mechanism of action and by number of cleaved DNA strands. Both hTop I and hTop II are targets of current anticancer drugs. [1-3] Compounds with acridine scaffold are widely studied due to many biologically active derivatives of this planar structure. [4,5] It was proved that 3,9-disubstituted acridine derivatives can be used as model molecules for cancer treatment. They also showed antiviral activity coupled with inhibition of topoisomerase II. [6-9] Besides, small group of dual acridine inhibitors of both topoisomerases have been described and the development of new topoisomerase targeted compounds with effect to both types is still an interesting field of study. [10]
The aim of this work was to study impact of selected 3,9-disubstituted acridine derivatives to the topoisomerase I and topoisomerase II. In conclusion, it can be seen that studied derivatives are capable to inhibit activity of both types of topoisomerase enzymes. First we proved that selected compounds don‘t have ability to trigger cleavage of plasmid DNA. Since, the nuclease activity assay was negative for all ligands we were able to conduct assays for topoisomerase I and II. Relaxation assay showed strong inhibitory potential against hTop I where full inhibition was observed at concentration 5 μM in all cases. This inhibitory effect was further study by unwinding assay. According to the results it can be seen that inhibition is caused by binding of ligands to the plasmid DNA instead of direct binding to the topoisomerase I. Moreover, the decatenation assay demonstrated that these molecules can inhibit also hTop IIα. However, in this case we are able to speak just about partial inhibition since even at the concentration 100 μM beside to the catenated form was kinetoplast DNA present also in form of mini circles. For assays for both enzymes the compound with weekest inhibitory effect was molecule with longest chain between acridine and benzene ring and stongest one was ligand with fluoro group at benzene ring with obvious preference for inhibition of topoisomerase I. This work is a strong motivation for further study of 3,9-disubstituted acridine derivatives as dual inhibitors of topoisomerase I and II.

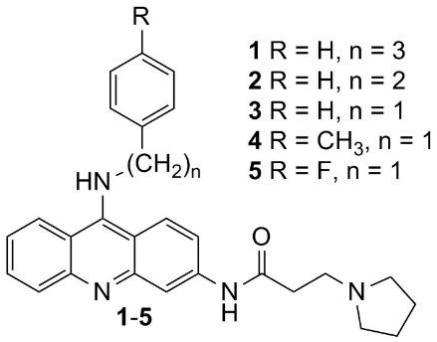

1 R = H, n = 3
2 R = H, n = 2
3 R = H, n = 1
4 R = CH_3, n = 1
5 R = F, n = 1

Figure 1 Structure of studied compounds **1**-**5**.

Acknowledgements

This work was supported by Grant VEGA No. 1/0016/18.

References

[1] Z. Topcu, J. Clin. Pharm. Ther. **26** (2001) 405 – 416.
[2] N. G. Bush, K. Evans-Roberts, A. Maxwell, EcoSal Plus **6** (2015) 1 – 36.
[3] J. L. Delgado, CH.-M. Hsieh, N.-L. Chan, H. Hiasa, Biochem J. **475** (2018) 373 – 398.
[4] M. Demeunynck, Expert Opin. Ther. Pat. **14** (2004) 55 – 70.
[5] M. Gensicka-Kowalewska, G. Cholewiński, K. Dzierbicka, RSC Adv. **7** (2017) 15776 – 15804.

[6] J. R. Goodell, A. A. Madhok, H. Hiasa, D. M. Ferguson, Bioorg. Med. Chem. **14** (2006) 5467 – 5480.
[7] J. R. Goodell, A. V. Ougolkov, H. Hiasa, H. Kaur, R. Remmel, D. D. Biladeau, D. M. Ferguson, J. Med. Chem. **51** (2008) 179 – 182.
[8] Z. Cui, X. Li, L. Li, B. Zhang, Ch. Gao, Y. Chen, Ch. Tan, H. Liu, W. Xie, T. Yang, Y. Jiang, Bioorg. Med. Chem. **24** (2016) 261 - 269.
[9] Q. Zhou, Ch. You, C. Zheng, Y. Gu, H. Gu, R. Zhang, H. Wu, B. Sun, Life Sci. **206** (2018) 1 – 9.
[10] J. Janočková, J. Plšíková, J. Kašpárková, V. Brabec, R. Jendželovský, J. Mikeš, J. Kovaľ, S. Hamuľaková, P. Fedoročko, K. Kuča, M. Kožurková, Eur. J. Pharm. Sci. **76** (2015) 192 – 202.

Extracellular Electron Transport for Reduction of Iron Deposits

J. Olajoš[a]*, R. Sůra[a], M. Antalík[a]
[a]Department of Biochemistry, Institute of Chemistry, Faculty of Science, Pavol Jozef Šafárik University in Košice, Moyzesova 11, 040 01 Košice, Slovak Republic
*jakub.olajos@student.upjs.sk

Except for cytochromes c, there are a large number of other heme proteins, but also other types of proteins that mediate electron transfer either in the respiratory chain but also in other redox processes. Recently, a very important process of extracellular electron transfer has been shown in this direction, which mediates the transfer of reducing sources from inside the cell to its surface and then to sparingly water-soluble rocks that contain iron in oxidation state 3+ (Fe^{3+}). Water-soluble iron salts are one of the bottlenecks for the growth of microorganisms and thus the basic food needs of other organisms, including humans. The low availability of iron for the existence of organisms is associated with the fact that in the oxidizing atmosphere such as exists on Earth, it is oxidized to Fe^{3+}, whose inorganic compounds are significantly less soluble in water than in the case of Fe^{2+} salts. Therefore, knowledge of the processes of external transfer of reducing equivalents outside cells is currently one of the very important scientific tasks that could lead to an efficient source of renewable energies as well as to the reduction of global warming.

Electron transfer from the cytoplasm to the extracellular spaces to reduce ferric oxide minerals requires an ingenious transport system involving low molecular weight substances and multicochemical cytochromes as well as protein aggregates formed from heme proteins that provide this process across the outer cell membrane and outside the cell. In the recent past, much knowledge has been gained to understand the nature of these structures as well as the mechanism by which such electron transfer occurs. Nevertheless, a lot of basic knowledge about these processes as well as the structures of multiheme aggregates is insufficiently researched [1].

The electron exchange reactions that take place between microbial cells and solid materials, referred to as extracellular electron transport (EET), have attracted a great deal of attention in the fields of microbial physiology, microbial ecology and biotechnology. Studies of model species of iron-reducing bacteria such as *Geobacter spp*. and *Shewanella spp*. revealed that redox active proteins, especially cytochromes type c outer membrane (OMC), play a key role in the EET process. Recent metagenomic analyzes have revealed that various microorganisms that have not been shown to have EET ability also contain OMC-like proteins, suggesting that EET via OMC could be more conserved in microorganisms than previously thought [2].

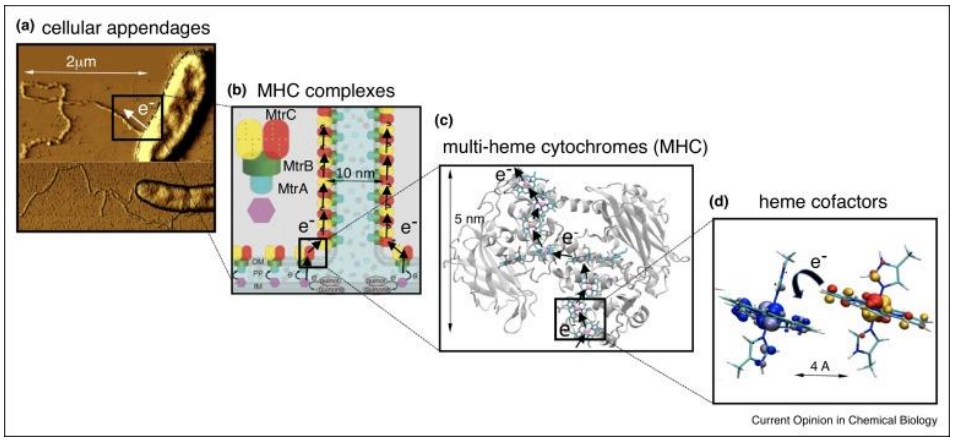

Figure 1 Electron transfer over multiple length scales in the bacterium *Shewanella oneidensis* [3].

Acknowledgements

This work was supported by the Grant Agency of Ministry of the Education, Science, Research and Sport of the Slovak Republic VEGA 1/0138/20.

References

[1] K. Tanaka et al., Frontiers in Microbiology **9** (2018) 1-7.
[2] S. Pirbadian et al., Proceedings of the Nat. Academy of Sci. of the USA **111** (2014) 12883-12888.
[3] J. Blumberger, Current Opinion in Chemical Biology **47** (2018) 24-31.

Interactions of Newly Synthesized Ag(I) Complexes with CT DNA

S. Sovová[a]*, G. Kuzderová[b], D. Sabolová[a]
[a]Department of Biochemistry, Institute of Chemistry, Faculty of Science, Pavol Jozef Šafárik University in Košice, Moyzesova 11, 040 01 Košice, Slovak Republic
[b]Department of Inorganic Chemistry, Institute of Chemistry, Faculty of Science, Pavol Jozef Šafárik University in Košice, Moyzesova 11, 040 01 Košice, Slovak Republic
*simona.sovova@student.upjs.sk

A number of anticancer drugs interact with the molecule DNA directly or prevent the relaxation of DNA due to inhibition of topoisomerases. These drugs are able to work at any phase of the cell cycle, however they are the most effective during DNA synthesis [1]. Drug – DNA interactions can be covalent (irreversible) or non-covalent (reversible). Irreversible binding leads to complete inhibition of DNA function and cell death. Reversible bindings are more desirable comparing to irreversible, considering drug metabolism and potential toxic effects, but also they can disrupt replication or/and transcription, which leads to cellular death [2, 3]. Non-covalent interacting drugs can be classified into intercalators, groove binders (minor-/major-) and external phosphodiester backbone binders [2, 4]. Some of drugs can interact with DNA combining two or more binding modes [4]. When the complex drug – DNA is formed (*via* electrostatic, hydrogen bonds or van der Waals interaction) the drug and the molecule DNA manifest some modifications, which can be determined using spectral methods [2].

This study was focused on silver dipeptide complexes. Silver nanoparticles (AgNPs) have a wide biological effects, such as antibacterial, antiviral, antifungal, anti-inflammatory and anticancer [5, 6]. AgNPs have potential in biomedical applications mainly due to their remarkable antimicrobial activity, low cost and low immunological response [6].

In the present work we have investigated DNA binding activity of newly synthesized silver dipeptide complexes $[Ag(GlyGly)]_n(NO_3)_n$ ***(1)***, $[Ag_2(GlyAla)(NO_3)_2]_n$ ***(2)*** and $[Ag_2(GlyAsp)(NO_3)]_n$ ***(3)*** using spectral methods as UV-Vis, fluorescence and CD spectroscopy. Also the standard plasmid (pBR322) cleavage assay and ATP dependent decatenation of kinetoplast DNA (kDNA) assay were used to study the effect of silver complexes on human topoisomerase I/II (Topo I/II) by DNA gel electrophoresis. The spectroscopic measurements have shown that all studied Ag(I) dipeptide complexes bind into DNA with binding constants K_b in a range from 0.6×10^5 M^{-1} to 14.4×10^5 M^{-1} and their Stern-Volmer (quenching) constants K_{sv} were estimated in the range from 4.5×10^4 M^{-1} to 8.3×10^4 M^{-1}. The circular dichroism spectra exhibit decrease of positive signal (at 275 nm) and increase of negative signal (at 245 nm) which is similar as in the case of the Hoechst – DNA complex. The electrophoretogram has shown inhibition of Topoisomerase I by all studied complexes already at concentration of 15 μM and inhibition of Topoisomerase II was observed in the case of complex ***(3)*** at concentration of 25 μM and 50 μM and complex ***(2)*** inhibited Topo II at concentration of 50 μM.

Acknowledgements

This work was supported by the Grant Agency of Ministry of the Education, Science, Research and Sport of the Slovak Republic VEGA 1/0016/18 and 1/0138/20.

References

[1] M. Navarro, W. Castro, S. González, M. J. Abad, P. Taylor, J. Mex. Chem. Soc. **57** (2013) 220-229.
[2] M. M. Aleksić and V. Kapetanović, Acta Chim. Slov. **61** (2014) 555-573.
[3] L. Strekowski and B. Wilson, Mutat. Res. **623** (2007) 3–13.
[4] L. Andrezálová and Z. Országhová, J. Inorg. Biochem. **225** (2021) 1-34.
[5] X. F. Zhang, Z. G. Liu, W. Shen, S. Gurunathan, Int. J. Mol. Sci. **17** (2016) 1-17.
[6] I. X. Yin, J. Zhang, I. S. Zhao, M. L. Mei, Q. Li, C. H. Chu, Int. J. Nanomedicine **15** (2020) 2555–2562.

LGGE - A New Method for Electrophoretic Analysis of Ligand-DNA Interactions

L. Trizna[a]*, V. Víglaský[a]
[a]Department of Biochemistry, Institute of Chemistry, Faculty of Science, Pavol Jozef Šafárik University in Košice, Moyzesova 11, 040 01 Košice, Slovak Republic
*lukas.trizna@student.upjs.sk

Electrophoresis is one of the most common methods used in biochemistry and molecular biology. The application of this method for the separation of protein chains and nucleic acids is a necessity in modern science. A new electrophoretic methodology for determining ligand-DNA interactions in a single separation, the so-called **L**igand-**G**radient **G**el **E**lectrophoresis (LGGE), has been developed in our laboratory. This method was developed to study the interaction of non-canonical G-quadruplex DNA (G4 DNA) with various ligands. LGGE is in principle a denaturing gradient gel electrophoresis (DGGE), but instead of a denaturing agent, a concentration gradient of ligand is applied perpendicular to the movement of the DNA sample [1]. The ligand-G4 interaction is a very attractive area of research for many scientific groups. Such G4 ligands may have great potential to be antiviral and anticancer drugs and / or probes. A wide range of biophysical methods are used for this purpose [2,3]. LGGE can also be useful for this purpose.

Methodology

LGGE is performed in standard PAGE apparatus; the laboratory-made specific spacers A-D and two glass-plates determine the shape of electrophoretic gel (Fig. 1, step 1 and 2). The mixture of acrylamide/bis-acrylamide (optional ratio 19:1), TEMED and 25 mM modified Robinson-Britton (RB) buffer is divided; solution S1 and S2. The optimal concentration of acrylamide for LGGE is in the range of 10-14 %. The desired ligand is resuspended in the S1 solution at the desired concentration. The solutions are carefully poured into a casting mold. An appropriate concentration of ammonium persulfate is always added to the solution just before pouring. After gel polymerization, the casting mold is rotated 90°, the spacers A and C are removed (step 6) and the spacer D is used as the barrier for buffer pouring. Apparatus is ready for standard and sample application (step 9). Finally, in the stained gel is clearly observable migration profile of DNA sample. On base of this profile, it is possible to determine the impact of ligand on topology of G4-DNA complex (step 10).

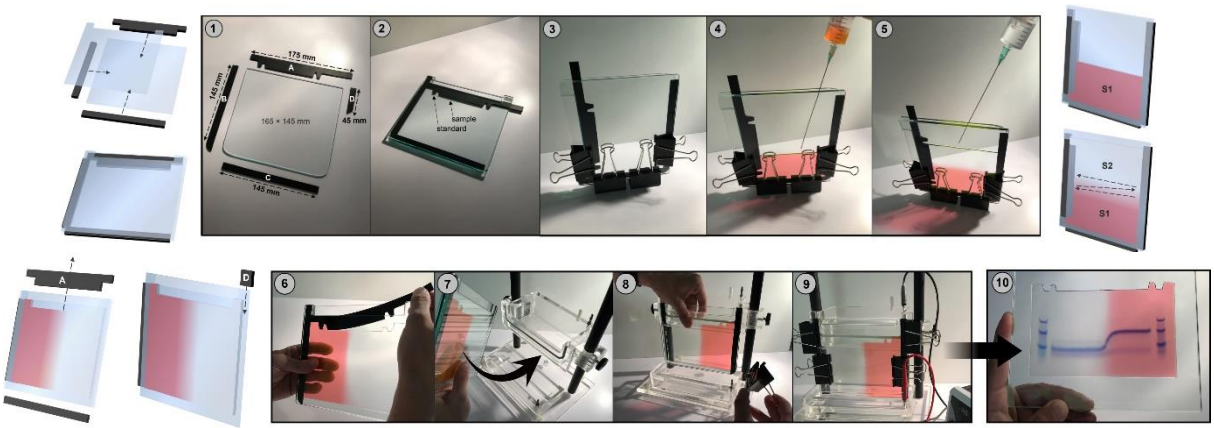

Figure 1 Apparatus for the gel pouring with spacers A-D (steps 1-3), preparation of gel for LGGE (steps 4-9) and example of LGGE gel containing ssDNA standards (d[AC]$_9$, d[AC]$_{18}$ and d[AC]$_{28}$) on both of sides and G4-DNA sample (d[G$_4$TCG$_3$CG$_3$CCG$_3$TG]) with 0-260 µM Rhodamine 6G in the gel (step 10).

Acknowledgements

This work was supported by the Grant Agency of the Ministry of Education, Science, Research and Sport of the Slovak Republic (VEGA No. 1/0138/20).

References

[1] L. Trizna, L. Janovec, A. Halaganová, V. Víglaský, Int. J. Mol. Sci. **22** (2021) 7639.
[2] T. Santos, G. F. Salgado, E. J. Cabrita, C. Cruz, Pharmaceuticals **14** (2021) 769.
[3] P. Murat, Y. Singh, E. Defrancq, Chem. Soc. Rev. **40** (2011) 5293.

Metal-Organic Framework MOF-76(Gd) as an Effective Humidity Sensor

A. Garg[a], J. Bednarčík[b, c], A. Sharma[d], M. Almáši[e]*
[a]Department of Physics, Suresh Gyan Vihar University, Jaipur 302017 India
[b]Department of Condensate Matter Physics, Institute of Physics, Faculty of Science, Pavol Jozef Safarik University in Košice, Park Angelinum 9, 041 54 Kosice, Slovak Republic
[c]Institute of Experimental Physics, Slovak Academy of Sciences, Watsonova 47, 040 01 Košice, Slovak Republic
[d] Department of Physics, School of Engineering & Technology, Central University of Haryana, Mahendergarh 123031 India
[e] Department of Inorganic Chemistry, Institute of Chemistry, Faculty of Science, Pavol Jozef Safarik University in Košice, Moyzesova 11, 040 01 Kosice, Slovak Republic
*miroslav.almasi@upjs.sk

The metal-organic frameworks (MOFs) material is a porous framework material assembled by metal ions and organic ligands. Compared with traditional porous materials, MOFs have the advantages of large specific surface area, ultra-high porosity, adjustable pore size, post-synthesis modification and high thermal stability. Featuring diversified structures and highly tunable micro/mesopore sizes, MOFs are able to cover the entire pore size gap between microporous zeolites and mesoporous silicas. With a large variety of metal nodes and a theoretically unlimited number of organic linkers, one can easily tune the compositions and structures of MOFs to achieve targeted functionality in a precise manner. In addition, the diversity of metal elements and organic ligands and their coordination modes determine the diverse types and functions of MOFs, such as magnetism, chirality, optical properties and catalysis [1, 2]. In nanoporous solids such as MOFs, gases can be stored in the adsorbed state. Due to the higher density of the adsorbed molecules, the effective storage capacity can be significantly increased by a factor of 2.5-3 as compared to empty cylinders. The modular concept of MOFs allows adjusting the chemical functionality to specifically remove the contaminants but release the stored gas. For such a "safe delivery system", MOFs need to be processed into compact bodies.

Humidity control is important in many areas, including moisture-sensitive products, package food, drug storage, agricultural or medical products automotive control systems, research labs and environmental control for paintings etc [3]. There are various commercially available sensors for detecting volatile substances at ppm-level concentrations, but there are still problems with humidity sensing below ~ 100 ppm (few percentages relative humidity (RH) at 298 K). There are numerous applications where humidity measurement in ppm or ppb level is required, such as semiconductor manufacturing, food or agricultural products storage, gas and fuel storage, and pharmaceutical preparations. Fabricating humidity sensors above around 90% RH and in few percentages RH is difficult, and thus, the RH sensors below 1 % are usually very expensive. There are very important industrial products that need humidity sensors to measure very low moisture content. For example, transformer oil from 5 to 25 ppm, plutonium pallets from 4 to 30 ppm and IC fabrication 10–100 ppm, require humidity sensors. Since there are number of research articles on humidity sensing but there are few ones which can detect in ppm level. In comparison with conventional amorphous nanoporous materials and polymers, MOF pore dimensions are highly defined. The ability of synthesis MOFs with a wide range of chemical, physical and morphological characteristics as well as the possibility of engineering the dimensions of the highly ordered pores and reversible sorption behavior of MOFs, makes them suitable materials for sensing. The change of the dielectric properties of the materials, caused by adsorption or desorption of molecules on the inner surface of MOF, is utilized to detect small amounts of analytes. Nevertheless a few studies have used MOFs as sensitive layers for gas sensing applications [4]. In this research work, synthesis and characterizations of a nanoporous MOF-76(Gd) ($[Gd(BTC)(H_2O)]\cdot DMF$, BTC – benzene-1,3,5-tricarboxylate; DMF – N,N´-dimethylformamide) for hydrogen adsorption/desorption and humidity sensing applications are presented. Morphological analyses performed by scanning and transmission electron microscopy indicate that synthesized MOF-76(Gd) has a rod-like assembly with an average dimension of the order of micrometres and do not agglomerate with each other to form a large cluster. Occurrence of BTC, water molecules and Gd(III) metal ions were confirmed by elemental analysis, infrared spectroscopy and EDS map scanning. PXRD measurement was used to determining the crystal structure and confirmed the presence of a pure phase of as-synthesized MOF-76(Gd). MOF-76(Gd) material is thermally stable between 300 °C to 550 °C temperature after the dehydration process based on thermogravimetric analysis, infrared spectroscopy and *in-situ* heating PXRD. Nitrogen adsorption/desorption measurement at 77K showed a BET surface area of 605 $m^2 g^{-1}$ and pore volume of 0.24 $cm^3 g^{-1}$ of the sample. Activated material was further used for hydrogen adsorption measurement and humidity sensing application. At a condition of 20 bar pressure and 77 K temperature, the maximal hydrogen storage capacity of MOF-76(Gd) was observed 0.18 wt. % which shows that an effective

activation process is required to significantly improve the uptake capacity. It may be suggested from the results that a good capacity of hydrogen storage may be accomplished, but a very high quantity could not be reproduced, which could meet the practical ideals for on-board hydrogen uptake systems. The humidity sensing measurements (water adsorption experiments) indicate that MOF-76(Gd) is a suitable material for moisture sensing applications. Humidity sensing recitation of the sample MOF-76(Gd) was appraised with several important sensing parameters. Variance method is used for % RH measurements. Figure 1(a) shows a linear increment for all the material, with varying % RH and out of these entire samples MOF-76(Gd) was observed for highly linear increment with maximum order change in resistance between 11-98 %RH which portrays outstanding sensing properties of MOF-76(Gd). Figure 1(b) gives the response and recovery time. It can be seen, response time was attained within 11s and the recovery time was observed within 2s. This clearly confirmed that the MOF-76(Gd) material is characterized by enhanced response and recovery times which provides its utility in futuristic humidity sensing application. Figure 1(b) shows hysteresis curve of sample based %RH sensor in which one line with downwards arrow represents the adsorption process from closed chambers of 11 % RH to 98 % RH and another line with the upwards arrow represent the desorption process take place from closed chambers of 98 % RH to 11 % RH. The hysteresis error (γH) was calculated by using the expression, $\gamma H = \pm \frac{\Delta H_{max}}{2F_{FS}}$, where ΔH_{max} is the difference in the output of the process of adsorption and desorption and F_{FS} is the full-scale output.

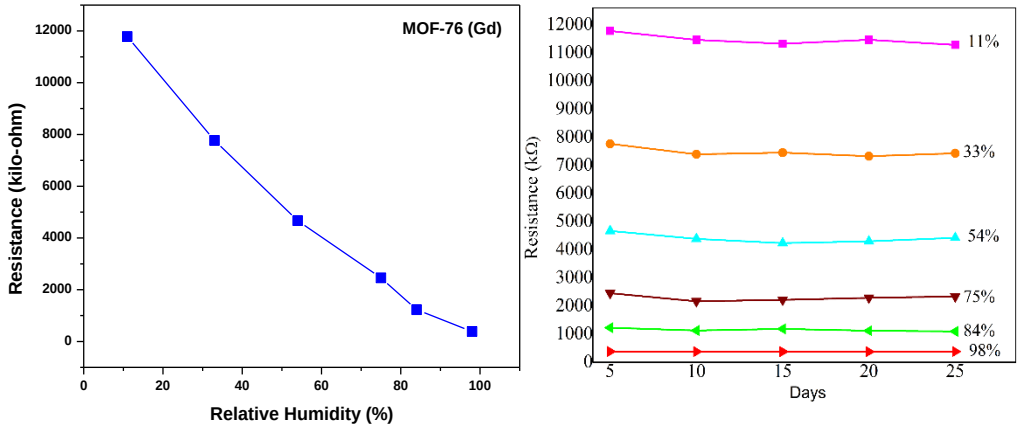

Figure 1 (a) Relative sensitivity of MOF-Tb(Gd) measured at each %RH, and **(b)** response of MOF-Tb(Gd) monitored at different humidity conditions for 30 days.

Figure 2 represents the stability of MOF-76(Gd) sensor, the resistance value at each % RH was measured for 25 days once every 5 days. The results show an excellent consistency, and a slight change in resistance was detected for a particular % RH level.

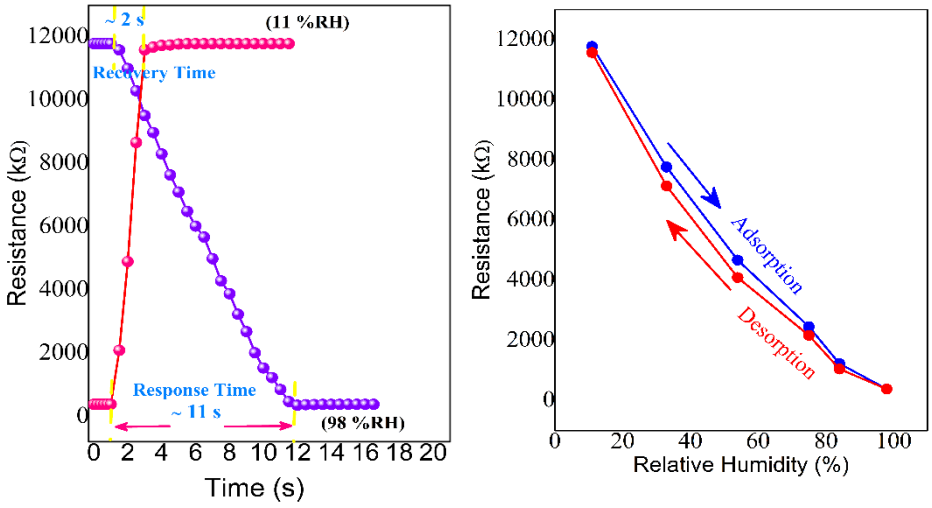

Figure 2 (a) Response/recovery time of the sensor MOF-Tb(Gd) measured between 11 % RH and 98 % RH and **(b)** hysteresis curve showing adsorption-desorption responses measured in the 11-98 % RH range for MOF-Tb(Gd).

Acknowledgements

This work was supported by the projects: VEGA 1/0865/21, APVV-18-0197, APVV-20-0138 and the University Grants Commission, Ministry of Human Resources and Development, Govt. of India.

References

[1] X. Lang, X. Wang, Y. Liu, K. Cai, L. Li, Q. Zhang, Int. J. Energy Res. **45** (2021) 4811-4820.

[2] J. Bellosta von Colbe, J. R. Ares, J. Barale, M. Baricco, C. Buckley, G. Capurso, N. Gallandat, D. M. Grant, M. N. Guzik, I. Jacob, E. H. Jensen, T. Jensen, J. Jepsen, T. Klassen, M. V. Lototskyy, K. Manickam, A. Montone, J. Puszkiel, S. Sartori, D. A. Sheppard, A. Stuart, G. Walker, C. J. Webb, H. Yang, V. Yartys, A. Zuttel, M. Dornheim, Int. J. Hydrogen Energy **44** (2019) 7780.

[3] J. Boudaden, M. Steinmaßl, H. Endres, A. Drost, I. Eisele, C. Kutter, P. Muller, Sensors **1** (2018) 1516.

[4] M. G. Campbell, M. Dinca, Sensors **17** (2017) 1108.

Activation or Carbonization of MOF-76(Gd) as a Matrix for Sulphur in Li-S Battery

N. Király[a]*, D. Capková[b], A. Straková Fedorková[b], M. Almáši[a]
[a]Department of Inorganic Chemistry, Institute of Chemistry, Faculty of Sciences, Pavol Jozef Šafárik University in Košice, Moyzesova 11, 040 01 Košice, Slovak Republic
[b]Department of Physical Chemistry, Institute of Chemistry, Faculty of Sciences, Pavol Jozef Šafárik University in Košice, Moyzesova 11, 040 01 Košice, Slovak Republic
*nikolas.kiraly@student.upjs.sk

Introduction

Metal-organic frameworks (MOF) also known as porous coordination polymers (PCPs) are one of the most exciting classes of porous materials to be discovered in the past three decades. MOFs are hybrid inorganic-organic materials composed of metal ions or clusters, which are bridged by organic linkers to form robust frameworks with permanent porosity. One of the characteristic features of MOFs is their topologically diverse and symmetrical structures, many of imitating minerals in nature [1]. The design of a target structure with specific functions and properties represents an eternal inspiration for scientists working in the field of materials chemistry. They find applications in many areas such as gas adsorption and separation, heterogeneous catalysis, drug delivery, ion exchange and energy storage [2]. Another currently intensively studied area of MOF materials application is their use as additives in Li-S batteries. MOFs offer immense possibilities in searching for sulphur hosts in Li-S cathodes due to their unique porous structure, large specific surface area and adjustable pore size. The presence of metal ions and conjugated aromatic linkers in the MOF structure can improve conductivity and material stability for high-performance Li-S batteries [3].

Results and discussion

We report the synthesis and characterization of metal-organic framework material, gadolinium(III) benzene-1,3,5-tricarboxylate (MOF-76(Gd)) with an exact chemical formula $[Gd(BTC)(H_2O)]\cdot DMF$ (BTC = benzene-1,3,5-tricarboxylate, DMF = N,N´-dimethylformamide)).). The crystal structure is built from benzene-1,3,5-tricarboxylate (BTC, trimesate) ligands as linkers and Gd(III) ions as nodes. Central Gd(III) ions are coordinated by seven oxygen atoms. Six oxygen atoms come from independent tridentate BTC linkers coordinated in syn-anti/syn-syn mode and each BTC ligand binds to six different Gd(III) cations. The last oxygen atom belongs to a coordinated water molecule. The thermal analysis showed that the desolvated [Gd(BTC)] framework is subsequently thermally stable up to 520 °C. PXRD confirmed that the material was successfully prepared in the pure phase, without the presence of other by-products. The material was studied in an activated (AC) and carbonized (C) form and the electrochemical behaviour of both materials as a sulphur matrix in the cathode of Li-S battery was investigated. In order to prepare a more conductive matrix, MOF-76(Gd) was carbonized and applied into the cathode material in Li-S battery. The 'flexible' pores can suppress electrode material damage of volumetric expansion during cycling, improve electrochemical kinetics, effectively capture and confine polysulphides, improve reversibility and inhibit polysulphide shuttle. The cells with the S/MOF-76(Gd) (AC) cathode show an initial discharge capacity of 684.4 mAh g^{-1} at 0.2 C and 620.8 mAh g^{-1} at 0.5 C, the capacity retention after 200 cycles at 0.5 C was 80.9 %. The S/MOF-76(Gd) (C) cathode exhibits an initial discharge capacity of 763.3 mAh g^{-1} at 0.2 C and 657.9 mAh g^{-1} at 0.5 C rate with a low fading rate of 0.036 % per cycle, the capacity retention after 200 cycles was 610.2 mAh g^{-1}. Even at a high current density (2 C), the discharge capacity was high with a low-capacity decrease. Overall, these results prove that MOF-76(Gd) based materials can accelerate polysulphide conversion, decrease capacity decay and restrain the polysulphides via strong interactions.

Acknowledgements

This research was sponsored by the following projects: VVGS-2021-1982 and APVV-20-0138.

References

[1] D. Kim, X. Liu, M.S. Lah, Inorg. Chem. Front. **2** (2015) 336-360.
[2] T. Ghanbari, F. Abnisa, W. M. A. W. Daud, Sci. Total Environ. **707** (2020) 35090.
[3] Y. Zheng, S. Zheng, H. Xue, H. Pang, J. Mater. Chem. A, **7** (2019) 3469-3491.

Characterization and Carbon Dioxide Adsorption of Holmium-Porphyrin Framework

N. Király[a]*, J. Kuchár[a], V. Zeleňák[a]
[a]Department of Inorganic Chemistry, Institute of Chemistry, Faculty of Science, Pavol Jozef Šafárik University in Košice, Moyzesova 11, 040 01 Košice, Slovak Republic
*nikolas.kiraly@student.upjs.sk

Introduction

In the past three decades, porous metal-organic frameworks (MOFs) have been intensively studied because of the variety in potential applications in the fields of gas adsorption, drug delivery, energy cycles, photocatalysis and photoreduction oxygen evolution reactions, sensing and explosive detection and many others. Microporous crystalline MOFs are formed by the self-assembly of inorganic metal clusters and organic linkers. Both inorganic (metal clusters) and organic (ligands) constituents of MOFs can be varied in their shape, size, composition, geometry, and branching modality. This allows tuning the structure and properties of MOFs to produce a versatile class of porous crystalline solids with a wide range of properties, high porosity, and surface area. Excellent examples of polytopic ligands with great potential to serve as building blocks in MOFs construction are porphyrins, metalloporphyrins, and their derivatives. These ligands offer rigidity and the possibility of a 4-connecting symmetry. For a long time, porphyrin ligands have been overlooked in MOF chemistry, although examples of porous MOFs based on porphyrins were known for a longer time. As a continuation of our research, in the present work, we focused on the synthesis of novel MOFs using a rigid anionic ligand derived from 4,4',4'',4'''-(porphyrin-5,10,15,20-tetrayl)tetrakis(benzenesulphonic) acid (H_6TPPS) with 4-fold symmetry (point group D_{4v}). [1,2].

Results and discussion

Presented work is focused on porous coordination polymer $\{[Ho(H_2TPPS)]\cdot nH_3O^+\cdot nH_2O\}_n$ (H_6TPPS = 4,4′,4″,4‴-(porphyrin-5,10,15,20-tetrayl)tetrakisbenzenesulfonic acid)), which was prepared by hydrothermal synthesis and characterized using a wide range of analytical techniques: infrared spectroscopy, UV/VIS spectroscopy, thermogravimetric measurements, elemental analysis, single crystal structure analysis (SXRD). Single crystal X-ray diffraction showed three-dimensional open porous framework constructed by mutually staggered H_2TPPS^{4-} ligands. Ho(III) ions are arranged in 1-D polymeric chains propagating along *c* crystallographic axis with Ho-Ho distance 4.889 Å and shortest distance between Ho(III) within the cavity is 15.393 Å. The framework contains three crossing cavities propagating along all crystallographic axes with sizes approximately 4.89 x 10.42 $Å^2$ and 5.16 x 8.40 $Å^2$. Infrared spectroscopy confirmed the presence of water and H_2TPPS ligand. Thermogravimetric analysis showed, that porous complex undergoes to dehydration process after heating to 100 °C and dehydrated form$\{[Ho(H_2TPPS)]\}_n$ is than highly thermally stable up to 350 °C. There are tree decomposition steps on TG, the first step with a weight loss of 3 % until 120 °C represents excluding of lattice water in the channel system. In the second step the decomposition of organic linker occurred and the final product of thermal decomposition was PrO_2. The activated porous complex was subjected to adsorption measurements of various gases which showed that the compound can be used as an effective adsorbent in the separation of CO_2 from N_2. Before the surface analysis materials were degassed for 2 hours at 40 °C, 2 hours at 100 °C and 16 hours for 150 °C. MPF adsorbs only limited amount of N_2 at -197 °C, but surprisingly compound adsorbs CO_2 at 0 °C with maximal storage capacity of 30 $cm^3.g^{-1}$ corresponding to 1.25 $mmol.g^{-1}$. The activated porous complexes were subjected to adsorption measurements of Ar at -186 °C. Fitting of argon adsorption isotherm using the Brunauer–Emmett–Teller (BET) equation gives estimated surface areas (BET) of 230 m^2/g.

Acknowledgements

This work was supported by the Scientific Grant Agency of the Slovak Republic (VEGA) under Projects 1/0865/21 and contract from P. J. Safarik University no. VVGS-2020-1667.

References

[1] R. J. Kuppler, et al., Coord. Chem. Rev. **253** (23-24) (2009) 3042-3066.
[2] W. Y. Gao, et al., Soc. Rev. **43** (16) (2014) 5841-5866.

Metal-Organic Frameworks UPJS-13 and UPJS-14 for Adsorption of Greenhouse Gasses

N. Király[a], V. Zeleňák[a], S. Bourrelly[b], M. Almáši[a]*
[a]Department of Inorganic Chemistry, Institute of Chemistry, Faculty of Science, Pavol Jozef Šafárik University in Košice, Moyzesova 11, 040 01 Kosice, Slovak Republic
[b]Aix-Marseille University, CNRS, MADIREL, Marseille Cedex 20, 133 97 France
*miroslav.almasi@upjs.sk

Metal-organic frameworks (MOFs) are one of the most exciting classes of porous materials to be discovered in the past decades. MOFs are crystalline materials constructed from organic molecules (linkers) coordinated to metal ions or clusters to form interesting polymeric frameworks with a larger surface area and the advantage of pore size changing. Due to the porosity and tunable textural properties, MOF materials find applications in gas storage and separation, heterogeneous catalysis, drug delivery, magnetic refrigeration, sensing and energy storage [1-3].
Global temperature has been rising since the first industrial revolution in the early 19th century, due to the emissions of large quantities of greenhouse gases. The main greenhouse gases are carbon dioxide and methane, but also nitrogen oxides and water vapour. Carbon dioxide is a major by-product of fossil fuel combustion, electricity generation and other anthropogenic activities. Major advances in carbon capture technology could provide power plants and road transport with an efficient and inexpensive way to remove carbon dioxide from their flue gas emissions, which is necessary to reduce greenhouse gas emissions to slow global warming and climate change. The 2030 Climate and Energy Framework commits all EU member states to a 40% reduction in greenhouse gas emissions over the coming years. For this reason, it is necessary to develop new and effective carbon dioxide and methane adsorbents as the main greenhouse gases. Many porous materials such as carbon dioxide adsorbents, e.g. MOFs or porous oxides, are modified with nitrogen-containing amine molecules to capture the CO_2 (chemisorption) at low-temperature steam to flush out the CO_2 for other uses or to sequester it underground are currently being developed and intensively studied. Examples are tetraamine-appended MOF Mg_2(dobpdc) (dobpdc = 4,4′-dioxidobiphenyl-3,3′-dicarboxylate, S_{BET} = 2880 $m^2.g^{-1}$), which can store up 90 wt.% CO_2 [4]. In order to avoid CO_2-intensive energy processes, CO_2 molecules must be captured in porous materials by physisorption as a chemisorption process. However, physisorption brings new challenges, because there is a lack of selectivity for CO_2 because no chemical bond is formed or when the functional groups are tuned to increase selectivity, the absorption of CO_2 is limited.
In the present study, extended tetrahedral nitrogen-rich tetraazo-tetracarboxylic acid (H_4MTA) was prepared by seven-step organic synthesis and used as a linker in the preparation of two novel aMOFs containing Zn(II) (UPJS-13) and Cd(II) (UPJS-14) ions. After characterisation, the textural properties of prepared materials were studied by nitrogen adsorption at -196 °C on as-synthesized (AS), ethanol exchanged (EX) and freeze-dried (FD) samples. After finding the best activation conditions, the materials were tested as adsorbents of greenhouse gases in high-pressure adsorption measurements of carbon dioxide and methane up to 20 bar.
The best textural properties were observed for materials after the freeze-drying (FD) process (see green curves in Figure 1) compared to ethanol exchanged (EX) or as-synthesized (AS) samples. The highest values of surface areas were calculated after activation of the samples at 80°C and corresponding values were 830 $m^2.g^{-1}$ (pore volume, V_p = 0.57 $cm^3.g^{-1}$; pore diameter, d = 0.73 nm calculated by DFT) for UPJS-13 (FD) and 1057 $m^2.g^{-1}$ (pore volume, V_p = 0.72 $cm^3.g^{-1}$; pore diameter, d = 0.87 nm calculated by DFT) for UPJS-14 (FD). Gradual heating to 120°C leads to a slight decrease in S_{BET} values and further heating did not affect the values of surface area for both compounds. In summary, it can be concluded that UPJS-14 material showed better textural properties compared to UPJS-13, regardless of the post-synthetic treatment and activation conditions. The highest values of surface areas of prepared materials were observed for samples after the freeze-drying process, followed by ethanol-exchanged and as-synthesized samples.

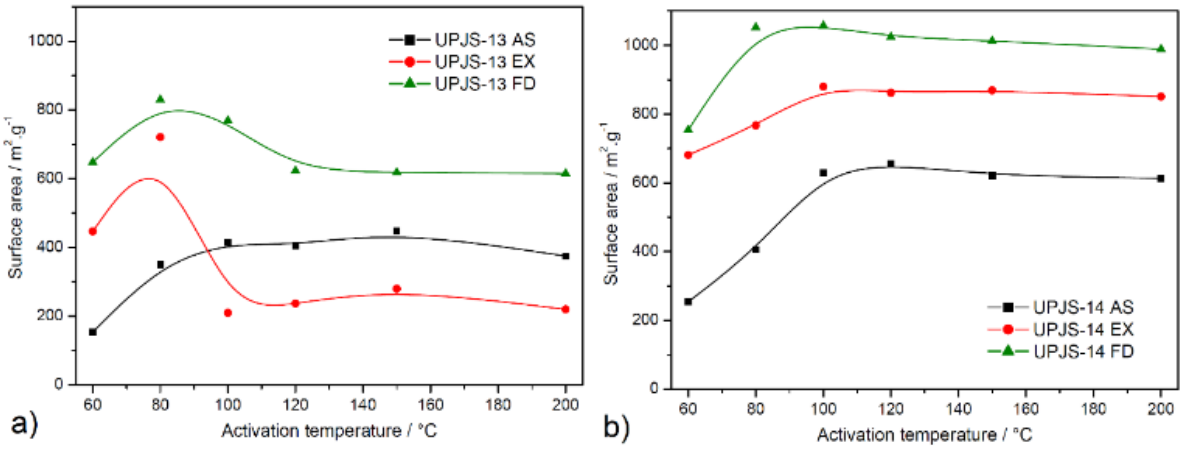

Figure 1 Calculated BET surface areas from nitrogen isotherms of activated materials at 60, 80, 100, 120, 150 and 200°C for a) UPJS-13 and b) UPJS-14.

As major components of greenhouse gases, carbon dioxide and methane have also been studied as probe molecules to investigate the sorption properties of prepared aMOFs. CO_2 and CH_4 high-pressure adsorption measurements were performed at 30°C and pressure up to 20 bar on freeze-dried samples activated at 80°C. Measured adsorption isotherms are shown in Figure 2. The absence of district plateaus in the isotherms indicated that the maximal capacities were still not achieved and compounds are not saturated by the gases at 20 bar. Both selected probes are non-polar molecules with different quadrupole moments (0 $C.m^2$ for CH_4, 14.3×10^{40} $C.m^2$ for CO_2), kinetic diameters (3.8 Å for CH_4, 3.3 Å for CO_2) and different boiling points (-161°C for CH_4, -78°C for CO_2) and described differences may influence the maximal adsorption uptake of gases.

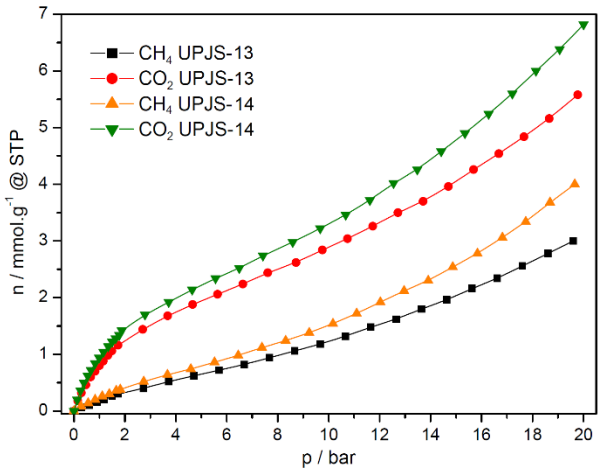

Figure 2 Methane and carbon dioxide high-pressure adsorption isotherms of **UPJS-13** and **UPJS-14** measured at 30 °C and pressure up to 20 bar.

aMOFs storage capacities of carbon dioxide at 1 bar and 30 °C were 0.94 $mmol.g^{-1}$ (4.14 wt. %) for UPJS-13 FD and 0.8 $mmol.g^{-1}$ (3.52 wt. %) for UPJS-14 FD. With increasing pressure, an increase in the amount of adsorbed carbon dioxide was observed. The maximal adsorption uptake and corresponding adsorption capacities were 6.82 $mmol.g^{-1}$ (30.01 wt. %) for UPJS-13 FD and 5.58 $mmol.g^{-1}$ (24.56 wt. %) for UPJS-14 FD at 30 °C and 20 bar. Both compounds show high CO_2 storage capacities, however, the UPJS-13 FD framework showed a higher affinity for CO_2 compared to UPJS-14 FD, although it has a smaller surface area. Due to the presence of an electron-deficient carbon atom, carbon dioxide is expected to interact with protic electronegative functional groups, leading to strong chemisorption.

Methane is the main component of natural gas and the second most abundant greenhouse gas in Earth´s atmosphere. CH_4 is a non-polar molecule with zero quadrupole moment and has a low volumetric energy density, which poses a challenge for efficient storage to reduce its concentration in the atmosphere or for energy application. For this reason, methane was also used as an adsorbate for high-pressure adsorption and measured isotherms are presented in Fig. 2. Materials adsorb methane with a maximal storage capacity of 0.22 $mmol.g^{-1}$ (0.35 wt. %) for UPJS-13 (FD) and 0.36 $mmol.g^{-1}$ (0.58 wt. %) for UPJS-14 (FD) at 30 °C and 1 bar and

3.02 mmol.g^{-1} (4.84 wt. %) for UPJS-13 (FD) and 3.98 mmol.g^{-1} (6.38 wt. %) for UPJS-14 (FD) at 30 °C and 20 bar. It could be noted that the adsorbed amounts are approximately four/five times lower compared to carbon dioxide. Contrary, the values of stored CH_4 are relatively high and can be explained by the pore size of aMOF materials. Several theoretical studies have shown that the optimum pore size for methane storage is 8 Å, which corresponds to distance between pore walls of about twice larger, than the molecule diameter [5].

Acknowledgements

This work was supported by the projects: VEGA 1/0865/21 and APVV-20-0138.

References

[1] Q. Qian, P. A. Asinger, M. J. Lee, G. Han, K. Mizrahi Rodriguez, S. Lin, F. M. Benedetti, A. X. Wu, W.S. Chi, Z. P. Smith, Chem. Rev. **120** (2020) 8161–8266.
[2] M. Fakhraei Ghazvini, M. Vahedi, S. Najafi Nobar, F. Sabouri, J. Environment. Chem. Eng. **416** (2021) 104790.
[3] H. Konnerth, B. M. Matsagar, S. S. Chen, M. H. G. Prechtl, F. K. Shieh, K. C. W. Wu, Coord. Chem. Rev. **416** (2020) 213319.
[4] E. J. Kim, R. L. Siegelman, H. Z. Jiang, A. C. Forse, J. H. Lee, J. D. Martell, P. J. Milner, J. M. Falkowski, J. B. Neaton, J. A. Reimer, S. C. Weston, J. R. Long, Science **369** (2020) 392–396.
[5] R. B. Getman, Y. S. Bae, C. E. Wilmer, R.Q. Snurr, Chem. Rev. **112** (2011) 703–723.

Novel Schiff Base-Functionalized Metal–Organic Framework for Dispersive Solid Phase Extraction of Heavy Metal Ions from Wastewater

P. Pillárová[a]*, Ľ. Zauška[a], M. Almáši[a]
[a]Department of Inorganic Chemistry, Institute of Chemistry, Faculty of Science, Pavol Jozef Šafárik University in Košice, Moyzesova 11, 040 01 Košice, Slovak Republic
*paula.pillarova@student.upjs.sk

One of the essential natural resources for life is water. However, with increased human activities and the rapid growth of modern industries, water pollution has become a serious issue worldwide [1]. Moreover, with the rapid expansion of industrialization, the environment is heavily contaminated by wastewaters generated from the industry. Among the various organic and inorganic pollutants, heavy metals are among the most dangerous contaminants due to their lack of biodegradation, water stability, and high toxicity for the environment [2]. The pollution of water ecosystems by heavy metals, which is mainly due to the discharge of industrial wastewater, causing damage to the health of humans and other beings, and this becomes a serious issue [3]. Heavy metals are usually considered environmental pollutants, including cadmium, mercury, lead, cobalt, nickel, copper, zinc, selenium, and tin ceausing endocrine disruption, congenital disorders, or general toxic effects in fish, plants, birds, or other aquatic organisms.

In the recent decades, design and development of various methods to remove the heavy metals from an aqueous medium, including chemical precipitation, ion exchange, nanofiltration, low-energy reverse osmosis, membrane processes, and adsorption [4]. Adsorption is accepted among all these methods because of its low cost, high efficiency, selectivity, and design simplicity. Heavy metal ions can be removed with different materials such as clay minerals, magnetic silica nanoparticles, chelating materials, activated carbons, chitosan/ natural zeolites, and nanofibers [5].

Nowadays, chemist researchers have shown a great deal of interest in novel materials in nanotechnology. Metal-organic frameworks (MOFs) are one of the promising class of nanomaterials to absorb hazardous pollutants from an aqueous medium [6]. MOFs are a new kind of crystalline porous compounds consisting of metal ions or clusters coordinated to organic ligands to form three-dimensional structures. They are a subset of coordination polymers that have a specific property, porosity. MOFs have chemical and physical properties such as excellent porosity and surface area, adjustable chemical structure, low density, and pore size. These advantages make the MOFs suitable for a different and wide range of applications such as storage and removal of gases, sensing, catalysis, separation/adsorption, detecting, targeted drug delivery, and other areas. MOFs are used as solid-phase sorbents to absorb and remove toxic metal ions as environmental pollutants from aqueous solutions [7].

In continuation of our interest in removing heavy metals, drugs, and other contaminants from aqueous media, we aimed to use of mesoporous metal-organic framework MIL-101(Fe)-NH_2 nanoparticles, which were post-sytetically modified with pyridine-2-carbaldehyde to form Schiff base within the framework (see Figure 1) for removal of Ni(II), Cu(II) and Cr(III) ions from aqueous samples. Described MOF was selected as dispesive solid phase due to its exciting properties such as high surface area, high thermal and chemical stability and simple separation. Schiff base-functionalized material has been shown to show efficient uptake of mentioned metal ions from solution compared to unmodified MOF.

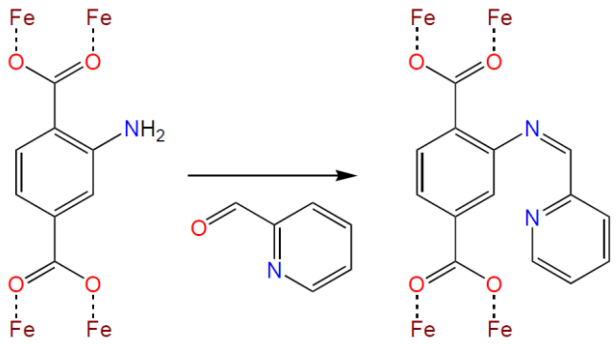

Figure 1 Post-synthetic modification of MIL-101(Fe)-NH_2 with pyridine-2-carbaldehyde within the framework under formation of Schiff base as an active site for ion binding.

References

[1] G. Mancuso, G. F Bencresciuto, S. Lavrnić, A. Toscano, Water **13** (2021) 1893.
[2] L. Cui, Y. Wang, L. Gao, L. Hu, Q. Wei, B. Du, J. Colloid Interface Sci. **456** (2015) 42-49.
[3] Y. Huang, X. Zeng, L. Guo, J. Lan, L. Zhang, D. Cao, Sep. Purif. Technol. **194** (2018) 462-469.
[4] Y. X. Ma, D. Xing, W. J. Shao, X. Y. Du, P. Q. La, J. Colloid Interface Sci. **505** (2017) 352-363.
[5] Q. Feng, D. Wu, Y. Zhao, A. Wei, Q. Wei, H. Fong, J. Hazard. Mater. 344 (2018) 819-828.
[6] M. M. Nilash, A. Hashemzadeh, A. R. Fakhari, M. M. Amini, Anal. Methods **11** (2019) 2683-2691.
[7] F. Boorboor Ajdari, E. Kowsari, M. Niknam Shahrak, A. Ehsani, Z. Kiaei, H. Torkzaban, M. Ershadi, S. Kholghi Eshkalak, V. Haddadi-Asl, A. Chinnappan, S. Ramakrishna, **422** (2020) 213441.

Metal-Organic Frameworks Containing Fluorinated Ligands

D. Princík[a]*, V. Zeleňák[a]
[a]Department of Inorganic Chemistry, Institute of Chemistry, Faculty of Science, Pavol Jozef Šafárik University in Košice, Moyzesova 11, 040 01 Košice, Slovak Republic
* david.princik@student.upjs.sk

The last two decades have received a huge expansion in the field of crystal polymeric porous materials also known as Metal-Organic Frameworks (MOF). These versatile materials dominate mainly due to their surface area and pore volume with various pore topologies, accessible cages and their potential applications in different fields, such as heterogenous catalysis [1], gas storage and gas separation materials [2] or drug delivery systems. Despite their great advantages, these materials also have certain disadvantages. From an industrial point of view, the main disadvantage is the hydrolytic lability, which is compensated by drying the used reactants, gases or solvents, which increases the production costs. Several methods are known to increase the hydrolytic resistance of MOF materials, but they often lead to pore occupancy and potentially decrease the sorption capacity of gases [3].

In this work we focus on increasing the hydrolytic resistance of MOF-type materials using a synthetic method that includes a completely new synthesis of MOF materials from a series of new, hydrophobic fluorinated ligands. Their hydrophobic effect is ensured by the aromatic skeleton of the ligand and the fluorine atoms bound to it. Two series of MOF complexes with non-fluorinated ligand as a reference material and fluorinated derivative were prepared. The first ligand represents biphenyl-4,4'-dicarboxylic acid (H_2BPDC), with which MOF complexes have been successfully prepared using Zn^{2+}, Ba^{2+}, Ce^{3+}, Fe^{3+}, Cr^{3+}, La^{3+}, Yb^{3+} and Zr^{4+} salts. The second ligand represents 3,3',5,5'-tetrafluorobiphenyl-4,4'-dicarboxylic acid ($H_2$4FBPDC), with which MOF complexes have been prepared using Ba^{2+}, Ce^{3+}, Cr^{3+} and La^{3+} salts and all prepared MOF complexes were subjected to IR, TG and SXRD measurements confirming their composition. Experimental results confirm the increased stability of fluorinated derivatives compared to reference complexes. Detailed information will be presented at the conference.

Acknowledgements

This work was supported by the Scientific Grant Agency (VEGA 1/0865/21).

References

[1] S. Li, Y. Zhang, Y. Hu, B. Wang et al., J. Materiomics. **7** (2021) 1029-1038.
[2] Q. F. Qiu, C. X. Chen, Z. Zeng et al., Inorg. Chem. **59** (2020) 14856-14860.
[3] S. Y. Jiang, W. W. He, S. L. Li et al., Inorg. Chem. **57** (2018) 6118-6123.

Postsynthetic Amine-Modified HKUST-1 for Enhanced Carbon Dioxide and Hydrogen Storage

K. Simanová[a]*, T. Zelenka[b], G. Zelenková[b], A. Sharma[c], M. Almáši[a]
[a]Department of Inorganic Chemistry, Institute of Chemistry, Faculty of Science, Pavol Jozef Šafárik University in Košice, Moyzesova 11, 040 01 Kosice, Slovak Republic
[b]Department of Chemistry, Faculty of Science, University of Ostrava, 30. dubna 22, 701 03 Ostrava, Czech Republic
[c]Department of Physics, School of Engineering & Technology, Central University of Haryana, Mahendergarh 123031 India
*klaudia.simanova@student.upjs.sk

Carbon dioxide emissions from fossil fuel combustion and industrial processes account for as much as 65 % of anthropogenic greenhouse gas emissions [1]. Carbon capture and sequestration (CCS), wherein CO_2 is separated from the flue emissions of large point sources and permanently sequestered underground, is widely recognized as an essential component of strategies for meeting the ambitious climate targets established at the Paris Climate Conference [2]. The development of capture technology has largely focused on coal flue emissions, but worldwide use of natural gas is projected to exceed that of coal by ~2032, necessitating the rapid development of CCS technology for natural gas emissions [3]. Aqueous amine solutions, the most mature carbon-capture technology as of now, are susceptible to oxidative and thermal degradation and have low carbon dioxide cycling capacities [4]. Porous solid adsorbents such as zeolites, silicas, and metal–organic frameworks are emerging as promising CO_2-capture materials because of their high surface areas, lower intrinsic regeneration energies, higher stabilities, and tunable surface chemistries. Taking inspiration from amine-functionalized silicas, it has been shown that amine-functionalized metal–organic frameworks can capture CO_2 in the presence of water and other molecules [5, 6].

Hydrogen can be a promising clean energy carrier for the replenishment of non-renewable fossil fuels. The set back of hydrogen as an alternative fuel is due to its difficulties in feasible storage and safety concerns. Current hydrogen adsorption technologies, such as cryo-compressed and liquefied storage, are costly for practical applications. Metal-organic frameworks (MOFs) are crystalline materials that have structural versatility, high porosity and surface area, which can adsorb hydrogen efficiently. Hydrogen is adsorbed by physisorption on the MOFs through weak van der Waals force of attraction which can be easily desorbed by applying suitable heat or pressure. The strategies to improve the MOFs surface area, hydrogen uptake capacities and parameters affecting them are studied. Hydrogen spill over mechanism is found to provide high-density storage when compared to other mechanisms [7].

Among many MOF representatives, HKUST-1 (Cu(II) benzene-1,3,5-tricarboxylate) is still considered to be one of the most promising adsorbents for CO_2 capture due to its high surface area, simple and low-cost synthesis, and high density of active metal sites, which can be effectively functionalized postsynthetically. Various molecular species were already used for incorporation within the HKUST-1 structure in order to improve different CO_2 capture performance parameters, for instance, incorporation of CuCl to enhance CO/H_2 and CO/N_2 separation [8], modification with pyrazine to improve CO_2/CH_4 selectivity [9], with N,N′-dimethylformamide [10] and polyethylenimine to enhance CO_2 adsorption [11] and separation [12] or with tetraethylenepentamine for CO_2 adsorption [13]. However, the modification of HKUST-1 with ethylenediamine to improve the CO_2 capture performance of HKUST-1 adsorbent has never been studied yet.

In our present research, we focused on the postsynthesic incorporation and detailed structural evaluation of ethylenediamine (en, diamine), diethylenetriamine (deta, triamine) and 1,2-bis(3-aminopropylamino)ethane (bapen, tetraamine) within the HKUST-1 framework for the first time (see Figure 1). HKUST-1 was prepared, solvent-exchanged by methanol, and structurally modified by the generation of additional amine-based sorption sites in order to investigate the impact of the modification process on carbon dioxide and hydrogen capture performances. The nature of amine moieties binding on coordinatively unsaturated metal sites (CUSs) of the HKUST-1 framework was evaluated by using different complementary spectroscopic techniques, elemental analysis, thermal analysis, powder X-ray diffraction, and gas adsorption of argon, carbon dioxide and hydrogen.

Postsynthetic modification of HKUST-1 with amines was performed in dry methanol using amines with different concentrations, through which materials with different molar ratios of HKUST-1 to amine: 1:0.05; 1:0.1; 1:0.25; 1:0.5; 1:0.75; 1:1; 1:1.5 were prepared. PXRD has shown that the structure of HKUST-1 is maintained at low molar ratios and that en and deta binding to CUSs occurs. In the case of higher molar ratios (1:1 and higher) and the use of bapen, a new non-porous phase or decomposition of HKUST-1 occurs. This phenomenon is probably caused due to the high pH of the solution because of the presence of a high concentration

of amines (en and deta), or the high basicity of the bapen. Subsequently, the thermal stability of the materials was studied by thermal analysis, and the compounds were shown to be stable up to 250 °C. Based on this information, it was possible to select the activation temperature of the materials before the adsorption measurements. The specific surface area (S_{BET}) and pore volume (V_p) of the prepared samples were calculated from the argon adsorption measurements. With increasing HKUST-1: amine molar ratio and amine bulk density, the observed values decreased. In addition, this analysis confirmed the non-porosity of materials with a high amine content. Adsorption measurements of carbon dioxide at 273 K and 1 bar (see Figure 2) have shown that the compounds are able to adsorb large amounts of carbon dioxide. In general, deta-modified samples showed higher adsorbed amounts of CO_2 compared to en, which can be explained by the higher number of amine groups within the deta molecule. With an increasing molar ratio of amines, there was a decrease in wt.% CO_2. The maximum storage capacity of CO_2 was 22.3 wt. % for HKUST-1: en / 1: 0.1 and 33.1 wt.% for HKUST-1: deta / 1: 0.05 at 273K and 1 bar. Hydrogen adsorption measurements showed the same trend as carbon dioxide, with the maximum H_2 adsorbed amounts being 2.07 wt. % for HKUST-1: en / 1: 0.1 and 2.28 wt.% for HKUST-1: deta / 1: 0.05 at 273K and 1 bar.

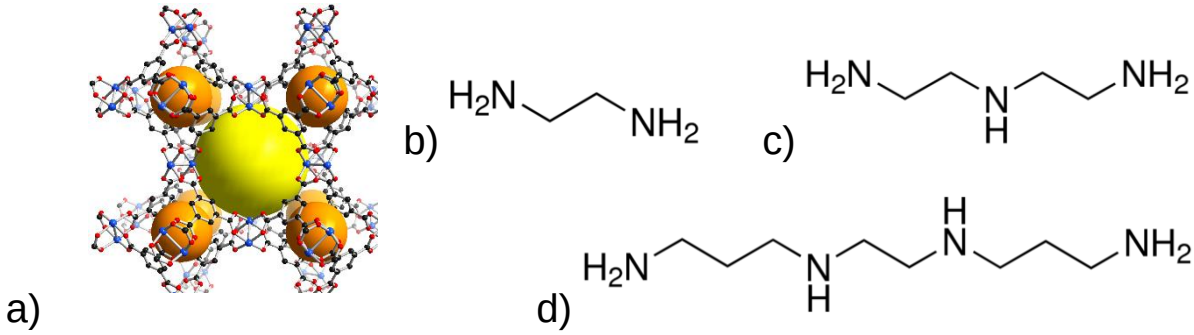

Figure 1 a) A view of HKUST-1 polymeric framework and molecular structure of amines used in the present study: **b)** ethylenediamine (en), **c)** diethylenetriamine (deta), and **d)** 1,2-bis(3-aminopropylamino)ethane (bapen).

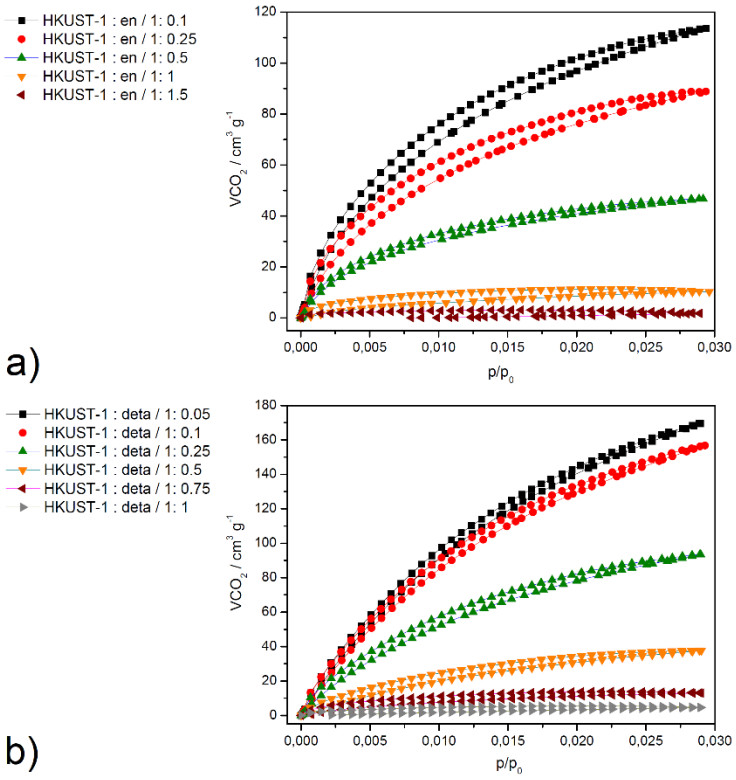

Figure 2 CO_2 adsorption/desorption isotherms of amine-modified HKUST-1 sample in the different molar ratios of en and deta at 273K.

Acknowledgements

This work was supported by the projects: VEGA 1/0865/21, APVV-18-0197, APVV-20-0138 and the University Grants Commission, Ministry of Human Resources and Development, Govt. of India.

References

[1] International Energy Agency, "CO_2 emissions from fuel combustion highlights" (International Energy Agency, 2016).
[2] M. Bui et al., Energy Environ. Sci. **11** (2018) 1062–1176.
[3] R. L. Siegelman, P. J. Milner, E. Kim, S. C. Weston, J. R. Long, Energy Environ. Sci. **12** (2019) 2161–2173.
[4] S. A. Mazari, B. Si Ali, B. M. Jan, I. M. Saeed, S. Nizamuddin, Int. J. Greenh. Gas Control **34** (2015) 129–140.
[5] Y. Lin, C. Kong, L. Chen, RSC Advances **6** (2016) 32598–32614.
[6] W. Chaikittisilp, H. J. Kim, C. W. Jones, Energy Fuels **25** (2011) 5528–5537.
[7] S. P. Shet, S. Shanmuga Priya, K. Sudhakar, M. Tahir, Int. J. Hydrogen Energy **46** (2021) 11782-11803.
[8] Y. Yin, Z. H. Wen, X.Q. Liu, L. Shi, A. H. Yuan, J. Porous Mater. **25** (2018) 1513.
[9] S. Salehi, M. Anbia, Energy Fuels **31** (2017) 5376−5384.
[10] L. Ma, H. Tang, C. Zhou, H. Zhang, C. Yan, X. Hu, Y. Yang, W. Yang, Y. Li, D. He, Int. J. Nanosci. **13** (2014) 1460002.
[11] V. Irani, A. Tavasoli, A. Maleki, M. Vahidi, Int. J. Hydrogen Energy **43** (2018) 5610−5619.
[12] A. Aarti, S. Bhadauria, A. Nanoti, S. Dasgupta, S. Divekar, P. Gupta, R. Chauhan, RSC Adv. **6** (2016) 93003−93009.
[13] F. Martínez, R. Sanz, G. Orcajo, D. Briones, V. Yanguez, Chem. Eng. Sci. **142** (2016) 55−61.

Solvothermal Reactions of Iron with Bidentate Aromatic *N*-Donor Ligands

J. Tomičová[a]*, M. Matiková Maľarová[a] J. Kuchár[a], J. Černák[a]
[a]Department of Inorganic Chemistry, Institute of Chemistry, Faculty of Science, Pavol Jozef Šafárik University in Košice, Moyzesova 11, 040 01 Košice, Slovak Republic
*jana.tomicova@student.upjs.sk

Iron undoubtedly belongs to the group of metals whose coordination compounds are studied from various aspects with potential practical applications. This is due to its various oxidation states, among which the most stable is II and III, and coordination numbers 4 and 6 with tetrahedron and octahedron geometry, respectively [1].

The amount of tetrahedral iron complexes in oxidation state II is significantly smaller compared to octahedral complexes. However, such iron complexes are interesting due to their magnetic properties. Tetrahedral complexes with oxidation state II are in high spin state and they belong into molecule magnets with one molecule, e. g. [$FeCl_2$(*neo*)] complex (*neo* = 2,9-dimethyl-1,10-phenantroline) [2].

Low-dimensional magnetic coordination polymers have attracted much attention since the discovery of anisotropic systems with remarkable properties such as single molecule magnets. In order to design materials with well-defined and precise properties, it is important to select a suitable ligand that efficiently transmits exchange interactions between paramagnetic centers. Possible bridging units, commonly small organic molecules with different donor atoms, are interesting because they allow enormous synthetic variability [3].

Complexes of iron in oxidation state II with ligands like 2,2´-bipyridine and 1,10-phenantroline and their derivatives are mostly octahedral in geometry and in low spin state. When these ligands in the complexes were replaced with monodentate *N*-donor ligands, transition from the low spin state to the high spin state was observed. If the halides ligand is used as a bridge and thus connects iron atoms, we can create a 1D structure in the shape of zigzag chain or oligomeric units [4].

In this work we focused on the preparation of iron complexes with oxidation state II or III with *N*-donor ligands under solvothermal conditions. Using solvothermal syntheses in acetylacetone we were able to prepare and characterize three new molecular complexes of unique composition that contained the iron as the central atom in oxidation state III surrounded by three different types of ligands. These types of complexes represent a very small group of octahedral complexes with various central atoms and there are only six similar compounds found in the Cambridge Crystallographic Database and only one of them with the iron as the central atom [5]. The molecular structure of [Fe^{III} ($acac^-$)$(py)_2Cl_2$] contains two monodentate ligands pyridine (*py*) coordinated on iron (Figure 1) [6].

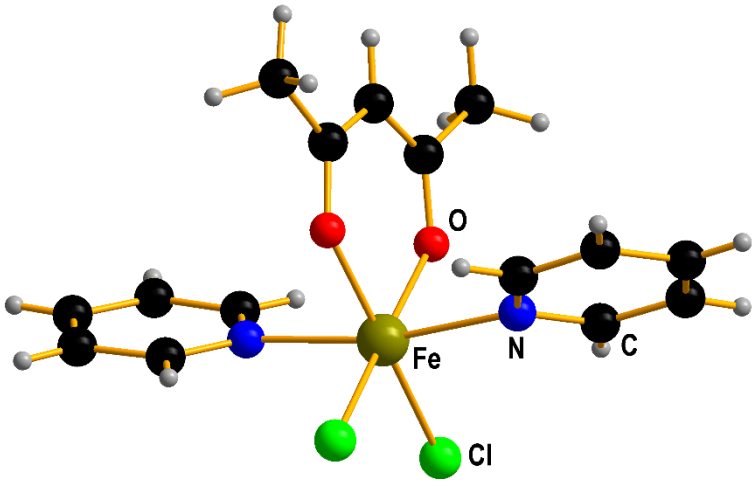

Figure 1 Molecular structure of complex [Fe^{III} ($acac^-$)$(py)_2Cl_2$].

From the syntheses of octahedral iron complexes with oxidation state III, we managed to prepare complexes with the acetylacetonate ligand coordinated on iron (III) by two oxygen atoms. The preparation of these complexes was carried out under solvothermal conditions using ferric chloride hydrate, *N*-donor type of ligand namely 2,2´-bipyridine, 1,10-phenantroline and 4,4´-dimethyl-2,2´-bipyridine in an acetylacetone as the solvent. The molecular structure of the prepared complexes with its π-π interactions is presented in the Figure 2.

All prepared heteroleptic complexes were characterized by IR and UV-VIS spectroscopy, elemental analyses and their molecular and crystal structure was solved. The thermal stability of complexes and the homogeneity of oxides prepared by thermal decomposition were studied by thermal analyses EDX and SEM analyses.

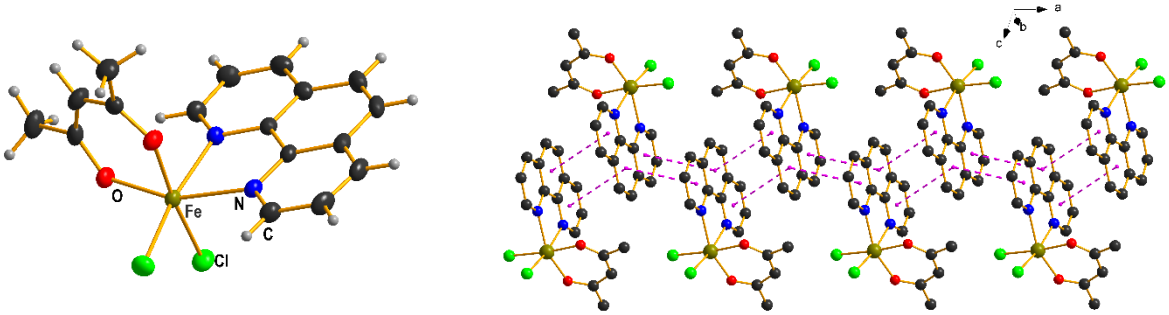

Figure 2 Molecular structure of prepared complex [Fe(*acac*$^-$)Cl_2(*phen*)] and π-π interactions.

References

[1] N. N. A. Greenwood, Chemie prvků II., (1993) ISBN 80-85427-38-9.
[2] O. Das, S. Chatterjee, T. K. Paine, J. Biol. Inorg. Chem. **18** (3) (2013) 401-410.
[3] P. Alborés, E. Rendschler, Dalton Trans. **42** (2013) 9621-9627.
[4] X. Sui, X. Lu, J. Coord. Chem. **61** (2008) 1568-1574.
[5] C. R. Groom, I. J. Bruno, M. P. Lightfoot, S.C. Warda, CSD. Struct. SC. Cryst. Eng. Mat. **72** (2) (2016) 171-179.
[6] V. M. Leovac, S. B. Novaković, G. A. Bogdanović, & M. D. Joksović, Struc. Chem. **18** (3) (2007) 337-341.

The Social Demand of the Professionally Focused Study Program "Chemical Laboratory Technician - Specialist"

Z. Vargová [a]*, M. Almáši[a], M. Rendošová[a], R. Oriňaková[a], S. Hamuľaková[a], R. Varhač[a], V. Víglaský[a], J. Šandrejová[a], M. Ganajová[a]

[a]Institute of Chemistry, Faculty of Science, Pavol Jozef Šafárik University in Košice, Moyzesova 11, 040 01 Košice, Slovak Republic

*zuzana.vargova@upjs.sk

With aim to prepare quality graduates for the needs of practice, the Institute of Chemistry PF UPJŠ in Kosice is preparing a new professionally focused study program for future students. Because of the present time point to the importance of science and mathematics teaching for the economic growth of countries, the emphasis in education is, in addition to quality teaching content, on the development of practical skills and competencies so necessary for a functioning state economy. Practical training must develop skills important for the workforce living in a technologically advanced economy [1]. If we want to keep up with developed Europe and the world, in Slovakia it is necessary to provide for young people the opportunities that foreign students use at advanced universities in the surrounding V4 countries as well as throughout Europe. In this case, Slovak young generation can see their future in Slovakia and not in other countries.

Our experiences from the solution of the project KEGA 008UPJŠ "Innovation of content, methods and forms of teaching practical exercises of chemical fields with direct participation of potential employers from practice" show that the Slovak industrial and institutional community in chemistry longs for such highly qualified graduates, but in Slovakia they are missing. Such graduates are educated by Slovak universities, but with the significant support of foreign and some domestic institutions, which have such a high-level instrument infrastructure. In Slovakia, such an instrument portfolio is missing at universities.

Based on the above-mentioned fact, it is necessary to create a study program within the field of chemistry in Slovakia, the graduates of which will be directly prepared for practice. However, for a student to see his real readiness for the labour market, he/she must gain vast instrumental experience during his/her studies. With such knowledge and skills, he/she will also shift the state economy based on science and research, which he/she will apply to industry and services. The teachers from Institute of Chemistry PF UPJŠ together with experts from practice involved in the creation of the professionally focused study program "Chemical Laboratory Technician – Specialist" will create materials for the elaboration of an accreditation file for quality education of the young generation ready for practice. The paper will present the starting points and procedures as well as the risks for launching a new study program.

Acknowledgements

This work was supported by Ministry of Education, Science, Research and Sport of the Slovak Republic under the grant no. KEGA 006UPJŠ-4/2021.

References

[1] E. A. Hanushek, L. Woessmann, The Knowledge Capital of Nations. Cambridge, MA: MIT Press, 2015, p.262.

Mesoporous Materials in Environmental Application

Ľ. Zauška[a]*, P. Pillárová[a], M. Almáši[a]
[a]Department of Inorganic Chemistry, Institute of Chemistry, Faculty of Science, Pavol Jozef Šafárik University in Košice, Moyzesova 11, 041 01 Košice, Slovak Republic
*l.zauska@gmail.com

Water is an essential part of our life. It is necessary for life being, biological and biochemical processes in the nature and human body and maintains heat balance of earth, etc. In decades, due to heavy industry, water ecology was decreased significantly. In European rivers, lakes and marines, high content of heavy metals [1], microplastics [2], and medicaments [3] were detected. Through water contamination, advanced water filtration technology could filtrate the majority of pollutants, which can change wastewater to service water. But these technologies are expensive, service cost is too high, and filtration media can not be reusable or recycled. The second majority problem is the toxicity of mentioned used media. But there are some methods how pollutants like heavy metal ions and organic compounds can be removed from wastewater without back elution from sorbent after filling it. The way is the ecologic oxidation of organic waste. Two conditions must be fulfilled. First, oxidation has to be established on physico-chemical reactions like photocatalysis [4] and second, the formation of kinetic stabile complexes or chelates with heavy metal ions on a solid matrix.

For ion capture, e.g. Cu^{2+}, Ni^{2+}, Cr^{6+} and NO_2^-, NO_3^-, CrO_4^{2-}, SO_4^-, Cl^- can be realised by ionic metal-organic frameworks (MOFs). These ionic materials (examples are cationic JUC-101 and anionic JUC-102) have nanoporous structures, and there is a possibility to chemisorb mentioned ions and make clusters or host-guest systems. There is also a possibility of using organosilane chelating agents attached to the substrate, specifically mesoporous silica. Depending on used organosilanes with organic function groups like -COOH, -OH, -SH, $-NO_2$, $-NH_2$, modified mesoporous silica will prefer specific cations. There is also a preference for bonds creations. Photocatalytic oxidation of organic pollutants and pathogens occurs on nanomaterials like TiO_2, ZnO_2, $BiVO_4$, etc. The photocatalytic effect arises during electron transfer from valence bands through the bandgap to the conduction band. This electron must be excited with UVA or visible light. Material doping with any atoms can reduce the required energy for electron transfer. This effect raises catalyst effectivity.

Our prepared materials SBA-16@N-TiO_2 and MIL-101 were characterised via analytical methods like Fourier-transformation infrared spectroscopy (FTIR), specifically, middle infrared attenuated total reflectance (MIR-ATR) and far infrared using CsI technique (FIR-CsI) on spectrophotometer IRTracer-100, Shimadzu Co. Nitrogen adsorption was realised at 77K in pressure range $p/p_0 = 0.05 – 0.95$ on APAP 2020 from Micromeritics Co. Surface area was determined with Brunauer-Emmett-Teller (BET) mathematical model and pore volume and pore diameter was characterised with Barret-Joyner-Halenda (BJH) method. Powder X-ray diffraction was also realised for TiO_2 phase and MIL-101 lattice cell determination. Angle range was set to 2θ 20-100º with speed scan $10º.min^{-1}$ on Ultima IV diffractometer from Rigaku Co. Thermal properties were studied with thermal analysis (TGA) and differential scanning calorimetry (DSC) with TGA Q500 from TA instruments Co. The samples were heated with a heating rate of $10ºC.min^{-1}$ in the air with a maximum of 800 °C. Texture properties and morphology of mesoporous silica were checked with the transmission and scanning electron microscope (TEM and SEM) TEM - JEM 2100F UHR, SEM - JSM 7600F from Jeol Co (see Figure 1). UV-VIS spectroscopy was used for quantification and effectivity of photocatalysis and ion capture. Organic compounds were determined in the range of 200-380 nm, and metal ions were detected in the range of 400-700 nm.

We have prepared two types of well-known materials with novel modifications and further tested them for water purification. Photocatalytic mesoporous silica with nanocrystalline anatase (TiO_2) surface modification had excellent sorption properties, and this nanomaterial has a self-cleaning effect. MIL-101(Fe)-NH_2 modified with Schiff base displayed good chelating properties for toxic metal ions (Ni^{2+}, Co^{2+} and Cr^{3+}), and there is no reverse elution of cations to the water.

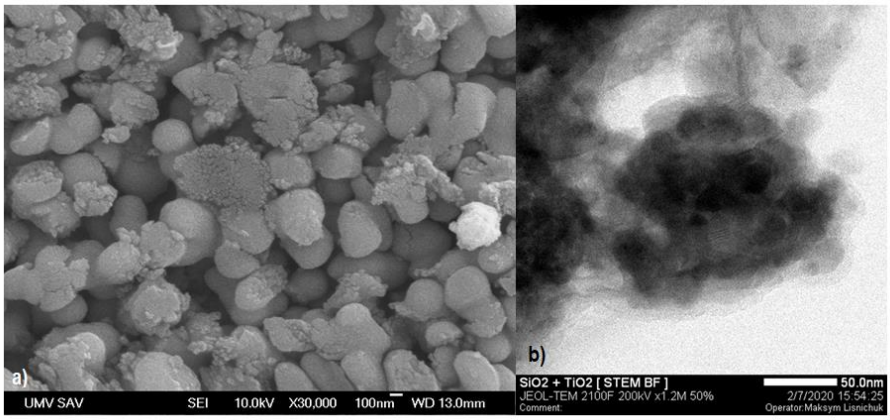

Figure 2 a) SEM image of SBA-16@N-TiO_2 and **b)** TEM image of SBA-16@N-TiO_2.

References

[1] B. L. Skjelkvåle et al., ICP Waters report 52/2000, Norwegian institute for water research (2000).
[2] Ch. Scherer et al., Sci. Total Environ. **10** (2020) 152.
[3] A. Al-Ahmad et. al., Spring. **37** (1999) 158.
[4] H. Park et. al., J. Photochem. Photobiol. C: Photochem. Rev. **15** (2013) 1.

Synthesis and Antiproliferative Evaluation of Novel 5-Fluorinated Indole Phytoalexins

M. Budovská[a]*, K. Krochtová[b], M. Kuba[a], V. Tischlerová[c], J. Mojžiš[c]
[a]Department of Organic Chemistry, Institute of Chemistry, Faculty of Science, Pavol Jozef Šafárik University in Košice, Moyzesova 11, 040 01 Košice, Slovak Republic
[b]Department of Biochemistry, Institute of Chemistry, Faculty of Science, Pavol Jozef Šafárik University in Košice, Moyzesova 11, 040 01 Košice, Slovak Republic
[c]Department of Pharmacology, Faculty of Medicine, Pavol Jozef Šafárik University in Košice, SNP 1, 040 11 Košice, Slovak Republic
*mariana.budovska@upjs.sk

Indole phytoalexins are known as low molecular mass secondary metabolites which are produced *de novo* by plants of the *Brassicaceae* family after exposure to biological (bacteria, fungi, viruses), physical (UV radiation, heat shock, injury), or chemical (heavy metals) stress. Indole phytoalexins are generally (*S*)-tryptophan derivatives and have different chemical structures [1]. Particularly, indole phytoalexins display antibacterial, antifungal, antiprotozoal, cancer chemopreventive and *in vitro* anti-proliferative activities. Indole phytoalexins have also antioxidative and anti-inflammatory properties [2].

This work provides information on the structure and synthesis of new 5-fluorinated indole phytoalexins. The design of target compounds is based on the bioisosteric replacement of a hydrogen atom with a fluorine atom at the C-5 position of indole phytoalexins. Evaluation of anti-proliferative effect showed that the 2'-(3,4-dichlorophenylamino) analogue of 5-fluorospirobrassinin was the most active against all tested cancer cell lines without causing toxicity to HUVEC cells. The structure-activity relationship (SAR) study revealed that prepared 5-fluoro analogues did not show improved anti-cancer activity compared to lead compounds, and the placement of a fluoro substituent at the C-5 position of the indole ring is not crucial to inducing cytotoxicity against a cancer cell line.

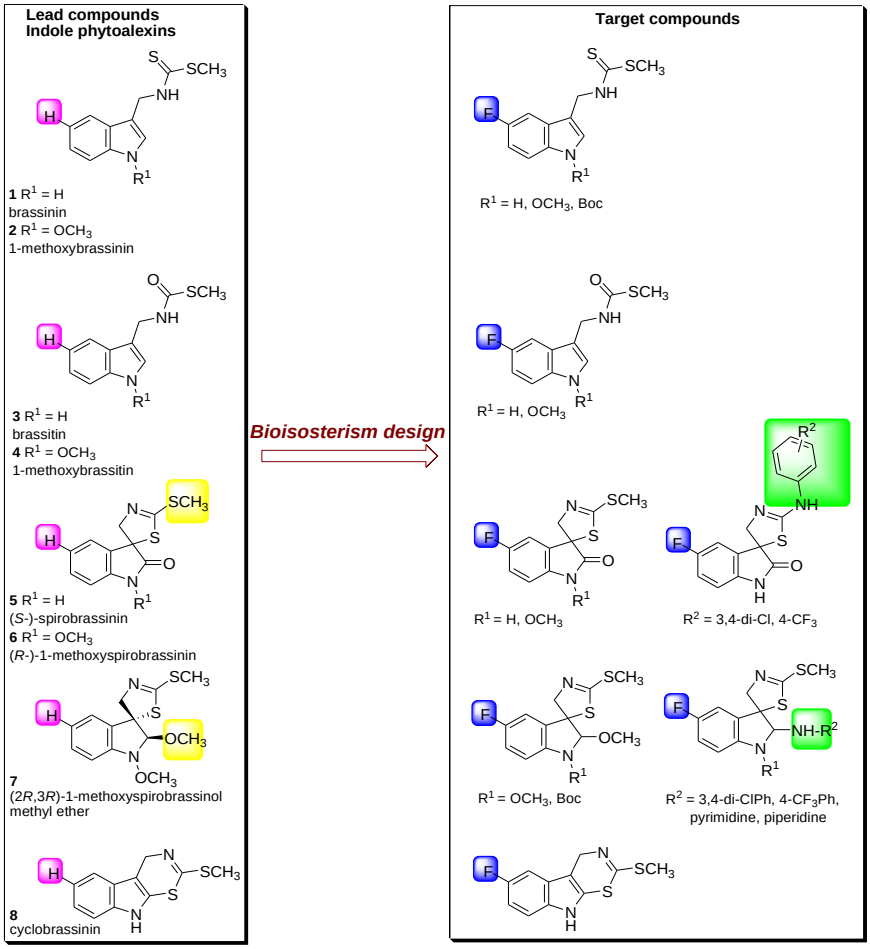

Figure 1 Indole phytoalexins and their bioisosteres.

Acknowledgements

The present study was supported in part by the Grant Agency of Ministry of the Education, Science, Research and Sport of the Slovak Republic (VEGA 1/0539/21 and VEGA 1/0138/20), and the Slovak Research and Development Agency under the contract No. APVV-16-0446.

References

[1] M. S. C. Pedras, A. Abdoli, RSC Adv. **7** (2017) 23633–23646.
[2] M. Chripkova, F. Zigo, J. Mojzis, Molecules **21** (2016) 1626–1640.

Design and Synthesis of Novel Biologically Active Proflavine Ureas

L. Janovec[a]*, E. Kováčová[a], M. Šemeláková[b], M. Kvaková[c], D. Kupka[d], D. Jager[d] and M. Kožurková[e, f]

[a]Department of Organic Chemistry, Institute of Chemistry, Faculty of Science, Pavol Jozef Šafárik University in Kosice, Moyzesova 11, 040 01, Košice, Slovak Republic

[b]Department of Medical Biology, Faculty of Medicine, Pavol Jozef Šafárik University in Kosice, Trieda SNP 1, 040 11 Kosice, Slovak Republic

[c]Department of Experimental Medicine, Faculty of Medicine, Pavol Jozef Šafárik University in Kosice, Trieda SNP 1, 040 11 Košice, Slovak Republic

[d]Institute of Geotechnics, Slovak Academy of Sciences, Watsonova 45, 040 01, Košice, Slovak Republic

[e]Department of Biochemistry, Institute of Chemistry, Faculty of Science, Pavol Jozef Šafárik University in Kosice, Moyzesova 11, 040 01 Košice, Slovak Republic

[f]Biomedical Research Center, University Hospital Hradec Králové, Sokolovska 581, 500 05 Hradec Králové, Czech Republic

*ladislav.janovec@upjs.sk

A novel series of proflavine ureas were synthesized on the basis of molecular modeling design studies [1]. The structure of the novel ureas was obtained from the pharmacological model, the parameters of which were determined from studies of the structure-activity relationship of previously prepared proflavin ureas bearing *n*-alkyl chains. The anticancer activity of the synthesized derivatives was evaluated against NCI-60 human cancer cell lines. The urea derivatives **azepyl**, **phenyl** and **phenylethyl** displayed the highest levels of anticancer activity, although the results were only a slight improvement over the **hexyl** urea, which was reported in a previous publication [2]. Several of the novel urea derivatives displayed GI_{50} values against HCT-116 cancer cell line which suggest the cytostatic effect of the compounds: **azepyl** – 0.44 μM; **phenyl** – 0.23 μM; **phenylethyl** – 0.35 μM; **hexyl** – 0.36 μM. In contrast, these novel urea derivatives exhibited levels of cytotoxicity three orders of magnitude lower than that of **hexyl** urea.

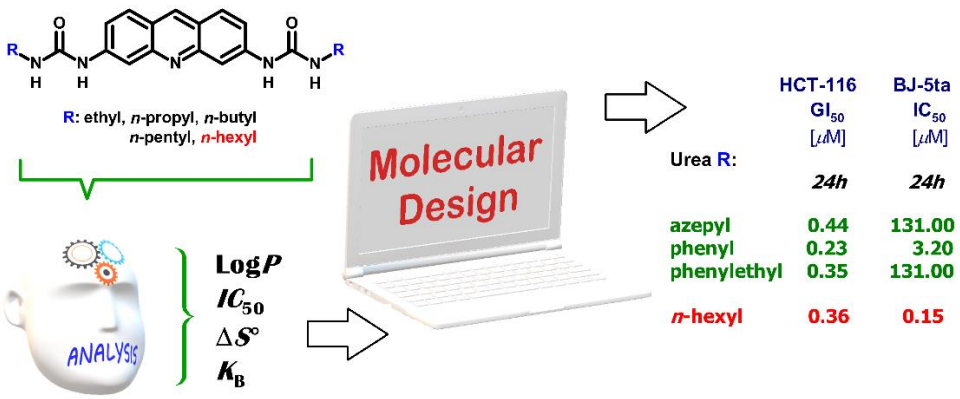

Figure 1 A strategy in the design of the novel acridine ureas.

Acknowledgements

The authors are also grateful to the National Institute of Health (NIH), National Cancer Institute Branch for the opportunity to use their Developmental Therapeutic Program (DTP) for the timely screening of our compounds using NCI-60 panels. This research was funded by the Ministry of Education, Science, Research and Sport of the Slovak Republic and the Slovak Academy of Sciences (SAS) (Slovak Grant Agency VEGA, grant No. 1/0016/18) and by the Czech Ministry of Health's (UHHK grant No. 00179906).

References

[1] L. Janovec, E. Kováčová, M. Šemeláková, M. Kvaková, D. Kupka, D. Jager, M. Kožurková, Molecules **26** (2021) art. no. 4860.

[2] M. Kožurková, D. Sabolová, L. Janovec, J. Mikeš, J. Koval', J. Ungvarský, M. Štefanišinová, P. Fedoročko, P. Kristian, J. Imrich, Bioorg. Med. Chem. **16** (2008) 3976–3984.

Stereoselective Synthesis of Cytotoxic Analogues of Natural Broussonetines and Penaresidins

T. Ponč áková[a]*, M. Fábian[a], M. Novotná[a], M. Martinková[a]
[a]Department of Organic Chemistry, Institute of Chemistry, Faculty of Science, Pavol Jozef Šafárik University in Košice, Moyzesova 11, 040 01 Košice, Slovak Republic
*tatiana.mitrikova@student.upjs.sk

Sphingolipids represent a widespread and interesting class of lipophilic compounds, which in addition to their pivotal structural roles in membrane construction are also involved in various significant cell signalling pathways and processes [1]. A general structural modulation of the basic sphingosine backbone of sphingolipids concerns its cyclisation into various types of conformationally constrained derivatives such as, for example, penaresidins and broussonetines.

Penaresidins A (**1**) and B (**2**) represent a special class of sphingolipid-derived compounds isolated by Kobayashi and coworkers [2] from the Okinawan marine sponge *Penares* sp. in 1991 (Figure 1). Moreover, the construction of the acetylated derivatives of **1** and **2** and their subsequent structural analysis assigned the relative configuration of the 2,3,4-trisubstituted ring [2]. The (2*S*,3*R*,4*S*) absolute stereochemistry of an azetidine core as well as the (*S*)-configuration of an alkyl side chain in these natural products was confirmed successively, by two research groups [3]. Both **1** and **2** were identified as potent actomyosin ATP-ase activators [2]. In addition, penaresidin B demonstrates cytotoxicity on murine lymphoma L1210 cells [4].

Broussonetines, including their stereoisomeric broussonetinines (Figure 1) represent a wide class of more than the 39 compounds isolated from the mulberry tree *Broussonetia kazinoki* by Kusano and coworkers [5]. Most of them possess a hydroxylated pyrrolidine unit with a variable 13-carbon side chain. The aforementioned common heterocyclic system is usually (2*R*,3*R*,4*R*,5*R*)-configured [5]. Theses sphingolipid-based copmounds were found to be potent and selective glycosidase inhibitors against various *β*-glycosidases obtained from various sources, with the IC_{50} values near to the nanomolar concentrations [5].

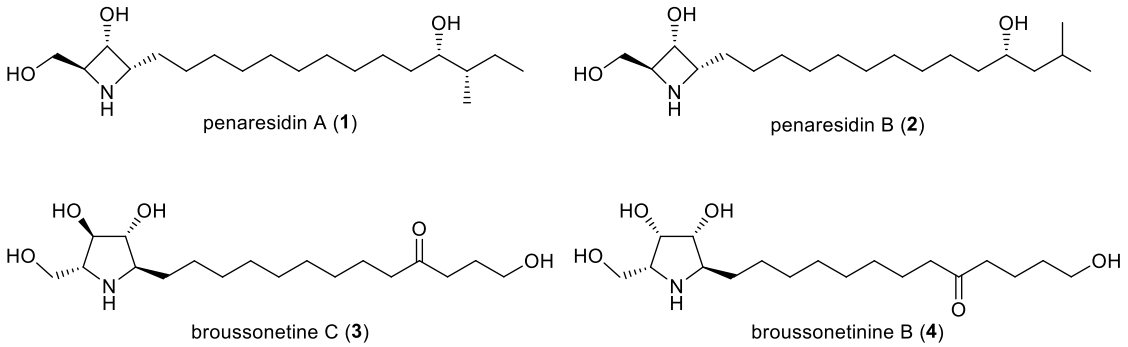

Figure 1 Representative structures of natural penaresidins and broussonetines.

Synthesis

We described the straightforward access to novel penaresidin- and broussonetine-based analogues bearing a simple alkyl side chain (compounds **5**.HCl and **6**.HCl, respectively) (Scheme 1). The construction of these alkaloids relies on a [3,3]-sigmatropic rearrangement to introduce the amino functionality, the late stage OCM reaction to install the hydrophobic segment, and NaH-mediated cyclization to create the heterocyclic unit. We envisioned that **5**.HCl and **6**.HCl would be constructed from intermediates **7** and **8**, respectively, using the olefin cross metathesis with tetradec-1-ene. The corresponding heterocyclic core in **7** and **8** would be obtained through the intramolecular S_N2 type reaction of the activated products **9** and **10** derived from the common derivative **11**. The novel C-N bond in **11** would be introduced via aza-Claisen rearrangement of the allylic substrate **12** prepared from D-glucose. The synthesized analogues **5**.HCl and **6**.HCl will be evaluated for their antiproliferative/cytotoxic activities on a panel of human malignant cell lines using a colourimetric MTT assay.

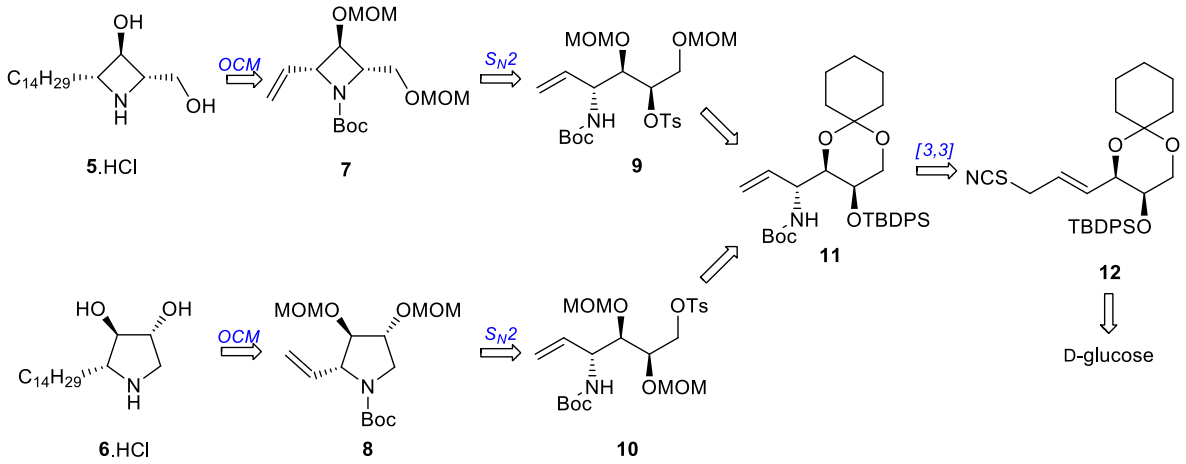

Scheme 1 Retrosynthetic analysis toward target compounds **5**.HCl and **6**.HCl.

Acknowledgements

Financial support from Slovak Grant Agency VEGA, grant no. 1/0375/19, and also from the Slovak Research and Development Agency under contract no. APVV-14-0883 is gratefully acknowledged. This publication is also the result of the project implementation: Open scientific community for modern interdisciplinary research in medicine (OPENMED), ITMS2014+: 313011V455 supported by the Operational Programme Integrated Infrastructure, funded by the ERDF.

References

[1] Y. Hirabayashi, Y. Igarashi, A. H. J. Merrill, *Sphingolipid Biology*; Springer-Verlag: Tokyo, 2006.
[2] J. Kobayashi, J. Cheng, M. Ishibashi, M. R. Walchli, S. Yamamura, Y. Ohizumi, J. Chem. Soc.-Perkin Trans. **1** (1991) 1135-1137.
[3] (a) H. Takikawa, T. Maeda, K. Mori, Tetrahedron Lett. **36** (1995) 7689–7692; (b) J. Kobayashi, M. Ishibashi, Heterocycles **42** (1996) 943–970; (c) J. Kobayashi, M. Tsuda, J. F. Cheng, M. Ishibashi, H. Tatikawa, K. Mori, Tetrahedron Lett. **37** (1996) 6775–6776; (d) H. Takikawa, T. Maeda, M. Seki, H. Koshino, K. Mori, J. Chem. Soc., Perkin Trans. **1** (1997) 97–111.
[4] K. Ohshita, H. Ishiyama, Y. Takahashi, J. Ito, Y. Mikami, J. Kobayashi, Bioorg. Med. Chem. **15** (2007) 4910–4916.
[5] M. Shibano, D. Tsukamoto, G. Kusano, Heterocycles **57** (2002) 1539-1553 and references cited therein.

Synthesis and *in vitro* Biological Profile of *N*-Acetyl-D-*ribo*-phytosphingosine and its 2-Epimer

K. Vargová[a]*, M. Fabišíková[a], S. Fazekašová[a], M. Martinková[a]
[a]Department of Organic Chemistry, Institute of Chemistry, Faculty of Science, Pavol Jozef Šafárik University in Košice, Moyzesova 11, 040 01 Košice, Slovak Republic
*kristina.vargova@student.upjs.sk

Skin aging is the sum of intrinsic aging and photoaging caused by repeated exposure to ultraviolet light. The photoaged skin shows coarse, deep wrinkles, dyspigmentation and telangiectasia. The alteration in collagen, the major structural component of the dermis, are thought to be responsible for wrinkle formation [1,2]. In skin aging are characteristic decreased procollagen expression and increased matrix metalloproteinases. Actual research is focused on searching for topical agents that prevent or retard cutaneous aging. For their effects on UV-induced MMP-1 expression in human dermal fibroblasts, several lipids have been studied [1]. D-*ribo*-Phytosphingosine **1** as well as its analogues such as *N*-acetyl-D-*ribo*-phytosphingosine **2**, tetraacetyl-D-*ribo*-phytosphingosine **3** and *N*-salicyloyl-D-*ribo*-phytosphingosine **4** demonstrate interesting anti-aging activity (Fig. 1) [1,2]. In 2007, Farwick and co-workers revealed that derivative **4** significantly increases the synthesis of procollagen-I by human adult dermal fibroblasts *in vitro* [2]. Sphingolipid **4** is expected to be a promising lead compound for novel therapeutic agents based on their ability to repair of the photoaged skin.

It should be noted that **1**, originally isolated from the mushroom *Amanita muscaria* [3] in 1911, is the principal sphingoid base in plants, mushrooms, yeasts, and other microorganisms. Recent studies on *Saccharomyces cerevisiae* have confirmed its key role as a signalling molecule in heat stress response [4]. In man, the amide-linked derivatives of **1**, colloquially referred to as "phytoceramides", occupy the uppermost layer of the epidermis and thus contribute to the generation of the water permeability barrier to prevent lethal dehydration [4].

These interesting biological findings have stimulated our synthetic effort and thus we present here a straightforward approach toward *N*-acetyl-D-*ribo*-phytosphingosine **2** and its 2-epimer **5** from D-ribose as the starting chiron.

As shown in our synthetic plan (Figure 1), the target compounds **2** and **5** would be constructed from the corresponding isothiocyanates **9** and **10**, respectively. The novel C-N bond in **9** and **10** could be introduced via a [3,3]-sigmatropic rearrangement of allylic thiocyanate **8** derived from the synthon **7** using HWE olefination, followed by DIBAl-H reduction. The desired template **7** was obtained from the protected L-erythrofuranose **6** through the Wittig reaction and subsequent olefin cross metathesis with tedradec-1-ene.

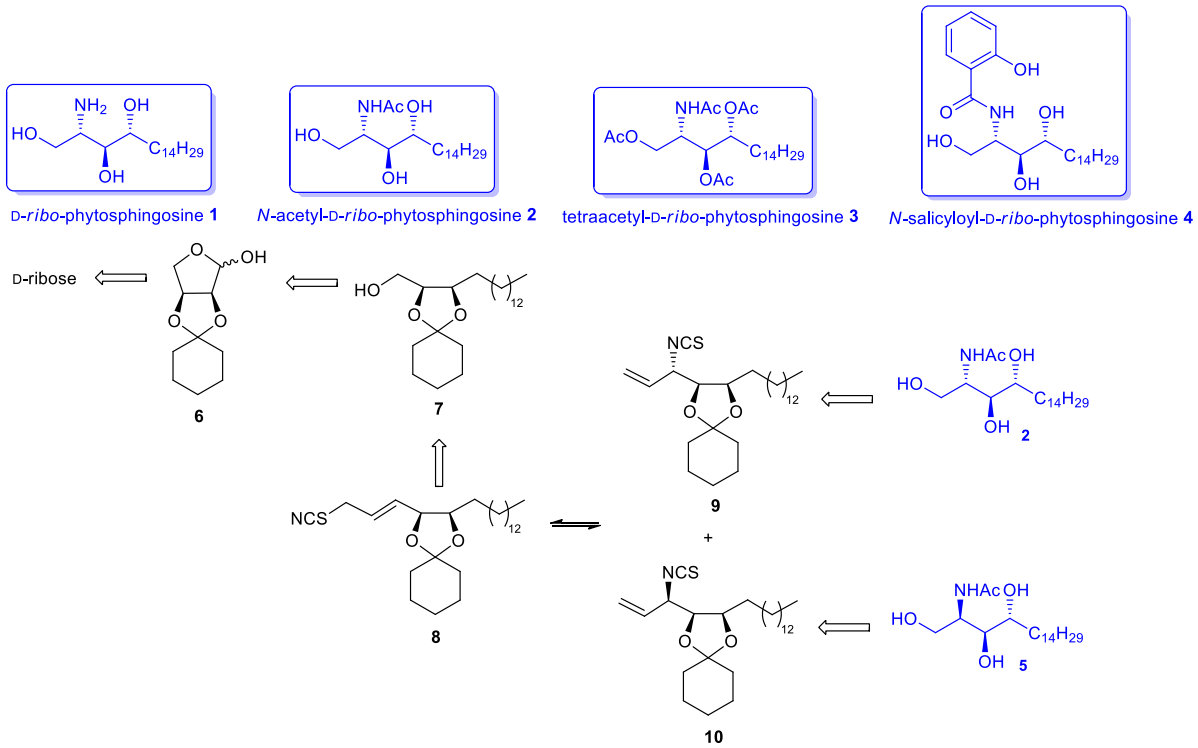

Figure 1 Synthetic plan toward *N*-acetyl-D-*ribo*-phytosphingosine **2** and its 2-epimer **5**.

Acknowledgements

Financial support from Slovak Grant Agency VEGA, grant no. 1/0375/19, and, also from the Slovak Research and Development Agency under contract no. APVV-14-0883 is gratefully acknowledged. This publication is also the result of the project implementation: Open scientific community for modern interdisciplinary research in medicine (OPENMED), ITMS2014+: 313011V455 supported by the Operational Programme Integrated Infrastructure, funded by the ERDF.

References

[1] S. Cho, H. Ho Kim, M. Jung Lee, S. Lee, Ch.-S. Park, S.-J. Nam, J.-J. Han, J.-W. Kim, J. Ho-Chung, J. Lipid Res. **49** (2008) 1235-1245.
[2] M. Farwick, R. E. B. Watson, A. V. Rawlings, U. Wollenweber, P. Lersch, J. J. Bowden, J. Y. Bastrilles, C. E. M. Griffiths, Int. J. Cosmet. Sci. **29** (2007) 319-329.
[3] J. Zellner, Monatsh. Chem. **32** (1911) 133–142.
[4] B. Školová, A. Kováčik, O. Tesař, L. Opálka, K. Vávrová, Biochim. Biophys. Acta **1859** (2017) 824–834 and reference cited therein.

Synthesis, Characterisation and DNA-Binding Activity of Acridine Based Chalcones

M. Vilková[a], D. Sabolová[b], M. Garberová[b], Z. Kudličková[a]*
[a]NMR Laboratory, Institute of Chemistry, Faculty of Science, Pavol Jozef Šafárik University in Košice, Moyzesova 11, 040 01 Košice, Slovak Republic
[b]Department of Biochemistry, Institute of Chemistry, Faculty of Science, Pavol Jozef Šafárik University in Košice, Moyzesova 11, 040 01 Košice, Slovak Republic
*zuzana.kudlickova@upjs.sk

Chalcones (1,3-diarylpropanones) are natural substances that are easy to synthesize and modify, in addition, they have a wide range of biological properties (antibacterial, antioxidant, antineoplastic, cytotoxic, antiulcer, antidepressant, anxiolytic, and anti-inflammatory). Hybrid molecules not only have more favorable properties such as enhanced activity and improved specificity, but also could overcome the drug resistance, so hybridization of chalcone moiety with other anticancer pharmacophores represents a promising strategy to develop novel anticancer agents with high efficacy. Chalcones and chalcone hybrids with other anticancer pharmacophores exhibited promising *in vitro* and *in vitro* activity against both drug-susceptible and drug-resistant cancers as novel anticancer candidates [1,2].
Acridine derivatives, due to the unique planar ring, can act as effective anticancer agents as DNA intercalators or topoisomerase inhibitors [3,4].
Two series of novel chalcone derivatives containing acridin-9-yl or acridin-4-yl moiety have been synthesized using Claisen-Schmidt condensation. The general methods for synthesis of target chalcones are depicted in Schemes 1, 2. Acridine-9-carbaldehyde (**1**) and acridine-4-carbaldehyde (**3**) were synthesized *via* Klanderman's method previously reported by our group [5]. The base-catalysed condensation of aldehyde **1** or **3** with substituted acetophenones in ethanol at room temperature gave chalcones **2a**–**g** and **4a**–**c,e,f** in 76–96 % yield using modified procedure described by Lahtchev [6]. Surprisingly, the treatment of acridin-4-carbaldehyde (**3**) with 4-bromoacetophenone in the presence of NaOH afforded 1,5-diphenyl-3-(acridin-4'-yl)pentane-1,5-dione (**4g**) instead of appropriate chalcone (Scheme 2). Structures of compounds were confirmed by NMR, IR and HR-MS spectral data.

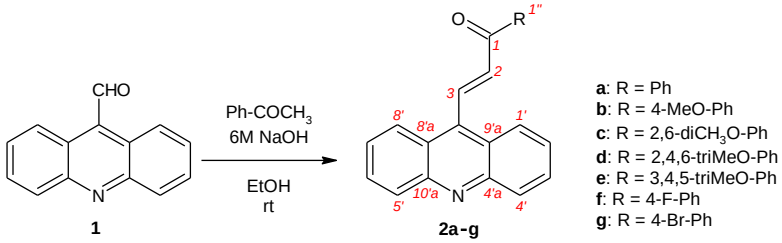

Scheme 1 Synthesis of substituted (2*E*)-3-(acridin-9-yl)-1-phenylprop-2-en-1-ones **2a**–**g**.

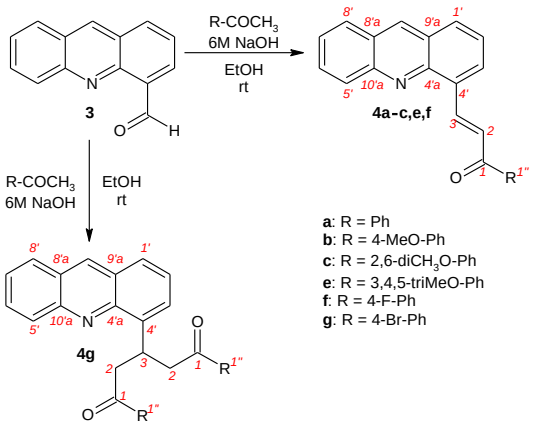

Scheme 2 Synthesis of substituted (2*E*)-3-(acridin-4'-yl)-1-phenylprop-2-en-1-ones **4a**–**c,e,f** and 1,5-diphenyl-3-(acridin-4'-yl)pentane-1,5-dione **4g**.

In the present work we have also investigated DNA binding activity of (2E)-3-(Acridin-4'-yl)-1-(3",4",5"-trimethoxyphenyl)prop-2-en-1-one (**4e**) using spectral methods as UV-Vis, fluorescence and CD spectroscopy. The achieved results obtained from spectroscopic analysis confirmed that derivative **4e** interact with CT DNA through bimodal binding mode, that means intercalation and groove-binding. The estimated Stern-Volmer constants (K_{sv}) are in the range from 1.28×10^3 M^{-1} to 1.37×10^3 M^{-1}. The current work may be supportive to the research of the anti-cancer mechanism of new hybrid chalcones and the design of the new potent anti-cancer drugs.

Acknowledgements

This work was supported by the Grant Agency of Ministry of the Education, Science, Research and Sport of the Slovak Republic VEGA 1/0016/18 and 1/0138/20.

References

[1] D. K. Mahapatra, S. K. Bharti and V. Asati, Eur. J. Med. Chem. **98** (2015) 69-114.

[2] F. Gao, G. Huang and J. Xiao, Med. Res. Rev. **40** (2020) 2049-2084.

[3] M. Gensicka-Kowalewska, G. Cholewiński and K. Dzierzbicka, RSC Adv. **26** (2017) 15776-15804.

[4] D. M. Ferguson, B. A. Jacobson, J. Jay-Dixon, M. R. Patel, R. A. Kratzke, A. Raza. Anticancer Res. **35** (2015) 5211-5218.

[5] M. Vilková, L. Ungvarská-Mąľučká, J. Imrich, Magn. Reson. Chem. **54** (2016) 8-16.

[6] K. L. Lahtchev, D. I. Batovska, S. P. Parushev, V. M. Ubiyvovk, A. A. Sibirny, Eur. J. Med. Chem. **43** (2008) 2220-2228.

Cathode Material for Li-S Battery Dopped by Pyrite

D. Capková[a], T. Kazda[b], J. Macko[a], O. Petruš[c], A. Baskevich[d], E. Shembel[d], A. Straková Fedorková[a]

[a] Department of Physical Chemistry, Institute of Chemistry, Faculty of Sciences, Pavol Jozef Šafárik University in Košice, Moyzesova 11, 040 01, Košice, Slovak Republic

[b] Department of Electrical and Electronic Technology, Faculty of Electrical Engineering and Communication, Brno University of Technology, Technická 10, 616 00, Brno, Czech Republic

[c] Institute of Materials Research, Slovak Academy of Sciences, Watsonova 47, 040 01 Košice, Slovak Republic

[d] Ukrainian State Chemical Technology University, Haharina Ave 8, 490 00, Dnipro, Ukraine

*dominika.capkova@upjs.sk

In an effort to reduce our dependence on fossil fuels, the energy storage systems that can be coupled to renewable sources need to be developed and adapt, e.g., solar, wind, wave. Lithium-sulfur (Li-S) batteries are one of the most promising systems that can satisfy requirements for energy storage devices [1]. The theoretical energy density of Li-S battery (~2600 Wh kg^{-1}) is up to five times greater than that of commercial Li-ion battery ($LiFePO_4$ - 580 Wh kg^{-1}). Furthermore, sulfur is abundant element, environmentally friendly, low-cost material and the theoretical capacity of sulfur is very high (1675 mAh g^{-1}) [2].

The electrochemical performances of the S/C/10 % FeS_2 and S/C/5 % FeS_2 electrodes are shown in Figure 1. The discharge capacities of the S/C/10 % FeS_2 electrodes are 720.2, 553.0, 418.3 and 297.0 mAh g^{-1} at the current rate of 0.2, 0.5, 1 and 2 C, respectively. In addition, when the current rate returns to 0.2 C, a stable discharge capacity of 787.9 mAh g^{-1} is recovered. In comparison, the discharge capacities of the S/C/5%FeS2 electrodes are 748.3, 421.6, 251.4 and 127.8 mAh g^{-1} at the current rate of 0.2, 0.5, 1 and 2 C, respectively.

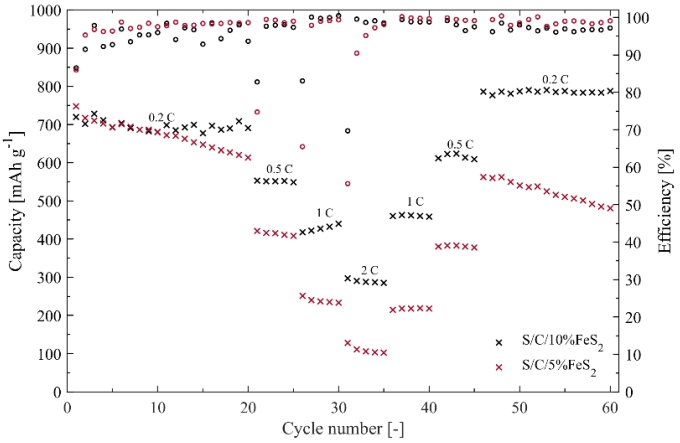

Figure 1 The dischagde capacities and the efficiency of the S/C/10 % FeS_2 and S/C/5 % FeS_2 cathodes.

Acknowledgements

This research was sponsored by the following projects: APVV-20-0138, Development of Novel 3D Materials for Post Lithium Ion Batteries with High Energy Density; APVV-20-0111, Towards Lithium Based Batteries with Improved Lifetime; iCoTS No. 313011V334, Innovative Solutions for Propulsion, Power and Safety Components of Transport Vehicles; VVGS-PF-2021-1756, Development of Electrode Materials for Lithium-sulfur Batteries; VEGA 1/0074/17, Nanomaterials and Nanostructured Layers with Specific Functionality, VEGA 1/0294/22, Porous Coordination Polymers for Environmental Applications, and specific graduate research of the Brno University of Technology No. FEKT-S-20-6206.

References

[1] J. Xiulei et al., Nature Materials **8** (2009) 500-506.
[2] D. Capková et al., Electrochimica Acta **354** (2020) 136640.

Surface Morphology of Zinc After 4 Weeks of Immersion in Hanks´ Solution

R. Gorejová[a]*, V. Čákyová[a], R. Oriňaková[a]
[a]Department of Physical Chemistry, Institute of Chemistry, Faculty of Science, Pavol Jozef Šafárik University in Košice, Moyzesova 11, 040 01 Košice, Slovak Republic
*radka.gorejova@student.upjs.sk

Biodegradable metals serving as temporary bone scaffolds are usually prepared from magnesium, iron, and zinc. Among them, zinc has received the most attention recently due to its favorable degradation properties in the environment of the simulated body fluids [1]. Biodegradation can be studied both electrochemically and by the static immersion tests. The electrochemical tests are a quick and simple method for the initial testing of absorbable materials. However, immersion tests can provide more accurate information about processes like those in the human body. In our work, zinc samples were prepared via uniaxial compression of raw powders into the form of pellets with a diameter of 12 mm. Subsequently, samples were sintered in an inert atmosphere at 350 °C in a tube furnace. Sintered samples were manually ground with three different grids and ultrasonically cleaned in acetone and 96 vol% ethanol. Ca^{2+}containing Hanks´ solution was prepared and metallic pellets were immersed into 50 ml of fresh corrosive medium. Temperature over the experiment was held at 37 °C for 4 weeks. The surface morphology of the non-corroded and corroded samples was studied using Scanning electron microscopy (SEM) coupled with Energy-dispersive x-ray analysis (EDX). While the non-corroded Zn sample surface (Figure 1a) consisted of pure zinc and only 3.8 w t% of oxygen originating in zinc oxide, the surface of the corroded sample was covered in corrosion products with several spherical deposits containing phosphorus and calcium (Figure 1b). The used corrosive solution contained Ca^{2+} and HCO^{-3} ions therefore precipitation of calcium phosphate took place in the case of studied samples (Figure 1b, inset). The corrosion speed of the pure zinc could not be calculated from the mass loss experiments due to the mass growth of corrosion products on the sample surface over the first 4 weeks. However, the pH of Hanks´ solution increased by ~0.4 after the first month of immersion. Corrosion speed of pure zinc sample evaluated electrochemically (in Hanks´ solution at 37 °C using the three-electrode system) was 0.549±0.07 $mmyear^{-1}$ Cytocompatibility of the deposited corrosion products and the corrosion rate after longer immersion needs to be further studied for biomaterial complex examination.

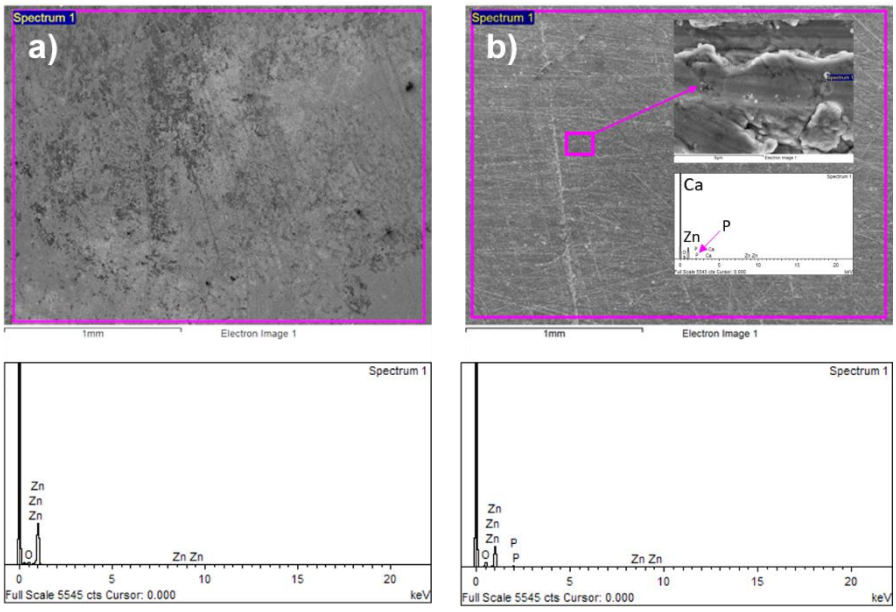

Figure 1 Surface of Zn sample before (a) and after (b) 4 weeks of immersion in Hanks´ solution at 37 °C.

Acknowledgements

This work was supported by the Slovak Research and Development Agency (project APVV-20-0278).

References

[1] P. K. Bowen, J. Drelich, J. Goldman, Adv. Mater. **25** (18) (2013) 2577-2582.

Highly Porous Iron/Iron-Nickel Metal Foams for Catalysis of Hydrogen Evolution Reaction

A. Gubóová [a]*, R. Oriňaková[a], M. Strečková[b], M. Paračková[a]
[a]Department of Physical Chemistry, Institute of Chemistry, Faculty of Science, Pavol Jozef Šafá ik University in Košice, Moyzesova 11, 040 01 Košice, Slovak Republic
[b]Institute of Materials Research, Slovak Academy of Sciences, Watsonova 47, 040 01 Košice, Slovak Republic
*alexandra.guboova@student.upjs.sk

Hydrogen is a clean energy alternative to fossil fuel, and it plays crucial role in development of renewable energy due to its recyclability and near zero-carbon-emission. Among various techniques of generating hydrogen, water electrolysis is considered as the most efficient process with high-purity product [1]. For efficient production of hydrogen from water, the development of non-noble-metal catalyst for hydrogen evolution is essential. Great efforts have been made to replace platinum as the best catalyst for hydrogen evolution. The most high-effective non- noble metal HER catalysts are based on transition metals such as Co, Ni, Fe, Mo, and their compounds. Hydrogen production by electrolysis in alkaline environment is the trend of industrial development.

In electrocatalysis, porous electrodes are used to decrease the reaction overpotential by increasing the real surface area [2]. In recent years porous metal materials are widely used due to their exceptional properties such as high porosity, strength and durability, outstanding electrical and thermal conductivity, large specific surface area, and excellent permeability. Among the porous metal materials, nickel ones have the advantages of salt and alkali corrosion resistance [3].

For this work, iron and iron-nickel metal foams were prepared by dissolving gelatine in distilled water and subsequently mixing in carbonyl iron powder and nickel powder. Samples were prepared by impregnating polyurethane foam with metal powders/gelatine suspension and then sintered at 1120 °C to obtain desired porous structure.

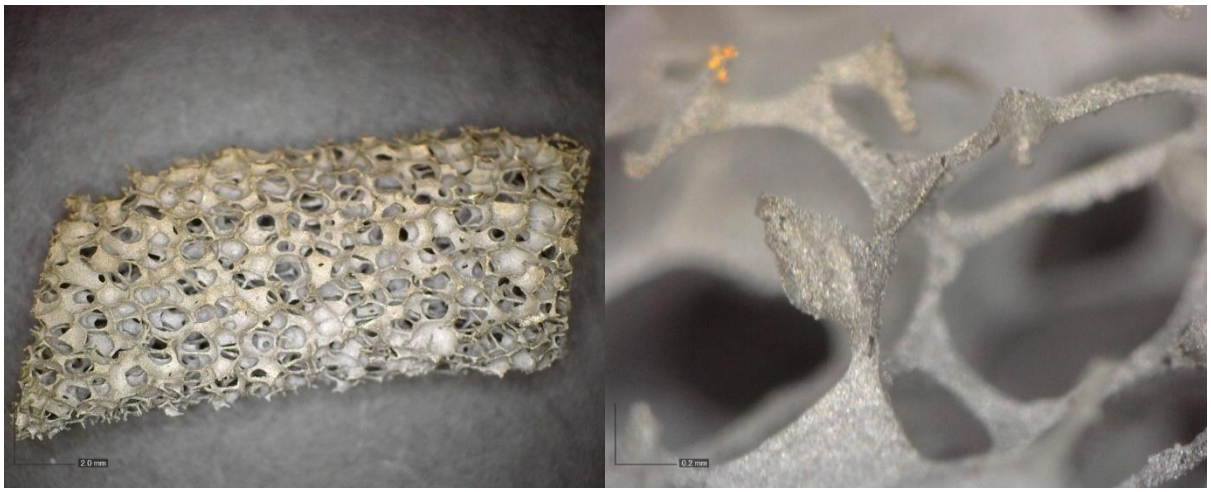

Figure 1 Images of iron foam porous structure at 20x and 200x magnification, respectively.

To evaluate catalytic activity of samples, electrochemical measurements were performed in alkaline media (1M NaOH) in three electrode system at ambient conditions. For a working electrode, a metal foam was used. A saturated calomel electrode (SCE) and a large area platinum foil were used as the reference and the counter electrode, respectively Tafel slopes derived from polarization curves and polarization curves themselves were obtained. All samples (*Fe w/15 % Ni, Fe w/5 % Ni, and pure Fe*) exhibited high electrocatalytic activity with value of overpotential to achieve a cathodic current density of 10 $mA.cm^{-2}$ being -294 mV for *Fe w/15 % Ni* sample. Tafel slope for this catalyst with value as low as 39.79 mV/dec indicates that the reaction took place via Heyrovsky-Tafel mechanism.

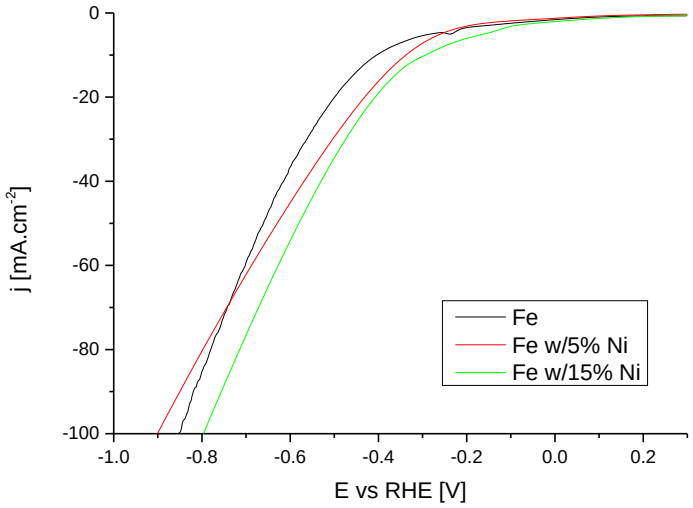

Figure 2 Polarization curves of iron and iron-nickel foams in 1M NaOH.

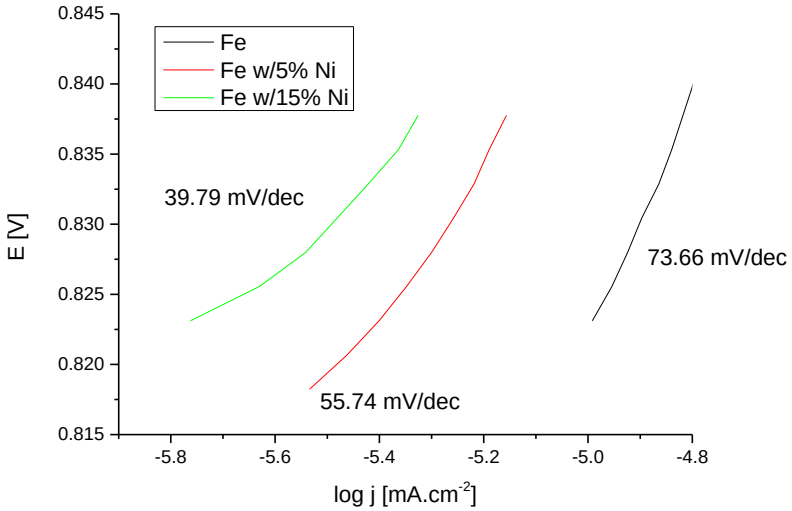

Figure 3 Tafel slopes for iron and iron-nickel foams with respective b-constant values.

Acknowledgements

This work was supported by Grant Agency of Slovak Academy of Sciences, project no. VEGA 1/0095/21 (Application of innovative nano catalysts and DFT simulations for efficient hydrogen production), Slovak Research and Development Agency under the contracts no. APVV-20-0299 (Electrocatalysts for efficient hydrogen production for future electrolysers and fuel cells) and no. APVV-20-0576 (Green ambitions for sustainable development (European Green Agreement in the context of international and national law).

References

[1] Z. Li, W. Niu, Z. Yang, A. Kara, Q. Wang, M. Wang, Y. Yang, Energy Environ. Sci. **13** (2020) 3110-3118.
[2] C Hitz, A Lasia, J. Electroanal. Chem. **500** (1–2) (2001) 213-222.
[3] H. Li, R. Liu, J. Chen, Z. Wang, X. Xiong, J. Mater. Res. Technol. **9** (3) (2020) 3149-3157.

Determination of Active Surface Area of Unmodified Screen Printed Carbon Electrode Compared to Modified by Polypyrrole and Nickel Nanoparticles

F. Chovancová[a]*, I. Šišoláková[a], J. Shepa[a], R. Oriňaková[a]
[a]Department of Physical Chemistry, Institute of Chemistry, Faculty of Science, Pavol Jozef Šafárik University in Košice, Moyzesova 11, 040 01 Košice, Slovak Republic
*frederika.chovancova1@student.upjs.sk

Insulin is synthesized in the beta cells of the pancreatic islets as a single chain precursor (proinsulin) from which a connecting peptide (C-peptide) is removed to yield the active insulin molecule. It is an anabolic hormone that regulates glucose levels and affects the metabolism of lipids, proteins and amino acids [1]. Diabetes is known as a chronic metabolism disorder with an amount number of patients worldwide [2]. The dysfunction of insulin secretion by B-cells of Langerhans caused hyperglycaemia (glucose level higher than 8 mmol/L) [3]. As a result, patients with diabetes face a higher risk of cardiovascular and renal failure [4].
Nowadays, the third generation of enzymatic glucose sensors is commercially used to monitor the level of glucose. However, these sensors are limited by the properties of an enzyme called glucose oxidase (GOx). Therefore, scientists have been developing electrochemical insulin sensors as a new diagnostics method [5]. Electrochemical insulin sensors have stood out due to their direct electrocatalytic detection and suitable analytical properties like high sensitivity, excellent selectivity, rapid response and low cost [6].
This work deals with developing an electrochemical sensor to determine insulin based on screen printed carbon electrodes (SPCE) modified by polypyrolle and nickel nanoparticles NiONPs/PPY/SPCE. The active surface areas of unmodified SPCE and NiONPs/PPY/SPCE were determined in a solution consisting of 1 mM $K_4[Fe(CN)_6]$ / 1 mM $K_3[Fe(CN)_6]$ and 1 M KCl via the electrochemical method - cyclic voltammetry. Active surface areas were calculated according to the Randles-Sefčik equation. The active surface area of unmodified SPCE was 0,31 cm^2, and nanomodified SPCE was 0,52 cm^2. After modification active surface area of the electrode is increased by more than 60 %.

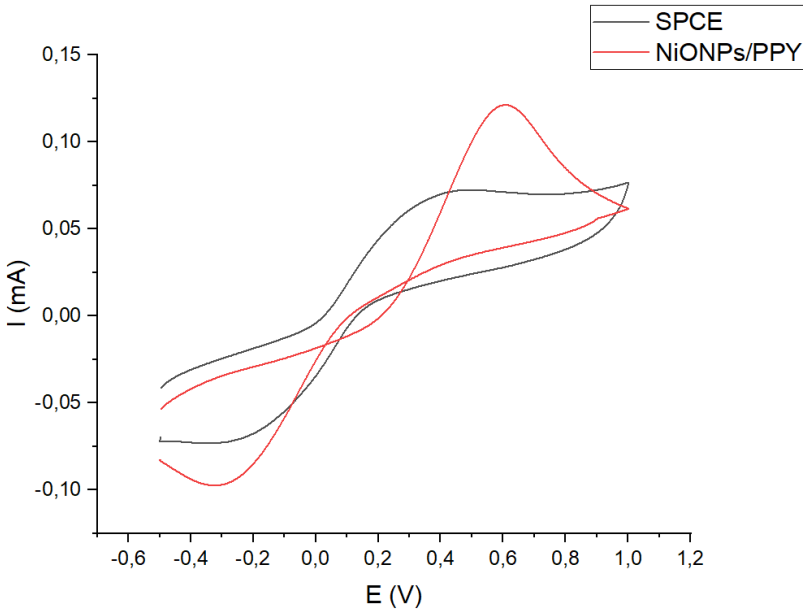

Figure 1 Cyclic voltammogram of 1 mM $K_4[Fe(CN)_6]$ / 1 mM $K_3[Fe(CN)_6]$ and 1 M KCl of unmodiefied SPCE (black line) and NiONPs/PPY/SPCE (red line).

Acknowledgements

This work has been supported by the APVV-PP-COVID-20-0036 and Visegradfound project number 22020140.

References

[1] A. K. Srivastava, P. Bajpai, and A. Jain, Elsevier Ltd. **1** (2018).

[2] J. Hovancová, I. Šišoláková, P. Vanýsek, R. Oriňaková, I. Shepa, M. Kaňuchová, N. Király, M. Vojtko, P. Čudek, A. Oriňak, J. Electroanal. Chem. **878** (2020) 114589.
[3] I. Šišoláková, J. Hovancová, R. Oriňaková, A. Oriňak, L. Trnková, I. Tříšková, Z. Farka, M. Pastucha, J. Radoňák, J. Electroanal. Chem. **860** (2020) 113881.
[4] I. Šišoláková, J. Hovancová, F. Chovancová, R. Oriňaková, I. Maskaľová, A. Oriňak, J. Radoňák, Electroanalysis **33** (2021) 627.
[5] I. Šišoláková, J. Hovancová, R. Oriňaková, A. Oriňak, L. Trnková, D. R. García, J. Radoňák, Bioelectrochemistry **130** (2019) 107326.
[6] J. Hovancová, I. Šišoláková, R. Oriňaková, A. Oriňak, J. Solid State Electrochem. **21** (2017) 2147–2166.

Porosity Dependence of Corrosion Parameters of Sintered Iron Samples

M. Kupková[a], M. Kupka[b], A. Morovská Turoňová[c]*
[a]Institute of Materials Research of SAS, Watsonova 47, 040 01 Košice, Slovak Republic
[b]Institute of Experimental Physics of SAS, Watsonova 47, 040 01 Košice, Slovak Republic
[c]Department of Physical Chemistry, Institute of Chemistry, Faculty of Science, Pavol Jozef Šafárik University in Košice, Moyzesova 11, 040 01, Košice, Slovakia
*andrea.morovska.turonova@upjs.sk

People have made useful things from metallic powders throughout the ages. In the present days, powder-forming routes are also used for fabricating various medical devices, which can save the human life and/or improve its quality. To do their job well, these devices have to be made from materials, which meet specific mechanical and chemical requirements. Prospective temporary implants, such as coronary stents or synthetic bone grafts, are expected to corrode at a rate that match the rate at which the tissue heals and regenerates, and to maintain mechanical integrity until the surrounding tissue becomes able to resist acted loads itself.

This contribution reports on preliminary results concerning corrosion parameters of a sintered iron, one of prospective biodegradable materials for temporary implantable medical devices.
Water-atomized iron powder, Höganäs ASC 100.29 grade, was die-pressed to prismatic bars (20mm×4mm×4mm) under compaction pressures of 100, 200, 400 and 600 MPa. The compacts were sintered at the temperature of 1120 ºC for 60 minutes in the H_2 atmosphere. Density of sintered compacts was obtained by weighing the compacts and measuring their dimensions. Obtained density and theoretical density of iron enabled to evaluate the porosity of specimens.
Taking into account the shape of pores and the total porosity of samples obtained, it was possible to assume that the pores formed a continuous inter-connected bar-spanning structure [1]. In such a situation, void spaces in a sintered body significantly enlarged the metal - environment interfacial area, which played an important role in the corrosion behaviour of sintered materials.

Potentiodynamic polarization measurements were carried out in a conventional three-electrode setup with the potentiostat PARSTAD 4000. A saturated calomel electrode (SCE) was used as the reference electrode, platinum acted as a counter electrode. An uncoated area of about 1 cm^2 of an otherwise coated surface of sintered iron sample acted as a working electrode. To simulate the internal environment of the human body, near-neutral Hanks' solution maintained at a temperature of 37ºC was used as an electrolyte. The samples were kept immersed in the electrolyte for 2 hours in order to stabilize the corrosion potential E_{corr} before the polarization curves began to be recorded. During the measurement, the potential varied from −250 mV to +250 mV at a rate of 0.16 mV/s.
Data obtained from potentiodynamic polarization measurements were converted to the corresponding Tafel plots. Corrosion characteristics were evaluated by the Tafel extrapolation technique applied to these Tafel plots. Note that current densities were evaluated by use of the electrode's geometric surface area exposed to the electrolyte, so the obtained current densities are actually the apparent ones. The values of E_{corr} and i_{corr} as functions of porosity are presented in Figure 1 a, b. It can be seen that the corrosion parameters of sintered iron samples varies significantly with the sample porosity.
To gain insight into the behaviour of sintered iron, the behaviour of a simpler model system undergoing dissimilar-metal-type corrosion has been considered [2]. It was supposed that the dissolution of iron (anodic reaction) took place on the outer surface of specimen as well as on the surfaces of inner walls of pores flooded with an electrolyte, while the reduction of dissolved oxygen (cathodic reaction) took place only on the outer surface of specimen. It was also supposed that both the solid phase and the electrolyte conducted electricity well enough to ignore potential drops except for that across the iron-electrolyte interface.

The corrosion potential and corrosion current density provided by the model were functions of areas of cathodic and anodic regions of the surface in contact with the electrolyte. It was found that the corrosion potential decreased with increasing porosity of samples. In the light of results obtained for a model system, such a dependence of corrosion potential on porosity is attributed to the decreasing cathode-to-anode area ratio of a sample undergoing dissimilar-metal corrosion. The external surface of sintered sample acts as the cathode and external surface together with the surface of internal walls of pores serve as the anode. The former surface decreases and the latter one increases with increasing porosity.

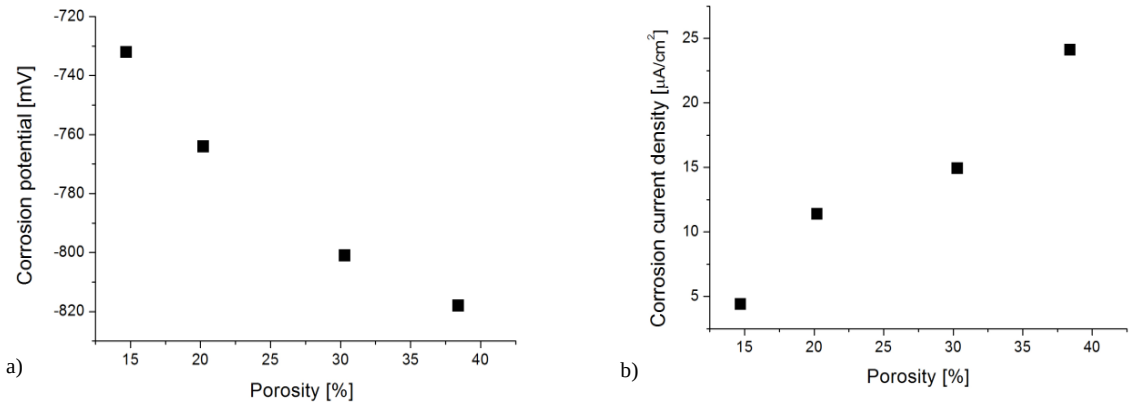

Figure 1 Corrosion parametrs of sintered iron samples in Hanks' solution as a function of sample's porosity a) corrosion potential as a function of porosity, b) corrosion current density (corrosion current per unit of geometric area) as a function of porosity.

Acknowledgements

The authors thank for financial support of the research by the Slovak Research and Development Agency under contract APVV-20-0278.

References

[1] E. J. Garboczi, K. A. Snyder, J. F. Douglas, M. F. Thorpe, Phys. Rev. E. **52** (1995) 819-828.
[2] M. Kupková, M. Kupka, M. Hrubovčáková, Int. J. Electrochem. Sci. **12** (2017) 3120-3132.

Nanostructured Carbon Materials for Li-S Batteries

J. Macko[a]*, D. Capková[a], A. Straková Fedorková[a], R. Oriňaková[a], A. Oriňak[a]
[a]Department of Physical Chemistry, Institute of Chemistry, Faculty of Science, Pavol Jozef Šafárik University in Košice, Moyzesova 11, 041 54 Košice, Slovak Republic
*jan.macko@upjs.sk

Lithium-sulfur (Li-S) battery attracts increasing attention because of its high energy density. However, sulfur cathodes suffer from several scientific and technical issues which are related to polysulfide ion migration. Lithium-sulfur batteries have a high theoretical energy density (~2600 Wh kg^{-1}) [1]. They are environmentally friendly, inexpensive and sulphur is naturally abundant in the environment [2]. Recently, nanostructured carbons, such as meso/micro-porous carbons, hollow carbon spheres, graphene, carbon nanotubes, and nanofibers, have been proposed to host sulfur materials [2]. There is an increasing demand for energy storage in modern applications, such as wearable electronics, electromobility, or stationary energy storage systems for renewable energy sources (photovoltaic or wind power plants, which are essential to meet climate goals) [3]. The polysulfide shuttle effect occurs during the charging and discharging of the Li-S battery. In the beginning, cyclo-S_8 is reduced during discharging to higher lithium polysulfides (Li_2S_8, Li_2S_6, Li_2S_4) between 2.4 and 2.1 V vs. Li and then, between 2.1 and 1.7 V vs. Li, lower lithium polysulfides (Li_2S_2, Li_2S) are formed (Figure 1). Currently, several methods to prevent the shuttle effect and decrease the influence of sulfur volumetric expansion are developed. A widely used technique is polysulfide trapping by porous carbon materials, which can bind lithium polysulfides in its porous structure and subsequently increase the conductivity of the electrode structure [3]. Despite enormous developments accomplished in the Li-S battery, the commercialization of this battery still has a long way to go, relying on technological breakthroughs in solving the key issues such as low sulphur conductivity, volume changes, and shuttle effect.

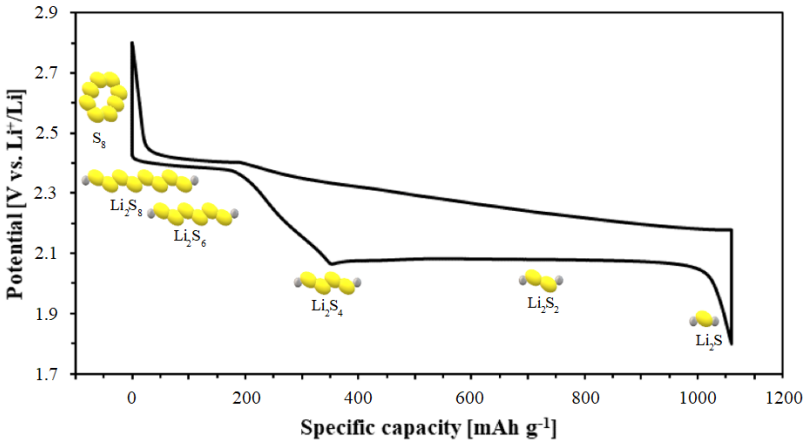

Figure 1 The polysulfide shuttle effect.

Acknowledgements

This work has been supported by grants APVV-20-0138 by Slovak Research and Development Agency.

References

[1] J. Z. Wang, L. Lu, M. Choucair, J. A. Stride, X. Xu, H. K. Liu, Journal of Power Sources **196** (2011) 7030-7034.
[2] J. Pu, Z. Shen, J. Zheng, C. Zhu, Q. Zhou, H. Zhang, F. Pan, Nano Energy **37** (2017) 7-14.
[3] T. Kazda, D. Capková, K. Jaššo, A. Straková Fedorková, E. Shembel, A. Markrvich, M. Sedlaříková, Materials **14** (2021) 5578.

Recycled Material for Cathode in Li-ion Battery

V. Niščáková[a]*, D. Capková[a], A. Straková Fedorková[a], S. Hatoková[b], M. Čigaš[b], Š. Hanigovský[b]

[a]Department of Physical Chemistry, Institute of Chemistry, Faculty of Science, Pavol Jozef Šafárik University in Košice, Moyzesova 11, 040 01 Košice, Slovak Republic
[b] Fecupral, Jilemnickeho 3578/2, 080 01, Prešov, Slovak Republic
*veronika.niscakova@student.upjs.sk

Lithium-ion batteries were first introduced on the market in 1991 by the company Sony Inc. This type of battery dominates many applications, from portable electronics to electric vehicles (EVs) [1,2]. The market for electric vehicles is growing rapidly and the number of electric vehicles in the world is also growing, so it is necessary to improve but at the same time reduce the cost of manufacturing such batteries [3]. The supply of lithium and cobalt, which are currently used as a major component in the production of Li-ion batteries, has been declining recently. Cobalt is suffering from scarcity and toxicity issues too [4]. Even based on this situation, the recycling of used lithium-ion batteries is considered to be a better approach to alleviate the enormous demand for raw materials for the synthesis of cathode and anode materials [2].
In this work was prepared positive electrode for Li-ion battery. The active material used in the production of the cathode came from the recycling of old NMC-based batteries.

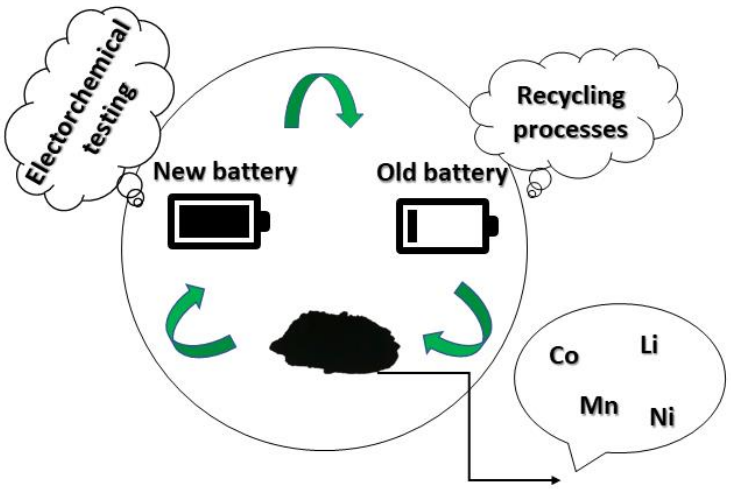

Figure 1 Preparing processes before electorchemical testing.

The composition of the prepared electrode was 80 % NMC, 10 % amorphous carbon and 10 % PVDF (as a binder). The individual compounds were dissolved in NMP (n-methyl-2pyrrolidone) and stirred for 24 hours. After thorough homogenization, the paste was applied to a carbon-modified aluminum foil and dried at 60 °C. The prepared electrode was tested by various electrochemical measurements such as cyclic voltammetry and galvanostatic cycling. Galvanostatic charge and discharge curves in potential window from 3 V to 4,2 V are in Figure 2. This curve was measured at 0,2 C. We observe a gradual decrease in capacity with an increasing number of cycles. The first discharge cycle was 84 mAh/g and the last 20th cycle was 33 mAh/g. This results is not so good but by adjusting the samples it is possible to improve the results.

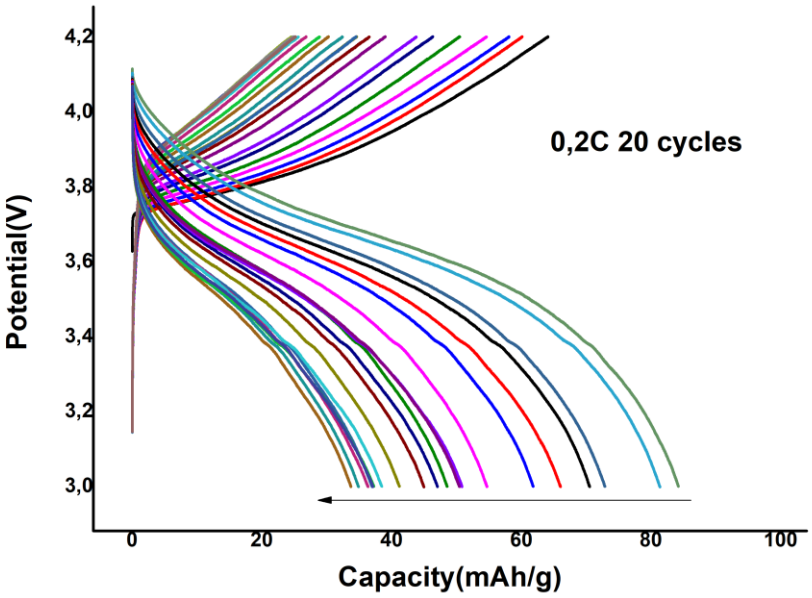

Figure 2 Charge and discharge curves of prepared electorde at 0,2C.

Acknowledgements

This publication was supported by the Operational program Integrated Infrastructure within the project: Innovative Solutions for Propulsion, Power and Safety Components of Transport Vehicles, 313011V334, cofinanced by the European Regional Development Fund and of the Slovak Research and Development Agency APVV-20-0138 and APVV-20-0111.

References

[1] M. Contestabile, S. Panero, B. Scrosati, J. Power Sources **92** (2001) 65–69.
[2] S. Natarajan, V. Aravindan, ACS Energy Lett. **3** (2018) 2101–2103.
[3] R. E. Ciez, J. F. Whitacre, Nat. Sustain. **2** (2019) 148–156.
[4] J. Loughran, Bad news for batteries: cobalt and lithium supplies 'critical' by 2050, (2019) 2018–2019. https://eandt.theiet.org/content/articles/2018/03/bad-news-for-batteries-cobalt-and-lithium-supplies-critical-by-2050/ (accessed October 20, 2021).

Influence of Bioactive Coating on Degradation Properties of Porous Iron-Based Materials

M. Petráková[a]*, R. Oriňaková[a], R. Gorejová[a]
[a]Department of Physical Chemistry, Institute of Chemistry, Faculty of Science, Pavol Jozef Šafárik University in Košice, Moyzesova 11, 040 01 Košice, Slovak Republic
*martina.petrakova@student.upjs.sk

Metallic biomaterials are widely used in many load-bearing orthopedic applications. However, the trend of recent years is biodegradable materials. Compared to permanent materials such as titanium, degradable implants gradually biodegrade over time, with the products of such degradation being resorbed and excreted from the human body. Even though metallic materials show good biocompatibility, their disadvantage is mainly sufficient osseointegration capacity for implant life due to undesirable interactions of degradation products with surrounding tissues after the release of metal ions from implant surfaces. To improve bioactivity and biocompatibility, various surface modification methods have been studied on porous biomaterials, such as alkaline heat treatment, electroplating, coating, or anodizing [1]. Metal implants have a different composition than human bone, so the healing process itself takes longer as the bone/implant interface forms more slowly. To improve this process, bioactive coatings are used to cover the surfaces of implants with thin layers [2]. Research is currently focused on the development of systems that can supply antibiotics locally. An example of such an antibiotic is gentamicin. Gentamicin is a relatively inexpensive broad-spectrum antibiotic with rapid, dose-dependent activity, which finds application precisely when applied topically in the form of a coating on the surface of a degradable implant [3].

In this work, the influence of bioactive polymer coating on the degradation of porous Fe biomaterials was studied. Iron-based cellular samples were prepared by sintering iron-impregnated polyurethane (PUR) foam. The porous samples were sintered in two steps, at which PUR foam was first removed at 450 °C for 120 min in an inert atmosphere and then at 1050 °C for 60 min. the samples were sintered in a reducing atmosphere. The surface of the iron samples (Fe) was modified with a polymer coating layer of polyethylene glycol (PEG). Part of the samples was coated with a PEG polymer layer containing gentamicin. Scanning electron microscopy (SEM) combined with EDX analysis was used to determine the surface morphology of both coated and uncoated samples. The addition of a layer of PEG as well as PEG with the addition of gentamicin slightly smoothed the surface of the sample (Fig. 1). The prepared samples showed the presence of macropores with a size of 400 to 1300 μm.

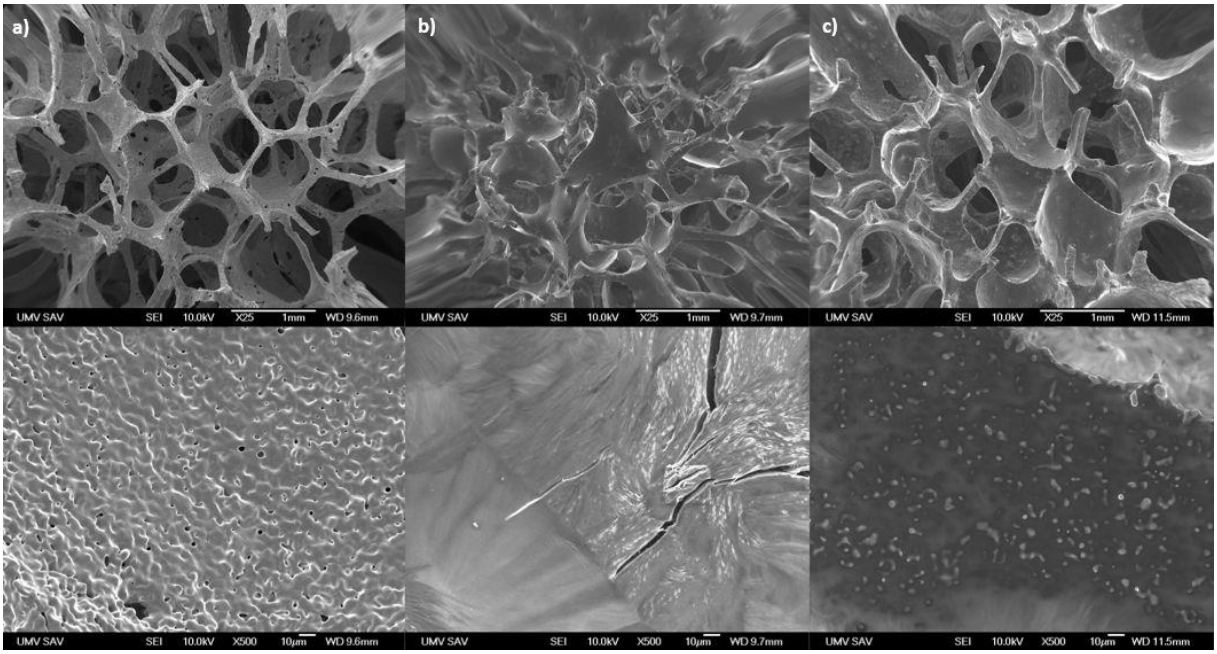

Figure 1 SEM images of the surface of the samples at surface enlargement 25x and 500x a) Fe b) FePEG c) FePEGGe.

The corrosion properties of coated and uncoated samples were studied by the method of anodic polarization in Hanks' solution (Figure 2). The measurements were performed in a standard three-electrode connection. The degradation properties of the samples were changed by the addition of a polymer coating. A shift to more negative potential values was observed for the PEG coated samples, indicating a higher tendency for corrosion compared to the non coated polymer coated samples. In contrast, a shift to more positive potential values was observed for antibiotic-coated samples, indicating increased corrosion resistance in the polymer-coated sample with gentamicin.

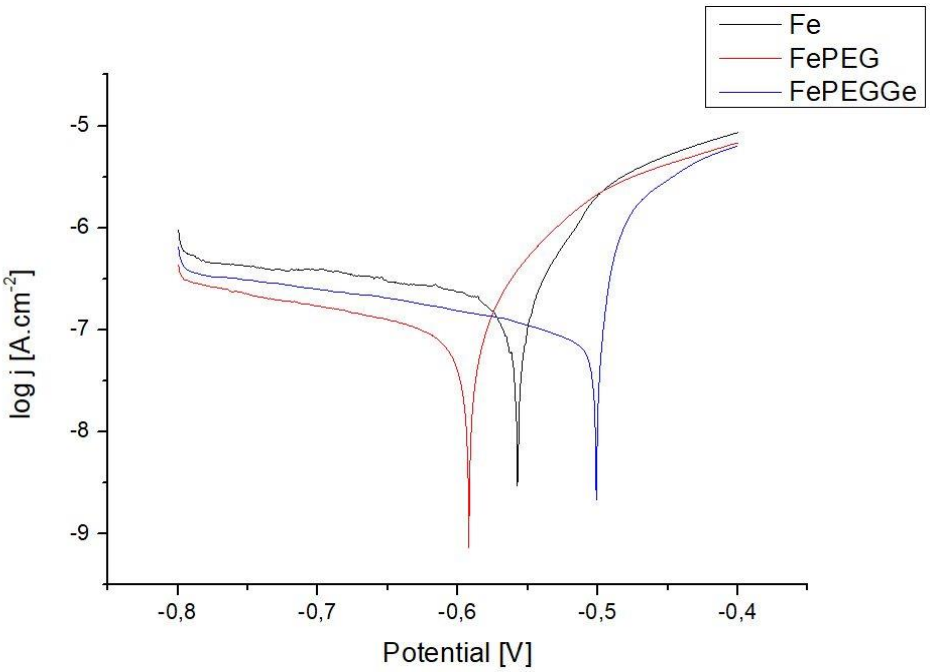

Figure 2 Potentiodynamic polarization curves of porous samples measured in Hanks' solution.

Acknowledgements

This work was supported by the project APVV-20-0278 of the Slovak Research and Development Agency.

References

[1] S. Grohmann et al., Biomedizinische Technik **64** (4) (2019) 383–395.
[2] K. Mediaswanti et al., Journal of Biomimetics Biomaterials and Tissue Engineering **18** (1) (2013) 1–8.
[3] M. Prodana et al., Coatings **11** (6) (2021) 1–20.

Experimental and Computational Studies of Catalytic CO_2 Valorisation

N. Podrojková[a]*, R. Oriňaková[a], A. Oriňak[a]
[a]Department of Physical Chemistry, Institute of Chemistry, Faculty of Science, Pavol Jozef Šafárik University in Košice, Moyzesova 11, 040 01 Košice, Slovak Republic
*natalia.podrojkova@student.upjs.sk

Catalyst modeling with computational simulations using quantum mechanics theory has great potential to contribute to the development of highly efficient CO_2 conversion catalysts. The functional density theory (DFT) of the CO_2 behavior on the catalyst surface provides valuable insight into the activation of the C = O bond, information on the adsorption and dissociation of CO_2. It can also help to understand the basic steps involved in the hydrogenation mechanism of CO_2.

Regarding heterogeneous hydrogenation of CO_2 the most commonly used catalyst is Cu together with different promoters (Zn, Zr, Ce, Al, Si, V, Ti, Ga, B, Cr, etc.) which is widely used mainly for production of methanol. The synthesis of methanol using copper-based catalysts can occur via three different reversible reaction pathways (Figure 1) [1]. The first mechanism is the formate mechanism, where the reaction of CO_2 with atomic H leads to the formation of formate as an intermediate. Chemisorbed formate can be formed from CO_2 reaction with dissociated surface hydrogen. Then, surface-bound formate is hydrogenated, which is the rate-determining step, to produce dioxomethylene that can lose oxygen with the formation of formaldehyde or lose hydroxyl and form H_2CO*. H_2CO* can be further hydrogenated to methoxy and methanol. The second reaction pathway is called RWGS and it produces a carboxyl intermediate. RWGS pathway involves the formation of CO* through the loss of hydroxyl from hydrocarboxyl. HCO intermediate is then hydrogenated to formyl that leads to methanol. During the third hydroxycarbonyl mechanism a $C(OH)_2$ intermediate is formed. It assumes that hydrocarboxyl can be hydrogenated to form COOH* which may subsequently lose hydrogen to form *COH. *COH is then hydrogenated to hydroxymethylene. All three reaction pathways lead to the formation of formyl (H_2CO*) which is subsequently hydrogenated to methoxy (H_3CO*) and methanol (CH_3OH) [1]

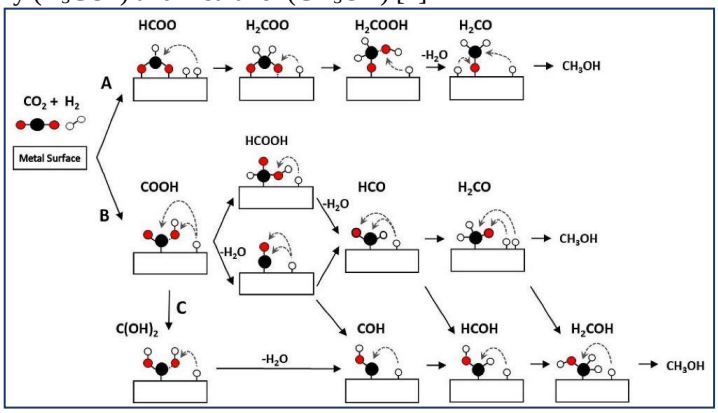

Figure 1 Possible mechanism and intermediates of methanol synthesis via CO_2 hydrogenation according to different studies a) formate mechanism, b) RWGS mechanism, c) hydrocarboxyl mechanism [1].

The use of quantum mechanics simulations for understanding the CO_2 hydrogenation process is effective in finding new intermediates, searching for new catalysts, and identifying reaction pathways. Our theoretical studies were oriented towards the effect of CuO on the mechanism of CO_2 hydrogenation to methanol to better understand the deactivation process of the catalyst. Using the DFT+U calculations in GPAW software we were able to optimize the CuO cell structure with calculation of U parameter. Also, values of lattice parameters were optimized, and surface structure was prepared for CO_2 adsorption simulations. The results from surface optimization provided the possibility to find the transition states and pathways of CO_2 hydrogenation to methanol which are the main goal of the work.

Acknowledgements

This work was supported by the Internal Scientific Grant System of Faculty of Science of Pavol Jozef Šafárik University in Košice, Slovak Republic project no. VVGS-PF-2019-1052 and by Scientific Grant Agency of the Ministry of Education, Science, Research, and Sport of the Slovak Republic project no. VEGA 1/0074/17.

References

[1] N. Podrojková et al., Chem. Cat. Chem. **12** (2020) 1802-1825.

Novel Catalysts for Production of Blue Hydrogen by Thermal Decomposition of Methane

K. Sisáková[a]*, R. Oriňaková[a], A. Oriňak[a]
[a]Department of Physical Chemistry, Institute of Chemistry, Faculty of Science, Pavol Jozef Šafárik University in Košice, Moyzesova 11, 040 01 Košice, Slovak Republic
*katarina.sisakova@student.upjs.sk

Introduction

Methane is widely used as a hydrogen source because of its high H/C ratio and abundance in natural gas fields. Green hydrogen can be produced by utilizing renewable energy sources, such as landfill gas and biogas from livestock manure and food processing waste, and methane feedstock and solar thermal energy as a heat source. Catalytic methane decomposition, CMD ($CH_4 \rightarrow 2H_2 + C$, $\triangle H_{298K} = 75.6$ kJ/mol) has attracted much attention as an alternative to conventional SMR process in terms of economic and environmental aspects. It is reported to produce COx-free hydrogen directly applicable for PEM fuel cells, and to dramatically reduce CO_2 emissions when coupled with heating source such as solar systems.

However, the thermal decomposition of methane to produce COx-free hydrogen entails several obstacles that need to be overcome. One of the disadvantages of the process is the high temperature at which the reaction takes place. Decomposition of methane without the use of a catalyst takes place at temperatures higher than 1200 ° C. The development of high-efficiency catalysts and the optimization of reactors are essential for the industrial production of TCDs [1]. Catalysts can reduce activation energy and shorten reaction times. Therefore, the selection of a suitable catalyst plays a crucial role in the TCD catalysed process. At present, research is mainly focused on Ni-based catalysts, noble metal doped catalysts, carbon catalysts and iron-based catalysts [2]. Another disadvantage is that the carbon formed is adsorbed on the active sites of the catalyst and causes the catalyst to be deactivated. Many industrial catalysts consist of Ni or Ni and other metal alloys supported on a suitable support. The main reason for this support is to keep the catalytically active phase in a highly dispersed state. The most important factors influencing carbon deposition during metal-catalysed methane decomposition are particle size, dispersion, and stabilization of the metal catalyst particles, which can be controlled by selecting a suitable support. In recent years, special attention has been focused on the use of SiO_2 as a support for a suitable catalyst for the process of thermal decomposition of methane [3]. The addition of a noble metal to a nickel-based catalyst, such as palladium, leads to a significant increase in stability and overall hydrogen yields, but modification with other noble metals reduces nickel activity.

Methods

TEM, SEM and AAS methods were used to characterize the structure of nanocatalysts. Microscopic images of the samples were taken with a HITACHI SU 6600 scanning electron microscope (SEM), which provides a resolution of up to 1.3 nm and a magnification of 60-600 000x. A Jeol 2100 (TEM) instrument was used for transmission electron microscopy, which provides a resolution of up to 0.19 nm and a magnification of 1000-800 000x. A ContrAA 300 atomic absorption spectrometer (Analytik Jena AG, Germany) with a flame ionization with a continuous radiation source was used to measure atomic absorption spectroscopy.

The DFT method was used to simulate and model the CMD. The General Gradient Approximation (GGA), which modifies the functional, is commonly used in catalysis and is referred to as the revised Perdew-Burke-Ernzerhof (rPBE), which uses double numerical plus polarization (dnp). This functional was used in conjunction with FD mode. The base set was used to balance electron exchange and correlation. The most stable crystallographic surface of Pd(fcc 111) was studied. The adsorption energy per 1 molecule can be calculated from the relation:

$$Eads = E_{surf\ +\ mol} - (E_{surf} + E_{mol}) \qquad (1)$$

where $E_{surf+mol}$ is the total energy of the adsorbate-substrate system; The E_{surf} is the energy of an uncovered surface cell; and E_{mol} is the energy of the isolated CH_4 molecule.

The nudged elastic band (NEB) was used to simulate the cleavage of C-H covalent bonds from a CH_4 molecule.

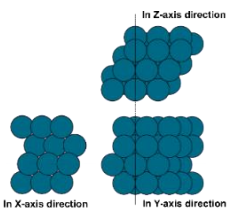

Figure 1 The surface of Palladium (fcc111) created and optimized by DFT method.

Results and Discussion

The structure of the catalysts was studied using a scanning and transmission electron microscope. Figure 2A, 2B and 2C shows TEM and SEM images of Pd nanoparticles deposited on a SiO_2 support. From the TEM images we can observe that palladium nanoparticles are deposited both on the surface and inside the pores of SiO_2. The Pd size of the nanoparticles is approximately 8 nm. In the figure 2G and 2H SEM and TEM images of $NiFe_2O_4$ nanoparticles deposited on a SiO_2 support are shown. From the TEM images we see that $NiFe_2O_4$ nanoparticles are absorbed mainly in the pores of SiO_2. $NiFe_2O_4$ nanoparticles are also more homogeneously dispersed compared to palladium nanoparticles. The average size of $NiFe_2O_4$ nanoparticles is approximately 10 nm. The TEM and SEM images of $Pd/NiFe_2O_4/SiO_2$ catalyst are shown in the figure 2D, 2E and 2F. The orange circle indicates palladium nanoparticles, while the blue circle indicates $NiFe_2O_4$ nanoparticles. From the TEM images we can observe that the Pd nanoparticles are surrounded by $NiFe_2O_4$ nanoparticles. It is also possible to observe empty pores of SiO_2. The nanoparticles are located mainly in the open pores of SiO_2.

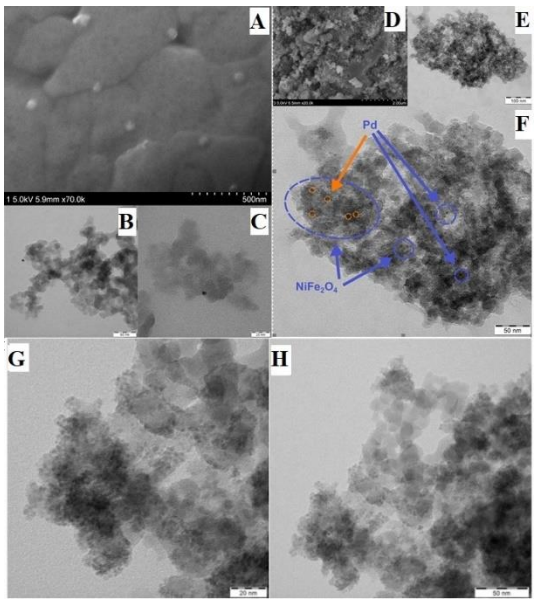

Figure 2 A- SEM images of Pd/SiO_2, B, C - TEM images of Pd/SiO_2, D - SEM images of $Pd/NiFe_2O_4/SiO_2$ catalyst, E, F - TEM images of $Pd/NiFe_2O_4/SiO_2$ catalyst, G, H- TEM images of $NiFe_2O_4$ nanoparticles deposited on SiO_2.

The prepared samples were also characterized by Atomic Absorption Spectroscopy (AAS). Under optimal conditions, a calibration dependence was made for all determined elements. Five calibration points were measured for palladium, nickel and iron. For Pd and Fe, a concentration range of 1-5 mg/L was determined. A calibration dependence in the range of 0.05-2 mg/L was determined for Ni.

The first step in the calculations and simulations of the TCD process using the DFT method was to optimize the surface of hydrogen and methane and calculate their adsorption energies. The adsorption energy of optimized methane is -23.973 eV and the adsorption energy of hydrogen is -6.704 eV.

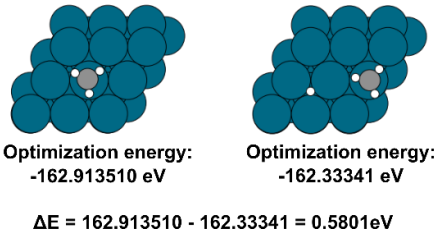

Figure 3 Adsorption energy of Pd surface before and after break of first hydrogen from methane molecule.

The adsorption energy of the Pd is -138,815 eV. In order to achieve the most accurate energy value, the grid parameter was also optimized in the values of 3.933 to 3.945 Å. The lowest value of adsorption energy was reached at the lattice parameter a = 3.942 Å. This value was used for surface creation and subsequent optimization. The distance between Pd atoms after optimization was 2.779 Å. In order to find out how the methane molecule is rotated during adsorption on the Pd surface, several possibilities have been optimized. It was shown that the lowest adsorption energy was achieved by methane, which was placed on the surface of the atom Pd, turned 1 with

hydrogen downwards - towards the surface of Pd. This location corresponds to the literature [4]. The lowest value of adsorption energy was -162.914 eV.
The activation barrier required to dissociate the first hydrogen bond from the methane molecule was calculated using the NEB calculation method.
The adsorption energy of the system before the cleavage of the hydrogen bond from the methane molecule on the palladium surface was -162.914 eV and after the cleavage of the bond: -162.333 eV. The calculated activation barrier is 0.581 eV for the palladium surface, indicating that from a thermodynamic point of view, this step does not require a large activation energy for dissociation. Arevalo et. al. studied using NEB simulation of DFT calculations of TCD methane on the surface of nickel and ruthenium [5]. The activation barrier they calculated for the nickel surface was 0.49 eV, while for the ruthenium surface it was 1.10 eV. From the given results we can see that while, from a thermodynamic point of view, the surface of ruthenium requires a high activation energy, on the contrary the surfaces of palladium and nickel do not need a large activation energy for dissociation. Liu et. al. studied the thermal decomposition of methane on the surface of palladium and ruthenium [6]. They calculated an activation barrier for the dissociation of the first hydrogen bond from a methane molecule on the palladium surface of 0.3 eV. Compared to the values presented in this work, their value is half lower. Such different values may be due to the use of other calculation methods than in the case of the simulations of Liu et. al., where they used the VASP program with the PW method for simulations and in the case of the DFT method they used the PBE functional with Dudarev correction instead of the Tkatchenko-Scheffler correction.
Similar to the first methane dissociation reaction on the palladium surface, the structures and adsorption energy were optimized for the other dissociation reactions. The adsorption energy calculated in this work for the CH_3 radical was 1.258 eV, for the CH_2 radical 3.198 eV, for the CH radical 5.655 eV.

Conclusion

A catalyst based on palladium, nickel and iron supported on SiO_2 support - $Pd/NiFe_2O_4/SiO_2$ was prepared. As part of a better study of properties, Pd/SiO_2, $NiFe_2O_4/SiO_2$ catalysts were also prepared. These catalysts were studied for their structure by SEM, TEM and AAS methods. From TEM and SEM analysis we know that the Pd size of the nanoparticles in the case of the Pd/SiO_2 catalyst was 8 nm. The AAS provided us with information on the palladium concentration, which was 4.045 mg/L. For $NiFe_2O_4/SiO_2$, the particle size averaged 10 nm and the metal concentration was 0.731 mg/L for nickel and 3.098 mg/L for iron. With a $Pd/NiFe_2O_4/SiO_2$ catalyst, we can observe that the palladium nanoparticles are surrounded by $NiFe_2O_4$ nanoparticles. Both types of nanoparticles are adsorbed mainly inside the pores of SiO_2, but also on the surface. The metal concentration in the catalyst was Pd - 0.246 mg/L, Ni - 1.456 mg/L, Fe - 4.121 mg/L.

Using the DFT method, we studied Pd nanoparticles for the TCD process. We used the GPAW program for calculation and simulation, and the ASE program for surface modeling. The implementation of a given program for the study of the TCD process brings new possibilities for the study of catalyst surfaces. The results are comparable to current research. The surfaces of methane, hydrogen, palladium and methane radicals were modeled and optimized. In addition, we implemented NEB calculations. We found that the activation barrier for the first hydrogen dissociation reaction from the methane molecule on the palladium surface is 0.581 eV. This value is higher than stated in the articles, but these minor differences were due to the use of other calculation methods. The adsorption energy calculated in this work for the CH_3 radical was 1.258 eV, for the CH_2 radical 3.198 eV, for the CH radical 5.655 eV.

Acknowledgements

This work was supported by the Scientific Grant Agency of the Ministry of Education, Science, Research, and Sport of the Slovak Republic Projects No. VEGA 1/0095/21, Research and Development Support Agency No. APVV-20-0299 and the Internal Scientific grant system PF UPJŠ VVGS-PF-2021-1783.

References

[1] K. Sisáková, A. Oriňak, R. Oriňaková, M. Strečková, J. Patera, A. Welle, Z. Kostecká, V. Girman, Catalysis Letters **150** (2020) 781-793.
[2] M. Pudukudy, Z. Yaakob, N. Dahani, M. Takriff, N. Hasaan, Journal of Cluster Science **28** (2017) 292-300.
[3] J. Qian, T. Chen, L. Enakonda, D. Liu, G. Mignani, J. Basset, L. Zhou, Int. J. Hydrogen Energy **45** (2020) 7981-8001.
[4] S. Kozlov, K. Neyman, Journal of Catalysis **337** (2016) 111-121.
[5] R. Arevalo, S. Aspera, M. Sison Escaño, H. Nakanishi, H. Kasai, Scientific Reports **7** (2017) 13963.
[6] Z. Liu, P. Hu, J. Am. Chem. Soc. **125** (2003) 1958-1967.

LIST OF POSTERS *Sessions 1-5*

Analytical Chemistry

P1 B. Benická, E. Kupcová: Isolation of anabolic androgenic steroids from oil-based samples

P2 A. Várfalvyová, E. Kupcová: Determination of Benzodiazepines in Alcoholic Beverages Using Microextraction Technique Coupled with HPLC/DAD

P3 D. Pavelek, R. Halko: Use of Infrared Spectrometry for Identification of Substances after their Separation by Liquid Chromatography

Biochemistry

P4 A.Gucký, S. Hamuľaková, M. Kožurková: Synthesis of Novel 7-Hydroxy-2-Oxo-*2H*-4-Chromenyl Metal Chelators

P5 K. Krochtová, L. Janovec, M. Kožurková: Topoisomerase inhibitory potential of 3,9-disubstituted acridine derivatives

P6 J. Olajoš, R. Sůra, M. Antalík: Extracellular electron transport for reduction of iron deposits

P7 S. Sovová, G. Kuzderová, D. Sabolová: Interactions of newly synthesized Ag(I) complexes with CT DNA

P8 L. Trizna, V. Víglaský: LGGE – A New Method for Electrophoretic Analysis of Ligand-DNA Interactions

Inorganic Chemistry

P9 D. Princík, V. Zeleňák: Metal-Organic Frameworks Containing Fluorinated Ligands

P10 J. Tomičová, M. Matiková Maľarová, J. Kuchár, J. Černák: Solvothermal reactions of iron with bidentate aromatic N-donor ligands

P11 Z. Vargová, M. Almáši, M. Rendošová, R. Oriňaková, S. Hamuľaková, R. Varhač, V. Víglaský, J. Šandrejová, M. Ganajová: The social demand of the professionally focused study program „Chemical Laboratory Technician - specialist”

LIST OF AUTHORS

New Trends in Chemistry, Research and Education at the Faculty of Science of Pavol Jozef Šafárik University in Košice 2021
Book of Abstracts

Edited by: prof. RNDr. Mária Kožurková, CSc.

Publisher: Pavol Jozef Šafárik University in Košice
Publishing ŠafárikPress

Year: 2021
Pages: 86
Author's sheets: 5,95
Edition: first

ISBN 978-80-574-0048-6 (e-publication)